Aluminum foams composite : elaboration and thermal properties for energy storage

Chuan Zhang

Thèse
de doctorat
de l'UTT

Chuan ZHANG

Aluminum Foams Composite: Elaboration and Thermal Properties for Energy Storage

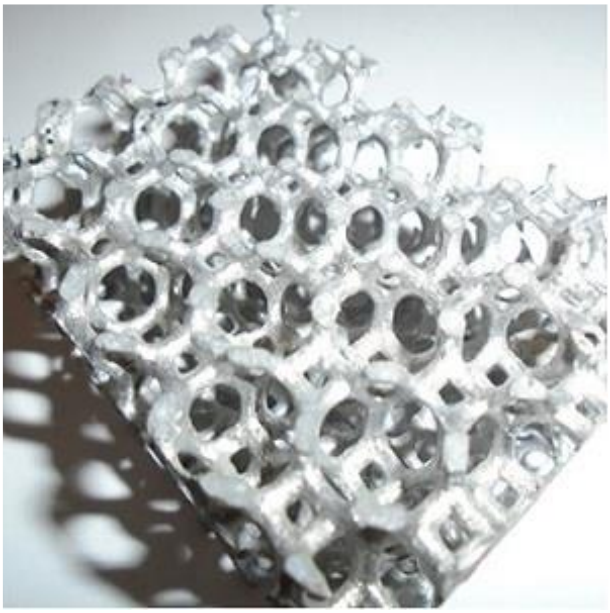

Spécialité :
Matériaux, Mécanique, Optique et Nanotechnologie

2017TROY0015 Année 2017

utt
UNIVERSITÉ DE TECHNOLOGIE
TROYES

THESE

pour l'obtention du grade de

DOCTEUR de l'UNIVERSITE DE TECHNOLOGIE DE TROYES

Spécialité : MATERIAUX, MECANIQUE, OPTIQUE ET NANOTECHNOLOGIE

présentée et soutenue par

Chuan ZHANG

le 7 juillet 2017

Aluminum Foams Composite: Elaboration and Thermal Properties for Energy Storage

JURY

M. Y.-Q. GUO	PROFESSEUR EMERITE	Président
M. H. BADREDDINE	MAITRE DE CONFERENCES	Directeur de thèse
M. A. EL HAMI	PROFESSEUR DES UNIVERSITES	Rapporteur
M. J. GARDAN	ENSEIGNANT CHERCHEUR EPF	Examinateur
M. X.-L. GONG	PROFESSEUR DES UNIVERSITES	Directeur de thèse
M. H. HADDADI	PROFESSEUR DES UNIVERSITES	Rapporteur
M. S. HE	PROFESSOR	Examinateur

Acknowledgements

Three years research experiences in France are challenging, unforgettable and meaningful, and it will be a valuable lesson for my life. During the study, all the work could not be completed without the assistance of the surrounding people in the University of Technology of Troyes (UTT). I would like to express my deepest gratitude to them and the China Scholarship Council (CSC) for the financial support.

First of all, I am especially grateful to my supervisors, GONG Xiao-Lu and Houssem BADREDDINE, for their valuable guidance, constructive suggestions and constant encouragement. They not only provide a good research foundation for this thesis, but also give me many precious advices in the experiment design and result analysis. Their positive attitude for work always prompts me to move forward in both scientific research and daily life.

Thanks to the defense committee.

I am hugely appreciative to F.WEIL and B.LESAGE for their assistances in the preparation of the samples in Halle industrielle. And thanks to J.GARDAN, who provides us with the mold prepared by 3d impression in EPF. Thanks to the project Effi-SiEMCE for the technical and material support.

I am also grateful to my friends HAN.HC, WEN.ZM, ZHANG XH, ZHANG Y and other friends at UTT, who help and accompany me along these years.

I would like to thank my parents their love and wait in expectation.

ZHANG Chuan

Abstract

The objective of this thesis is to study and optimize the manufacturing process of metal foams and the thermal behavior of the aluminum foam/phase change material (PCM) composite by experimental and numerical methods. The manufacturing process of open-cell aluminum foam is developed and optimized to precisely control the parameters of manufacturing. Two pore-scale models of high porosity aluminum foams (HPAF)/PCM composite and low porosity aluminum foams (LPAF)/PCM composite are established for numerical simulation. By simulating the melting process of a layer energy storage system, the HPAF/PCM and LPAF/PCM composite are compared numerically in order to evaluate the energy storage performance. The results show that aluminum foam improves greatly the heat transfer process in PCM due to its high thermal conductivity. The porosity of aluminum foams could not only influence the melting process of composite but also the energy storage performance. Thanks to the collaboration with EPF, a new manufacturing method of periodic open-cell aluminum foams is developed based on 3D rapid tooling. The thermal behavior of the periodic open-cell aluminum foams/PCM composite is experimentally and numerically analyzed.

Keywords: Metal foams; Heat storage; Metallic composites; Thermal analysis; Simulation methods; Three-dimensional printing

Résumé

L'objectif de cette thèse est d'étudier et d'optimiser, par des méthodes expérimentales et numériques, le processus de fabrication des mousses métalliques et le comportement thermique des mousses composites aluminium/matériau à changement de phase (MCP). Le processus d'élaboration des mousses d'aluminium à pores ouverts est développé et optimisé pour contrôler précisément les paramètres des échantillons. Deux modèles de mousse d'aluminium à haute porosité (MAHP)/MCP composite et de mousse d'aluminium à faible porosité (MAFP)/MCP composite sont définis pour la simulation numérique. La comparaison de ces deux modèles est réalisée numériquement en simulant le processus de fusion d'un système de stockage d'énergie thermique permettant d'évaluer les performances de stockage. Les résultats obtenus montrent clairement que l'utilisation des mousses améliore le processus de transfert thermique dans le MCP. La porosité des mousses pourrait non seulement affecter le processus de fusion du MCP mais aussi influencer les performances de stockage d'énergie. La méthodologie d'élaboration des mousses d'aluminium à pores ouverts et périodiques mise en place est basée sur l'utilisation de techniques d'impression 3D. Le comportement thermique des mousses composites d'aluminium à pore périodiques ouvert et MCP est analysé expérimentalement et numériquement.

Mots clés : Mousses métalliques; Chaleur -- Stockage; Composites à matrice métallique; Analyse thermique; Simulation, Méthodes de ; Impression 3D

Table of contents

General introduction

Metal foams, especially aluminum foams, are widely studied thanks to their exceptional properties. They have a low density, an excellent capacity for energy absorption, heat transfer and sound absorption. Metal foams also have a large internal surface due to the porous structure. The mechanical properties of open-cell aluminum foams have been studied since over ten years in our laboratory. The open-cell aluminum foams are a promising functional material which could be widely applied in energy storage filed. This thesis focuses on the study of the enhancement effect of the aluminum foams on the heat transfer in phase change materials (PCMs).

In the first chapter, the preparation methods, structure characteristics, thermal properties of open-cell aluminum foams and 3D printing technology are introduced. Besides, the classification and characteristic of PCMs are presented, because they are the critical materials in the energy storage. The whole additive manufacturing (AM) process and several AM technologies are described.

In the second chapter, the preparation process of aluminum foams with the negative pressure infiltration method is presented. The advantages and disadvantages are analyzed. Thus the improvement and upgrading methods are proposed and achieved. After the improvement and upgrading methods, the properties of aluminum foams could be accurately controlled. The porosities of aluminum foams under different negative pressures are compared.

In the third chapter, a model of the high mechanical property open-cell metal foam is proposed and validated by comparing with the experimental results. The melting processes of paraffin in two models are both simulated and the results are compared and discussed.

In the chapter 4, a fabrication method of periodic open-cell metal foams is presented, combining the traditional casting method and the 3D printing by plaster and binder jetting. With the help of this method, the morphological and geometrical parameters of open-cell metal foam is designed and controlled according to the manufacturing constraints. After manufacturing the metal foam based on tetrakaidecahedron geometry, the thermal performance of energy storage system is investigated

In the chapter 5, the main conclusions of this thesis are summarized and some perspectives are provided for future studies.

Chapter 1 Bibliography

1.1 Introduction

Metal foams appeared in the early forties. They have advantages such as low density, thermal insulation properties, sound insulation and electrical insolation. The use of this material is very promising in the following fields: civil engineering, aeronautics, naval, automobile, medical, transport, etc. (Ashby et al., 2000)

We can separate the metal foams into two large families according to their pore types: closed-pore metal foams and open-pore metal foams as shown in Figure 1.1. It should be noted according to Figure 1.1 that the microstructure of the open pores is better arranged than that of the closed pores, but the cost of making open pores is much higher than that of closed pores during industrial production. Typical commercial products are currently: Cymat, Alulight, Alporas (brands of closed-pore metal foams); And ERG, Inco (open pore).

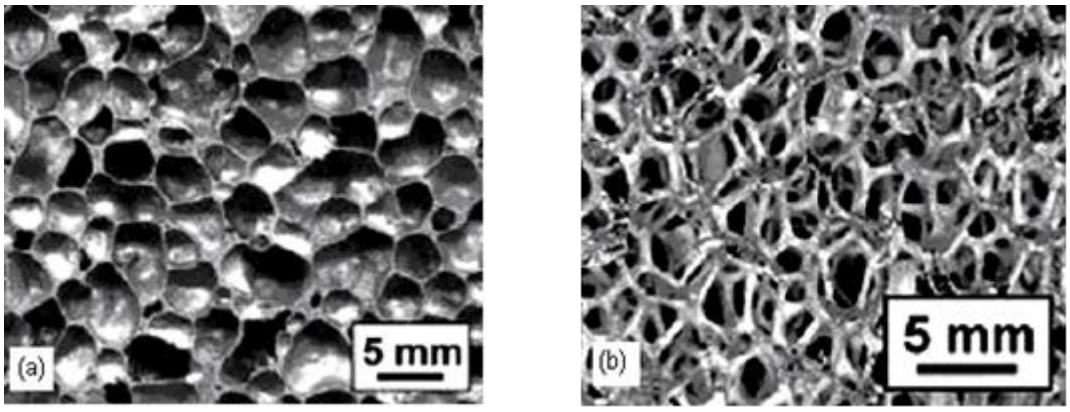

Figure 1.1 Metal foams: (a) closed pores and (b) open pore

1.2 Preparation methods of metal foams and structure characteristics of metal foams

Thanks to the development of manufacturing technology, many kinds of preparation methods of metal foams have been proposed and developed in recent decades (Wadley, 2002). In order to obtain pore structure of metal foams, there are several preparation methods for open-cell and closed-cell metal foams in this part. Depending on the manufacturing method, the structures and properties of metal foams are also different, such as porosity, pores per inch (PPI), and permeability. In this section, several common manufacturing techniques for metal foams are described.

1.2.1 Manufacturing techniques of closed-cell foams

Foaming of molten metal by gas injection

The first method of making metal foams was developed by *Hydro Aluminum Corporation* in Norway and sold by *Cymat Aluminum Corporation* of Canada. Figure 1.2 presents this method of manufacture.

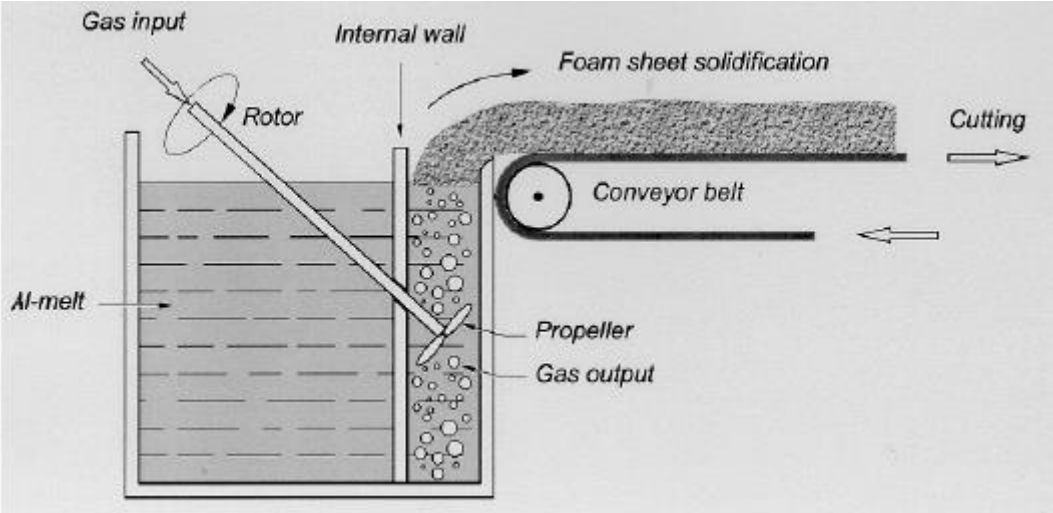

Figure 1.2 Foaming of molten metal by gas injection(Banhart, 2001)

The open-cell metal foam is produced by gas injection below the surface of a melted molten and SiC particles mixture. The bubbles thus created then rise towards the surface but do not burst. The stable foam is formed and it is necessary to obtain this foam on the surface, then it is put in the form of a slab before cooling it on a conveyor to obtain semi-finished products. The size of the cells, and also the density, is controlled by adjusting the flow rate of the injected gas.

Foaming of molten metal with foaming agent

The modern method of metal foam was developed by Shinko Wire, Amagasaki in 1985, and this type of metal foam is known as the "Alporas" brand. Figure 1.3 describes this method in which calcium is added to the molten aluminum at 680 ° C, the molten metal is stirred for several minutes during which the viscosity of the molten metal increases substantially and continuously. Once the viscosity is high enough, the emulsion of titanium hydride generally is added and then decomposed, thereby emitting the hydrogen gas causing the emulsion process. The emulsion

process is carried out at a constant pressure. After the crucible has been cooled below the melting point of the aluminum alloy, the liquid foam solidifies and could thus be removed from the mold for subsequent machining.

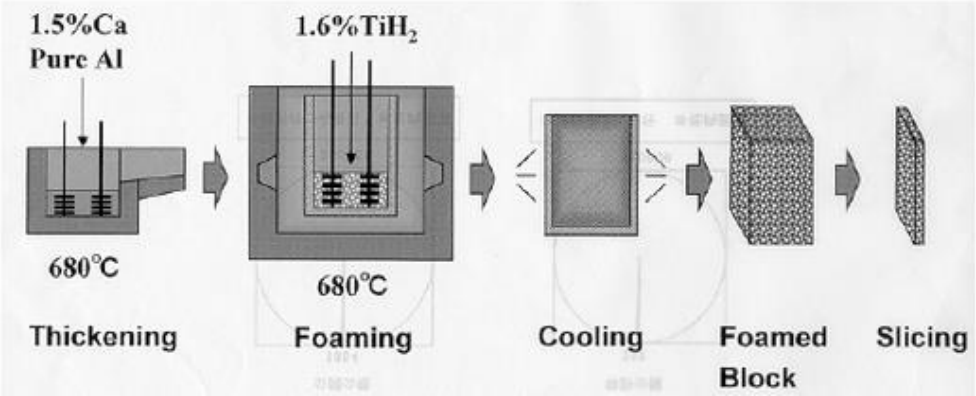

Figure 1.3 Foaming of molten metal with foaming agent(Banhart, 2001)

Powder metallurgy

The method of powder metallurgy for the production of metal foams is carried out by TIFAM (the Fraunhofer Institute for Applied Materials Research) (Ashby et al., 2000; Banhart, 2001) and by the Bratislava University in collaboration with the Karmann company. The foams produced by this technique are known as the trade mark "Alulight". Figure 1.4 describes the principle of the powder metallurgy method. The metal powders and an emulsifying agent (often titanium dichloride) are mixed and then this mixture is consolidated by pressure, the semi-finished product assembly takes the form of the cold mold under compression. The foaming process is controlled by heating the semi-finished product assembly above 550 °C (for aluminum binder), decomposing the foaming agent at high

temperature. This technique allows produce the production of the mold-shaped metal foam.

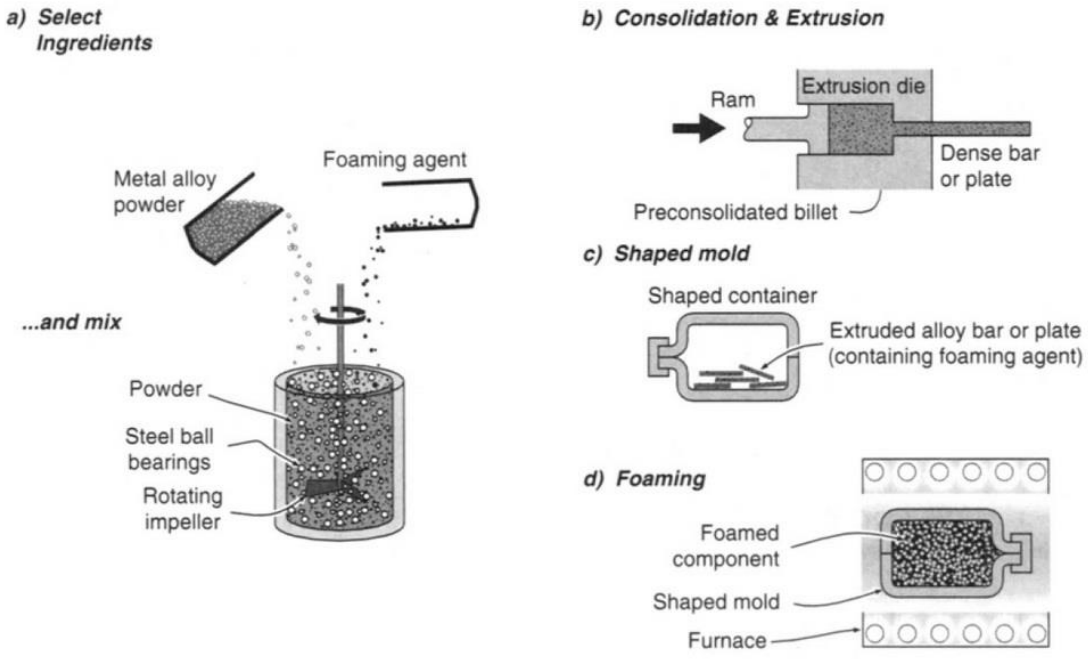

Figure 1.4 The sequence of powder metallurgy steps used to manufacture metal foams by gas-releasing particles in semi-solids (the Fraunhofer and the Alulight processes) (Ashby et al., 2000)

1.2.2 Manufacturing techniques of open-cell foams

Infiltration flow with polymeric foam

Figure 1.5 presents the method of making open-cell foams under the trademark "Duocel". In this technique, the polymeric foam of the open cell structure is placed in a mold and then filled with different materials such as mud, sand or plaster.

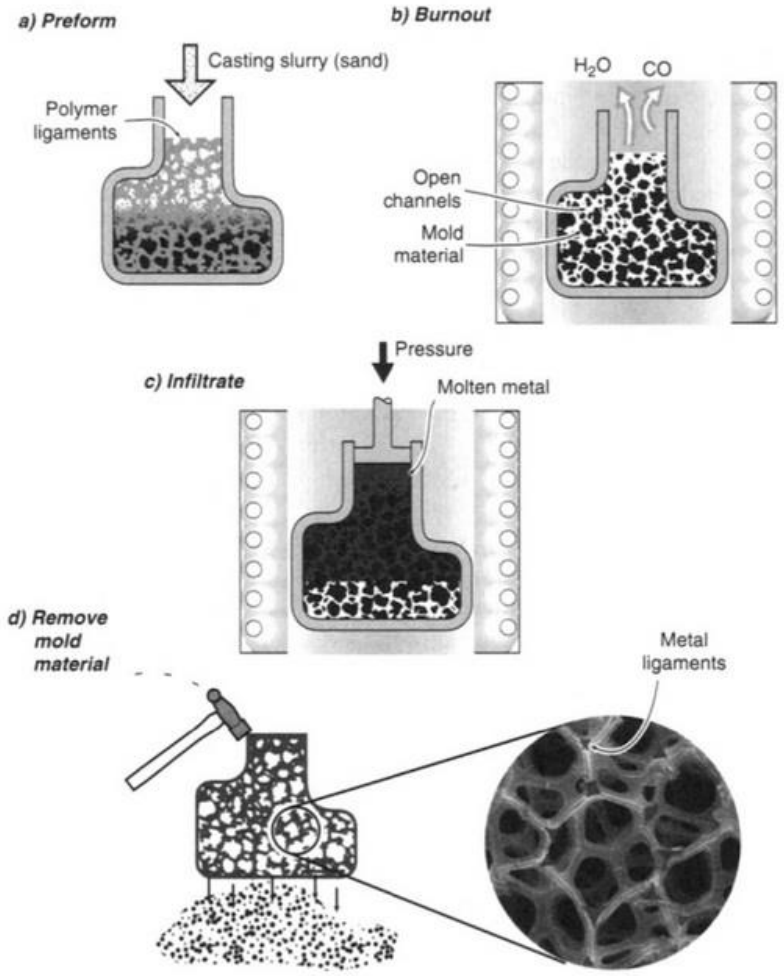

Figure 1.5 Investment casting method used to manufacturing open cell foams (DUOCEL process) (Ashby et al., 2000)

After filling, the blown polymer foam of the mold volatilizes and the molten metal is filtered in place of the polymeric foam by gravity or suction pressure and heating of the mold. Finally, after the demolding, metal foams are obtained and take up the initial structure of the polymeric foam, as shown in Figure 1.6 (Ashby et al., 2000; Yamada et al., 2000).

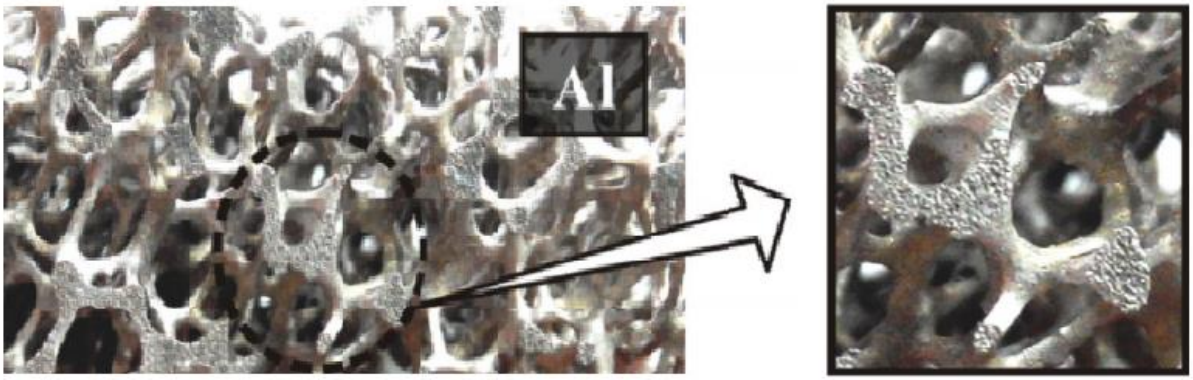

Figure 1.6 metal foam produced by investment casting method(Yang et al., 2016b)

Depot of metal by vapor in the cellular preform

Open-cell nickel foams are manufactured by the technique of metal vapor deposition. The metal foams produced take the trade mark "Inco". In this technique, the polymeric foam of the open cell structure is placed in a mold and then the vapor of composition of the nickel ($Ni(CO)_4$) decomposes. The nickel metal is deposited on the surface of the polymeric foam, and the polymeric foam is then burned. After the sintering, open-cell nickel foams could be obtained. This technique is described in Figure 1.7.

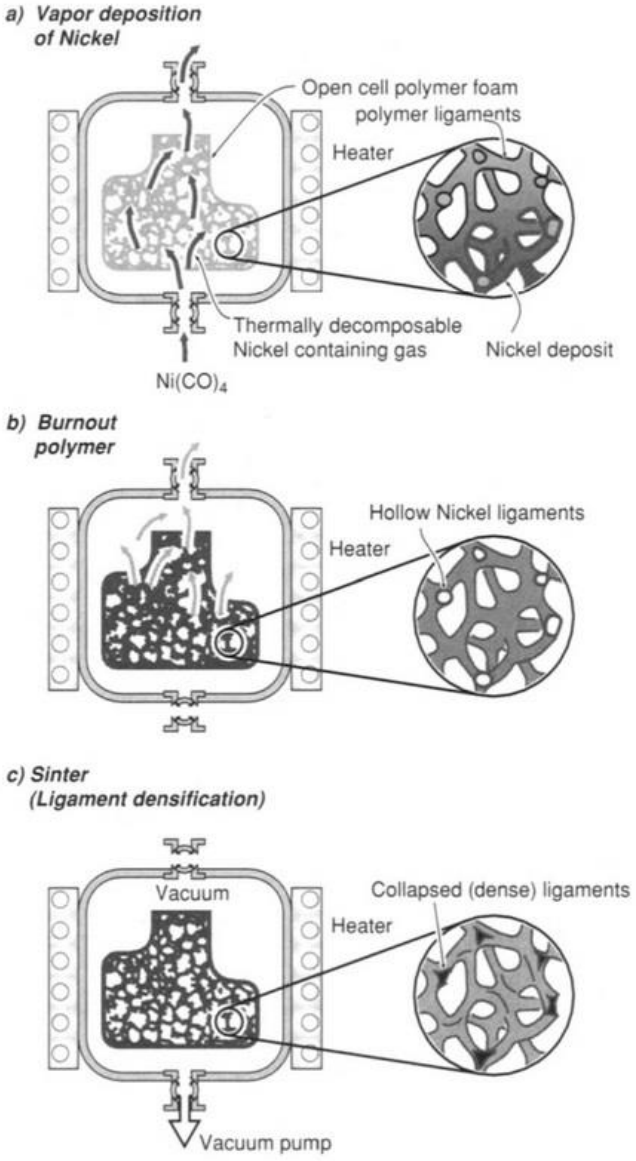

Figure 1.7 Depot of metal by vapor in the cellular preform(Ashby et al., 2000)

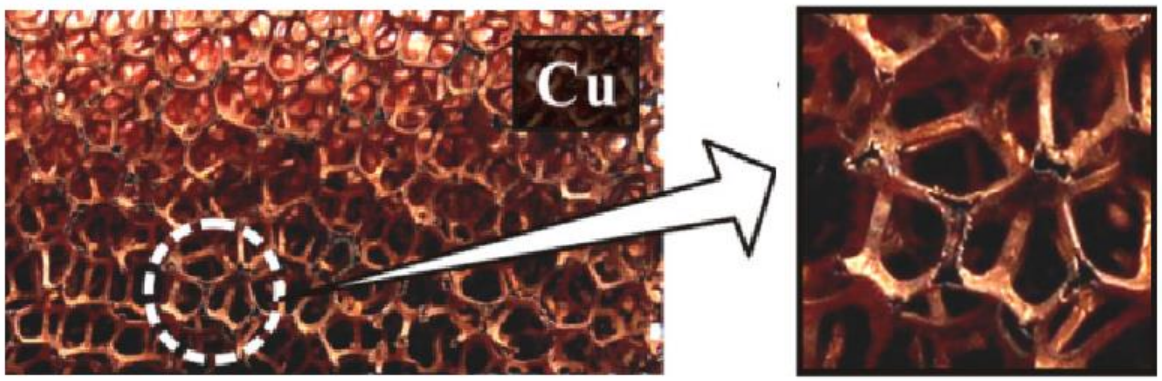

Figure 1.8 Metal foam produced by electro-deposition method (Yang et al., 2016b)

Infiltration flow with filler

Figure 1.9 describes this technique for the preparation of open-cell metal foams. The molten metal is filtered in a heated preform, and this preform is often inorganic particles, sand or salt (San Marchi and Mortensen, 2001), organic (such as polymer) or even hollow spheres. Firstly, the preform of the salt particles is sintered to improve its quality. The molten metal will be filtered under a specific pressure. The cooling of the mixture is subsequently dissolved by washing with water, and the aluminum foams are thus obtained(San Marchi and Mortensen, 2001).

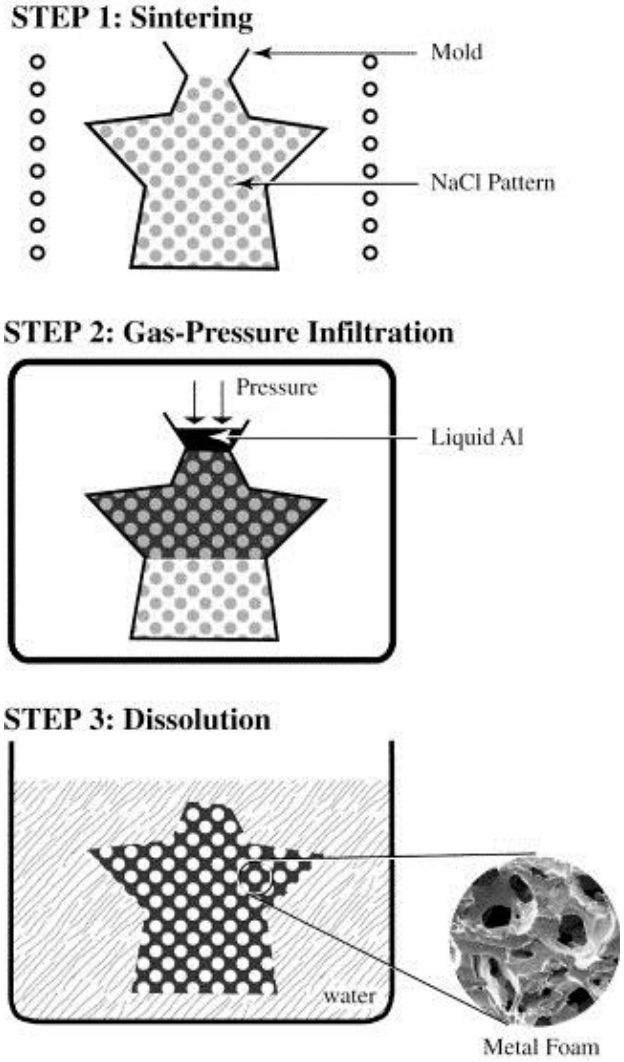

Figure 1.9 Schematic of the replication process for the production of metallic foam

Among all manufacturing techniques above, it could be concluded that the infiltration technique with filler is the most easily controllable. At the same time, other advantages such as the low cost of equipment and the simple implementation are also reasons why we chose this technique for our study, which is described in detail in Chapter 2 and the ameliorated method based on this method in Chapter 4.

1.3 Structure and Property of Metal Foams

1.3.1 Characteristics of the structure of metallic foams

The metal foam can be considered a composite composed of two elements: a metal and air. To describe the structure of metallic foams, two characteristics are important: the relative density and the porous structure. In most of the research articles published in this field, the mechanical properties of metal foam are mainly represented by two characteristics: properties of solid metal and relative density of metal foam (Ashby et al., 2000). In recent years, more and more researches are concentrating on the porous structure of metal foams.

The relative density is the most important characteristic of metal foams. It is one of the macroscopic characteristics, defined by the density of the metal and the percentage of metal and air. For some typical metal foams, their relative density is less than 0.35. Sometimes the structure of real foams is very complex, so the determination of the density is relatively difficult due to its inhomogeneity. Moreover, the exact measurement of the actual structure is virtually impossible. However, it could be obtained by the Archimedes' principle. It is difficult to find a specimen that has a closed complement surface in order to obtain the total volume.

The porous structure is other important characteristic of metal foams. A pore can be composed of knots, edges and walls (in closed-cell metal foams). The mechanical behavior of metal foams depends on local stresses within metal foams, where flexion, wrinkling, plastic creep and local fracture occur. Moreover, the density of the foam is also inhomogeneous because of the inhomogeneity of the porous structure, and this leads to a change of mechanical behavior of the metal

foams. Because of this complicity of pores, the following parameters are often used to describe it:

The pore: volume fraction, pore size, orientation and measured diameter (maximum, minimum and average diameter, and shape).

The arrangement of the pore: the pore arrangement rule, the number of adjacent pores, the length, the thickness and the flexion of the edge, the distance of the adjacent pores.

The structure of the pore: the number of nodes, the number of edges and walls in each pore, the angle of the edge, the shape of the edge, the number of walls that connects to an edge, Length and thickness of the wall, the number of walls that connects to a knot, the curvature and the fold on a wall ... etc.

Most metal foams have defects which unfortunately affect their mechanical and thermal properties. Typical defects include bending of the edge, crushing (bending) on the wall and on the edge etc. The macroscopic modulus of elasticity is thus decreased. In addition, other factors may also influence the mechanical and thermal properties of metal foams, such as:

Micro-cracks

Existing lumpy surfaces on the wall

The shrinkage cavities

The cavities without complete filling

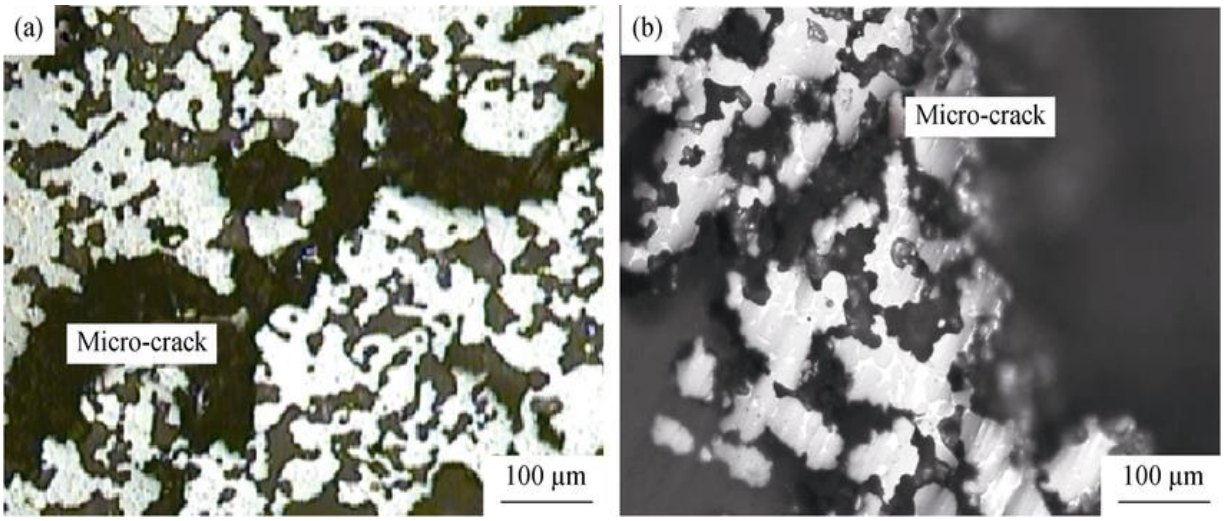

Figure 1.10 Micro-cracks of spheres' shells (a)specimen Cu5 and (b) specimen Cu20(Narayana)

Figure 1.10 shows the micro-cracks in the metal foams, from this figure, it could be observed that the width of these micro-cracks is not great, but the length is very long, which forms a long gap. The formation of these micro-cracks is associated with many factors, such as the casting process, cooling process and demolding process.

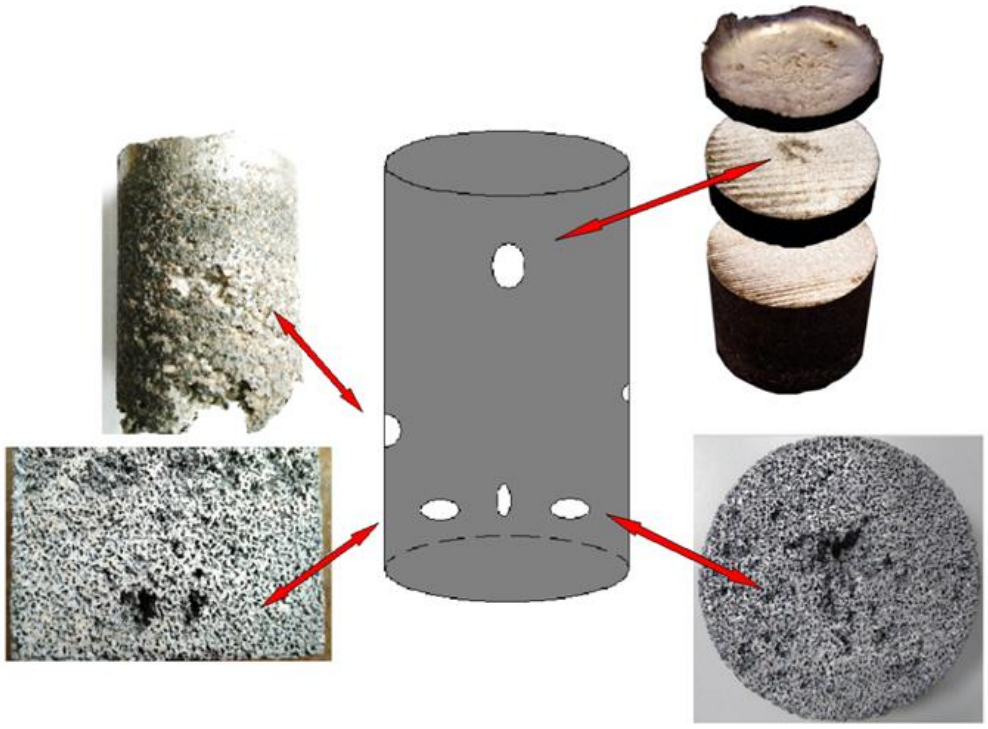

Figure 1.11 cavities in the sample of aluminum foam

Figure 1.11 shows the cavities in the sample of metal foam. These cavities are large in size, about 10-20mm. They greatly affected the quality of the sample.

These micro-cracks, cavities and other defects will have a significant impact on the properties of metal foams. Therefore, we should try to reduce the defects in the metal foam in order to obtain metal foams with great mechanical and thermal properties.

These parameters could not explain precisely the influence of structures on mechanical properties. Recently, some new researches in the literature (Brezny and Green, 1990; Chen and Lakes, 1995; Grenestedt and Bassinet, 2000) have presented the relationships between metal foam structures and their mechanical

and thermal properties but so far this field of research is far from complete and remains many important points to study.

1.3.2 Thermal properties and applications

Due to the deepening of the research, the mechanical properties of metal foam are no longer the only focus, the thermal properties and the acoustic properties of metal foams were studied. In the field of thermodynamics, that open-cell metal foams are promising materials for heat exchangers (Boomsma et al., 2003; Mellouli et al., 2009) because of their high internal surface areas and porous structures, which may contribute to the heat transfer process. Compared with traditional metal fins, metal foams have larger specific surface area and higher mechanical strength. This section describes the thermal properties of metal foams and their applications in the field thermodynamics.

Thermal properties

Thermal properties include the following thermal parameters: melting temperature, specific heat, coefficient of expansion, thermal conductivity, thermal diffusivity and thermal radiation ... etc.(Boomsma et al., 2003; Zhao and Wu, 2011). Thermal conductivity is the determining property of heat response in steady state; the thermal diffusivity determines the transient behavior. Figure 1.12 shows that aluminum foams have low thermal conductivities and that thermal diffusivities are relatively high. All aluminum foams with closed cells have almost the same value of thermal diffusivity α.

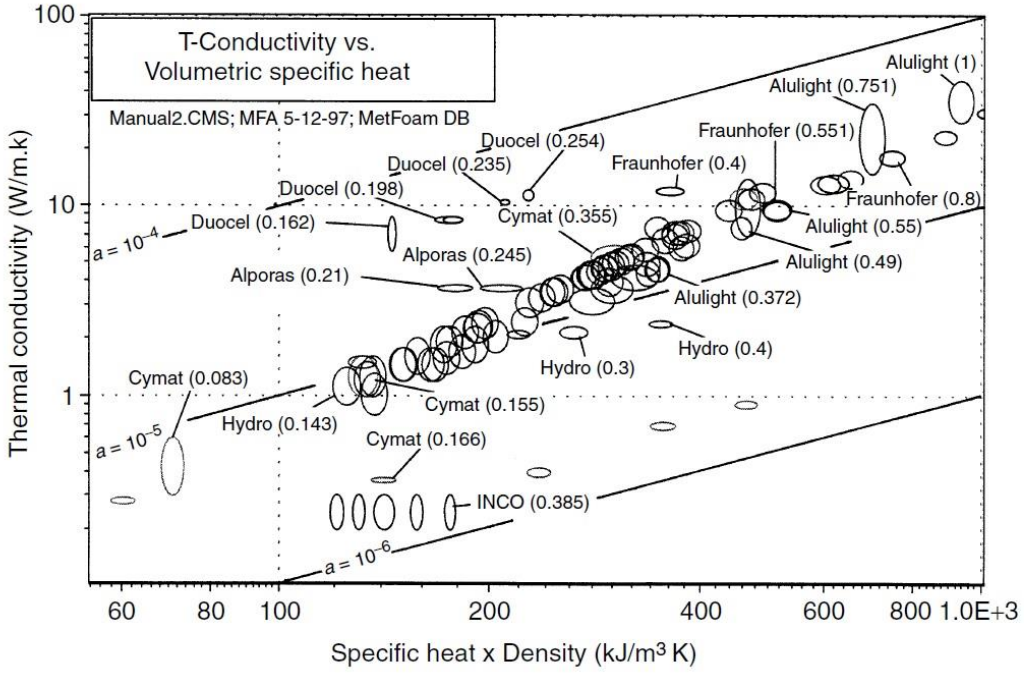

Figure 1.12 Thermal conduction according to the specific heat for different metal foams (Ashby et al., 2000)

Applications

The thermal conductivity of metal foams is higher than that of non-metal foams, for closed-cell metal foams, their thermal conductivity is lower than that of solid metal, so they could be use as fire protection materials. For open-cells metal foams, they can be used to improve heat transfer in applications such as heat exchangers for embedded equipment, compact heat sinks for electronic equipment, heat shields, air-cooled condenser towers and the regenerators (Antohe et al., 1996; Kaviany, 1985). We also have some remarks such as:

(1) If the porosity rate is high, leads to a low thermal conductivity;

(2) In open-cell metal foams, the interconnected cells have a large specific area. This characteristic makes it possible to be used as catalyst support, heat exchanger and energy absorber of mechanical shock.

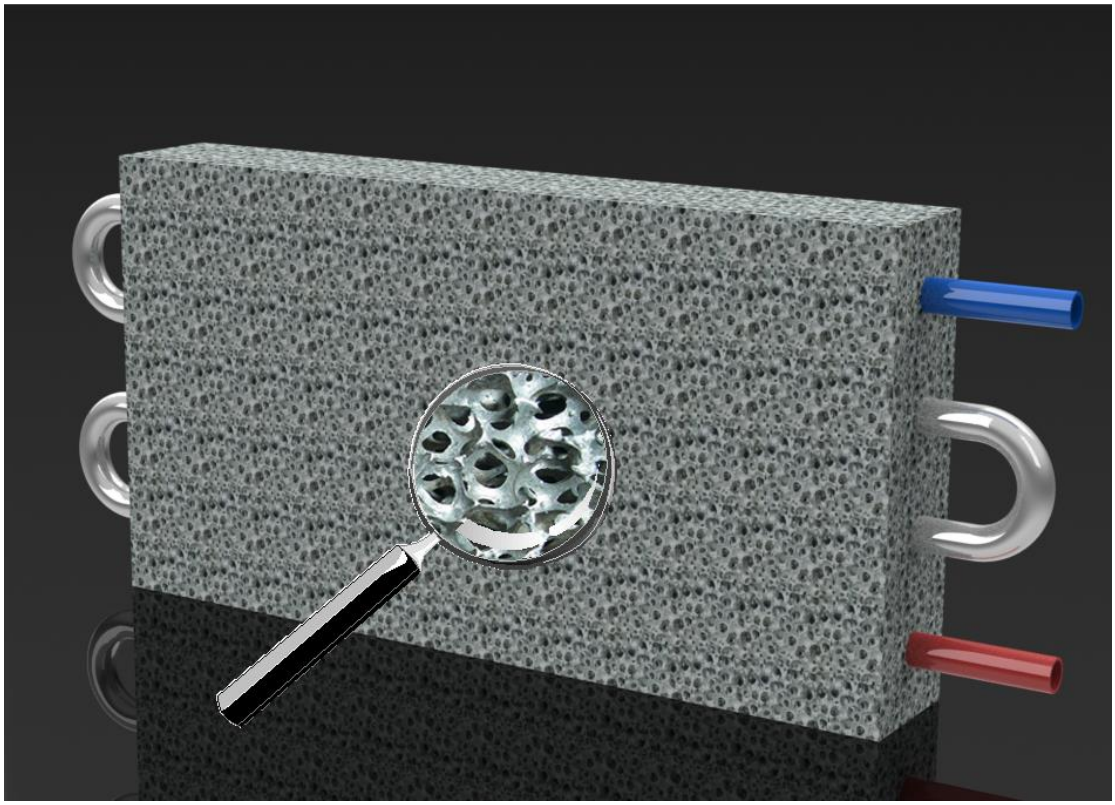

Figure 1.13 Heat exchanger element based on metal foam

Figure 1.13 shows a heat exchanger based on metal foam, the metal foams could enhance the performance of the heat exchanger thanks to their high specific surface area.

1.4 Phase change material

In recent years, with development the economic and social, the energy becomes the main focus of researches in every country. We should not only study new energy, but also study the energy storage and reuse in order to reach the purpose of saving energy. The phase change material becomes the promising material in the field of energy storage due to its thermal performance.

1.4.1 Various phase change materials

There are three main methods to store energy, sensible heat, latent heat and chemical energy. They are all used in different field according to their different thermal properties. Figure 1.14 shows the classification of energy storage material. In this figure, there are two types of PCM, the organics and the inorganics.

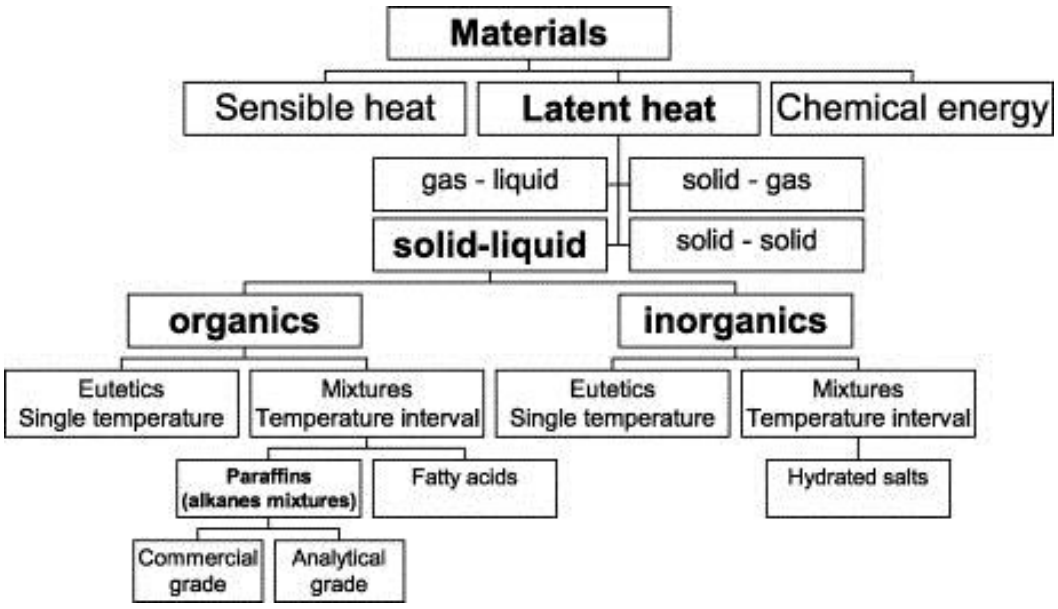

Figure 1.14 Classification of energy storage materials(Abhat, 1983)

Table 1-1 shows the comparison of thermal and physical properties between sensible heat storage materials (rock and water) and latent heat storage materials (organic and inorganic). By comparing the relative storage mass and the relative storage volume, the advantage of the latent heat storage materials is very clear. The latent heat storage materials could store same amount of energy with lighter weight and less volume.

Table 1-1 Comparison between the different methods of heat storage (Hasnain, 1998)

Property	Rock	Water	Organic PCM	Inorganic PCM
Density, kg/m^3	2240	1000	800	1600
Specific heat, kJ/kg	1.0	4.2	2.0	2.0
Latent heat, kJ/kg	–	–	190	230
Latent heat, kJ/m^3	–	–	152	368
Storage mass for 10^6 J, kg	67,000	16,000	5300	4350
Storage volume for 10^6 J, m^3	30	16	6.6	2.7
Relative storage mass	15	4	1.25	1.0
Relative storage volume	11	6	2.5	1.0

Figure 1.15 shows the basic principle process of energy storage in PCMs. When the temperature increases, the energy stored in PCMs is mainly the sensible heat. When the melting point is reached, the solid-liquid phase transition occurs in PCMs. In this step, the temperature increases much more slowly and the energy stored is mainly the latent heat. After PCMs are totally melted, the sensible heat becomes again the main form of energy storage. This energy storage process is repeatable and reversible. The PCMs always have a large value of latent heat,

which makes the PCMs could absorb or release a large amount of energy with a small temperature variation during the phase change process. Therefore, PCM could store large amounts of energy during the phase change process with small temperature variation, which brings great convenience to a variety of applications.

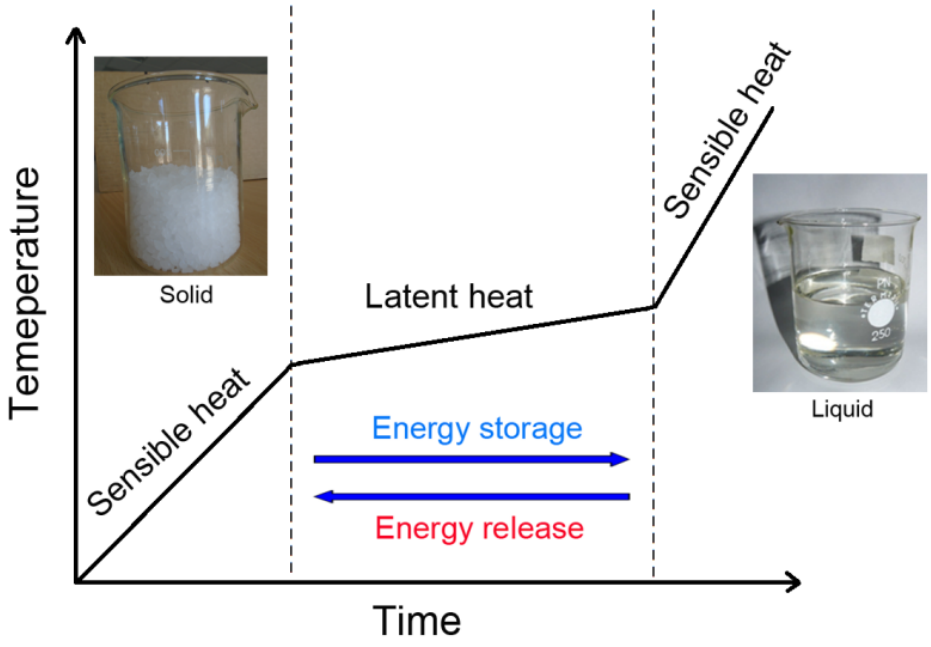

Figure 1.15 Principle process of energy storage and release of PCMs

1.4.2 Advantages and disadvantages of different PCMs

There are two main types of PCMs, the organic PCMs and the inorganic PCMs. The representative organic PCMs are paraffin, polyethylene glycol and fatty acid. For inorganic PCMs, the representative materials are $Na_2SO_4 \cdot 10H_2O$, $Na_2HPO_4 \cdot 12H_2O$ and $Na(CH_3COO) \cdot 3\ H_2O$. The advantages of organic PCMs are anti-corrosive, low undercooling, chemical stability and thermal stability.

However, they have also disadvantages, low latent heat, low thermal conductivity and inflammability. For inorganic PCMs, they have a larger latent heat than organic PCMs. But they have great disadvantages, undercooling, corrosion and phase separation, which largely limit their applications in the field of energy storage. The thermal stability of PCMs is very important, because the application environment is very complex.

There are some important properties of PCMs are necessary if they are used in the field of energy storage. They are described as following (Abhat, 1983): (1) the latent heat of PCMs should be as great as possible, and the temperature of phase change should be fitted to the application condition; (2) the variation of the volume before and after the phase change should be small; (3) their chemical properties should be stability, safety, nonflammable; (4) the phase separation should be avoided. According to these limits, it is seen that both types of PCM are not perfect, thus we should chose the suitable PCMs according to different application conditions.

Table 1-2 Advantages and disadvantages of the organic/inorganic PCMs

Type	Representation materials	Advantages	Disadvantages
Organic PCMs	Paraffin Polyethylene glycol Fatty acid	No corrosive; Low undercooling; Chemical and thermal stability	Low latent heat; Low thermal conductivity; Inflammability
Inorganic PCMs	$Na_2SO_4 \cdot 10H_2O$ $Na_2HPO_4 \cdot 12H_2O$ $Na(CH_3COO) \cdot 3\ H_2O$	Large latent heat	Undercooling; Corrosion; Phase separation;

1.5 Modeling of metal foam

The metal foam structures are inhomogeneous, their geometric profiles are very complex and the thermal and mechanical behavior shows a strong nonlinearity. It is important to model and simulate metal foams to predict their properties and give useful information in the production and application of this material. In recent years, much research has focused on the modeling and numerical simulation of metallic foams (Gibson and Ashby, 1999; Weaire et al., 1995; Weaire and Drenckhan, 2008).

Numerical modeling studies could be classified by scale of dimensions: microscopic, mesoscopic and macroscopic. The scale of the microscopic dimensions is represented by the size of the pore. We consider a single pore (or some pores) which is composed by walls, edges and nodes in order to obtain the structural relation with thermal and mechanical behavior. The property of the materials is thus obtained by the statistical method. The mathematical general equations are established on a pore and the experimental results allow us to validate these theoretical equations.

The mesoscopic scale is the scale between "micro" and "macro". The inhomogeneity of metal foams and the change in the pore are the points often studied by researchers.

The scale of the macroscopic dimensions is one hundred or one thousand times more than the size of a pore, for example the modeling on a whole specimen. Supposing the pores are homogeneous and continuous, mechanical behavior such

as elastic limit, plasticity, damage and rupture, are also widely studied in the literature (Deshpande and Fleck, 2000; Liu, 2007a).

The numerical simulation studies of metal foams could also be classified by their research aims: for the design of a structure using metal foams; for the elements of the metal foams are used in a complex structure. Manufacturers are more interested in manufacturing technology, the microscopic structure and the behavior of the use of foam. For these reasons, they prefer microscopic and mesoscopic modeling in order to better fit their needs and their demands.

Metal foams are an excellent functional material because they have a special microscopic structure. It is used in many fields such as radiators, filters and catalyst supports. Therefore, the modeling and simulation of heat transfer and fluid property are important. In recent years, some publications have presented the modeling of the process of foaming, in particular the fabrication by melted metallurgical method (Ma et al., 1999; Nieh et al., 1998).

1.5.1 Pore geometry models

The 2D is often applied for materials with the regular cell structure, such as hexagon cell. The 3D geometric modeling is used for porous materials of random shape. In the case, the pores are assumed to be ideal. Researchers have often used the models: spherical model (Andersen et al., 2000; Lim et al., 2002), cubic model (Lu et al., 1998), dodecahedral model (Bhattacharya et al., 2002) or tetrakaidecahedron model (Kelvin) as shown in Figure 1.16.

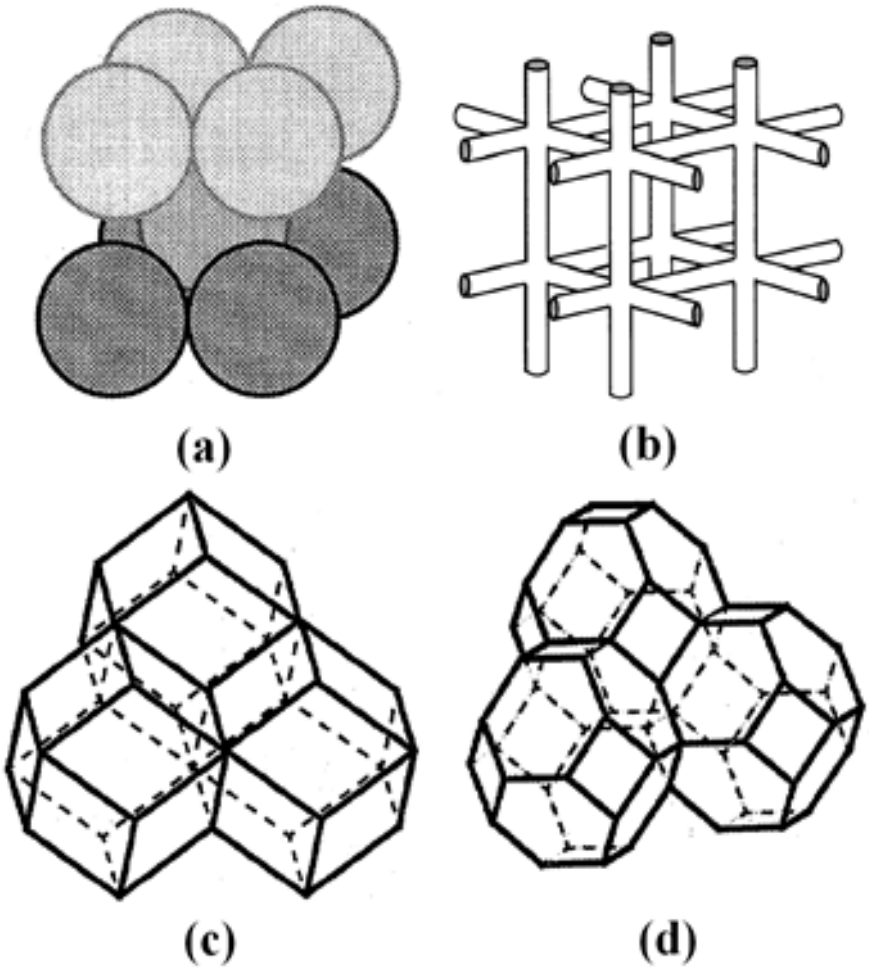

Figure 1.16 (a) spherical models; (b) cubic models; (c) dodecahedral models(d) tetrakaidecahedron (Kelvin) model

1.5.2 The advantage of the Tetrakaidecahedron model

The advantage of the tetrakaidecahedron model (Figure 1.17) is that it has an amount of faces and edges as much as the actual pore structure, and therefore closer to reality. It is widely used in numerical 3D foam modeling. The development of a tetrakaidecahedron model structure was done by Weaire and Phelan in 1994(Weaire and Phelan, 1994). They discovered a periodic unit of cells:

Voronoi (Figure 1.18). This Voronoi periodic unit contains: six polyhedras of 14 faces (including 12 pentagons + 2 hexagons) and two polyhedras of 12 pentagonal faces. They indicated that this model has the minimum of surface energy and closer to the real structure of metal foam pores.

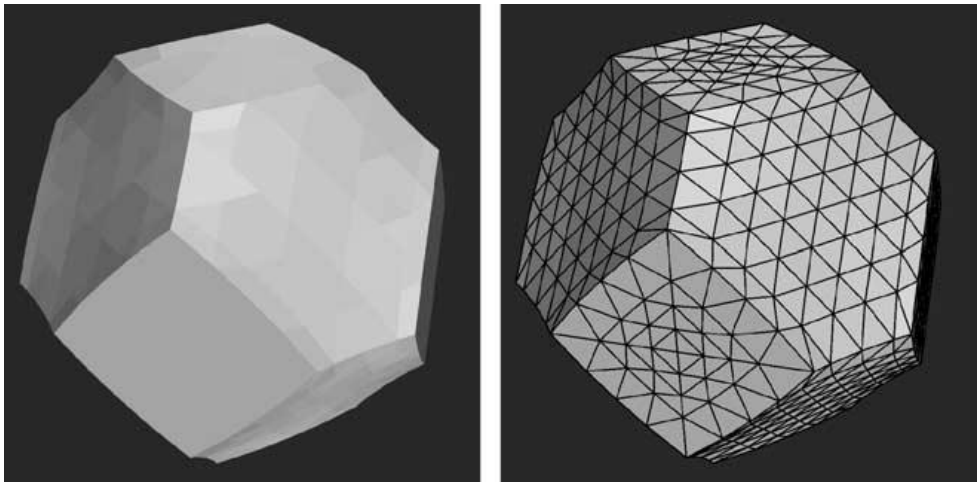

Figure 1.17 Tetrakaidecahedron model cell

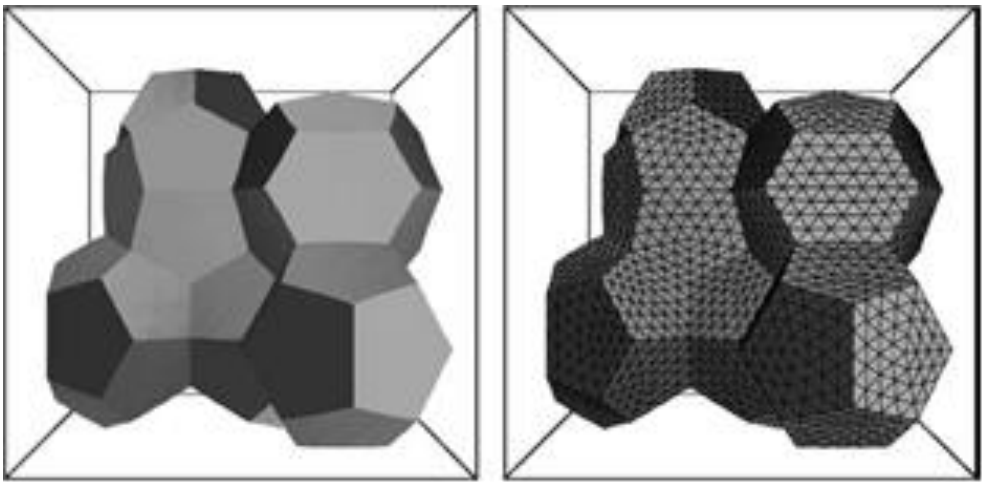

Figure 1.18 Periodic unit of eight tetrakaidecahedron cells

1.6 Technology of 3D printing

3D printing technology, also known as additive manufacturing or laminate manufacturing (Additive Manufacturing, AM), could refer any printing process of three-dimensional objects (Excell and Nathan, 2010). 3D printing is mainly a continuous process by adding material under computer control (Gibson et al., 2010). 3D printed objects could have any shape and geometric according different applications. 3D printers are a kind of industrial robots.

1.6.1 Main steps of 3D printing process

There are several steps in the 3D printing process (AM) in order to transfer a virtual CAD description to a real objet. This process is a complex and sophisticated process. The complexity of the whole process varies depending on the material, dimension, accuracy requirements and so on. The main steps of 3D printing process are shown in Figure 1.19.

Step 1: CAD

All AM objects should start from the geometric model. The professional CAD software is needed in order to output a 3D solid or surface model. A reverse engineering software (laser or optical scanning) could also be used in this step.

Step 2: STL file

Almost AM machines could accept the file format of STL, which becomes a standard in the field of AM. Nearly every professional CAD software could output a STL file, so this step becomes very simple.

Step 3: File transfer

The STL files must be transferred to the AM machines. This step involves the correct dimension, position and orientation of the models.

Step 4: AM machine setup

Several parameters need to be set correctly, such as the material constraints, energy source, layer thickness and timings.

Step 5: Build

The building of the parts is automate and controlled by the AM machine. We should observe the process to ensure no errors during the building.

Step 6: Removal

The objects should be removed after the step 5 from the AM machines. In this step, we should follow the rules of the AM machines.

Step 7: Post-processing

The extra material should be removed from the parts. For some materials and some special structures, the surface treatment, the cutting off, special cleaning and other operations are also needed.

Step 8: Application

Once the 3D printed productions are obtained, the quality check is required before the application. According different application conditions, the temperature, the humidity and other environment conditions should be suitable for the parts.

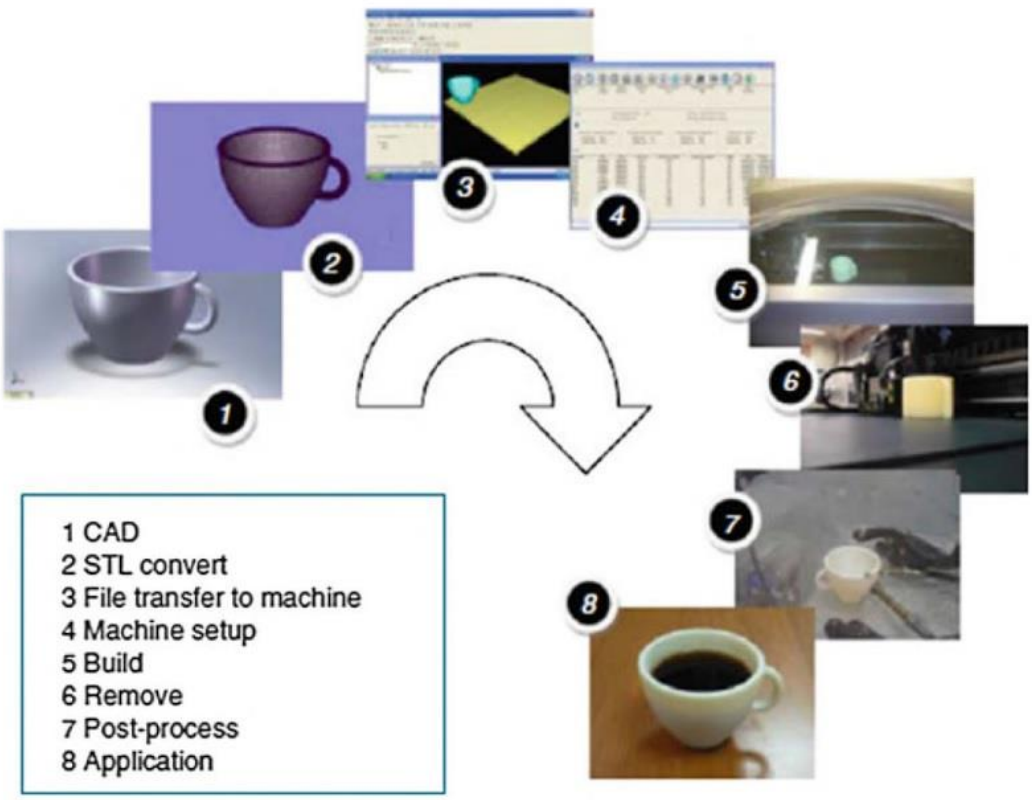

Figure 1.19 Main steps of 3D printing process(Gibson et al., 2014)

1.6.2 Various AM processes

In the early researches, AM process was used to produce plastic prototypes, and several AM processes (i.e., SLA, SLS, FDM) have been developed to make different parts with various plastics. After many developments and explorations, AM technology becomes more and more mature and common. The materials are no longer just plastics, the metals, ceramics, composites and other materials could

be also used in AM process. Table 2 lists the types of materials that can be processed by AM technology and the corresponding processes. The various AM technologies are widely investigated, such as Stereolithography (SLA) (Jacobs, 1992), Fused Deposition Modeling (FDM)(Comb et al., 1994), Selective Laser Sintering (SLS) (Beaman et al., 1997), Laminated Objective Manufacturing (LOM) (Mueller and Kochan, 1999), Three Dimensional Printing(3DP) (Sachs et al., 1993) and Laser Metal Deposition (LMD) (Mazumder et al., 1999).

Two representative technologies, the stereolithography and selective laser sintering technology, are presented as follow.

Stereolithography (SLA)

SLA is one of the most widely used AM technologies. This AM technology is usually used for liquid epoxy resin based photopolymer. Figure 1.20 shows the whole SLA process.

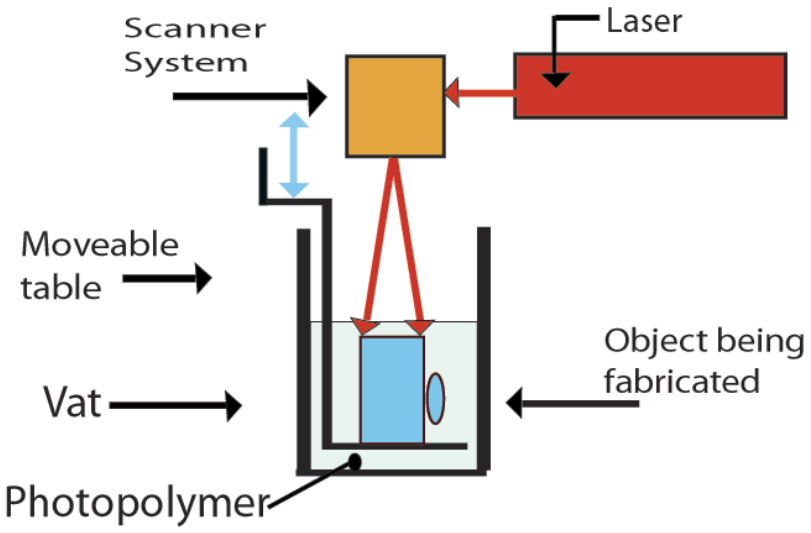

Figure 1.20 Stereolithography (SLA)

Selective Laser Sintering (SLS)

Selective Laser Sintering is an effective technology for durable and functional black or natural-colored parts. However, the surfaces are not enough smooth and the edges are not enough sharp. A laser beam is used to selectively fuse powder material into solid. Many materials could be used by this technology, such as nylon, thermal plastic elastomers and metals. Figure 1.21 shows the selective laser sintering (SLS) process.

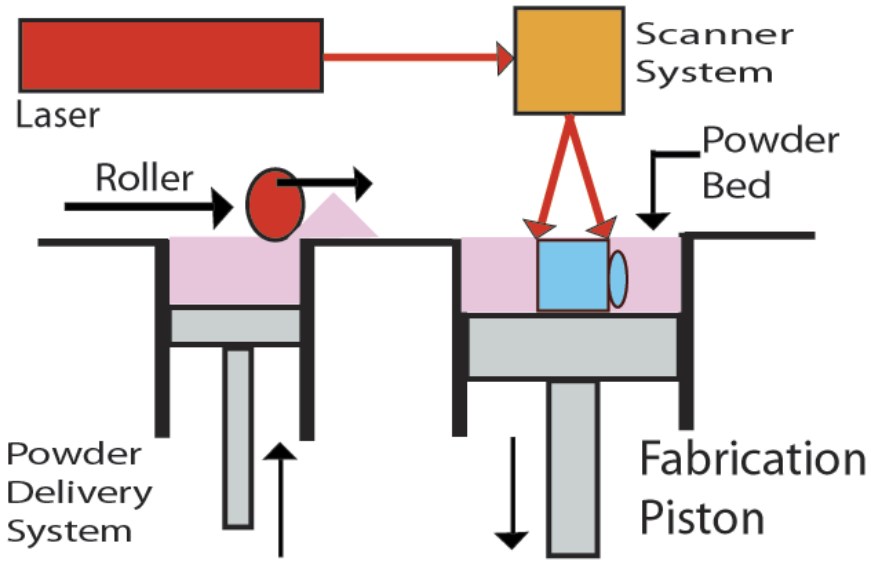

Figure 1.21 Selective Laser Sintering (SLS)

1.7 Conclusion

Metal foams are very interesting materials for energy storage applications. The bibliographical studies make it possible to highlight the research already carried out on the manufacturing methods, the microscopic structures of metal foams, the

mechanical and thermal properties and the AM technology, etc. After many years of manufacturing development, several manufacturing methods are already mature, which offers necessary experience for the improvement and upgrading. The numerical modeling of the porous structure makes the numerical simulations possible. Therefore, the comparison of porosities and structures could be achieved. The AM technology offers a possibility to obtain periodic aluminum foams with a designed structure.

Chapter 2 Manufacturing process of the aluminum foam

2.1 Introduction

In the second chapter, the preparation process of aluminum foams with the negative pressure infiltration method is presented. The advantages and disadvantages are analyzed. Thus the improvement and upgrading methods are proposed and achieved. After the improvement and upgrading, the properties of aluminum foams could be accurately controlled. The porosities of aluminum foams under different negative pressures are compared.

2.2 Traditional manufacturing process of the aluminum foam

The method used to prepare the aluminum foam in our research is called 'Infiltration casting method' or 'Negative pressure casting process'(Niu et al., 2000). This method is a traditional manufacturing method of open-cell metal foam based on gravity casting process(Rabiei and O'Neill, 2005; Vendra and Rabiei, 2007). It is often used to prepare the foam of Al, Mg, Zn, etc. Many advantages are offered by this method such as low cost, controllable pore size, simple process and great sample size. There are three principal steps in this method:

-Preparation of mold: a kind of soluble particles should be used as preform to prepare a mold. We chose salt particles as the soluble particles because of its low price, high melting point and controllable particle size. Certain size salt particles are filled in a steel tube to obtain this mold. The final procedure in this step is to heat the mold to keep the fluidity of the molten aluminum during the next step.

***-Infiltration**:* the molten aluminum is poured into the mold in order to fill the spaces between the salt particles. Due to the surface tension, the gravity is not enough to make the molten aluminum fill the entire mold; a negative pressure must be applied under the mold as soon as the molten aluminum is poured into the mold(Niu et al., 2000). The pressure difference between the upper and lower surface allows the molten aluminum to fill the entire mold. This step is shown in Figure 2.1.

***- Solidification**:* after the step of infiltration, the mixture of aluminum and salt is immersed in water during several hours until the salt particles are all dissolved. The sample of aluminum foam is finally obtained after the water remained in the sample evaporates. Then the sample can be cut into different dimensions for various experiments.

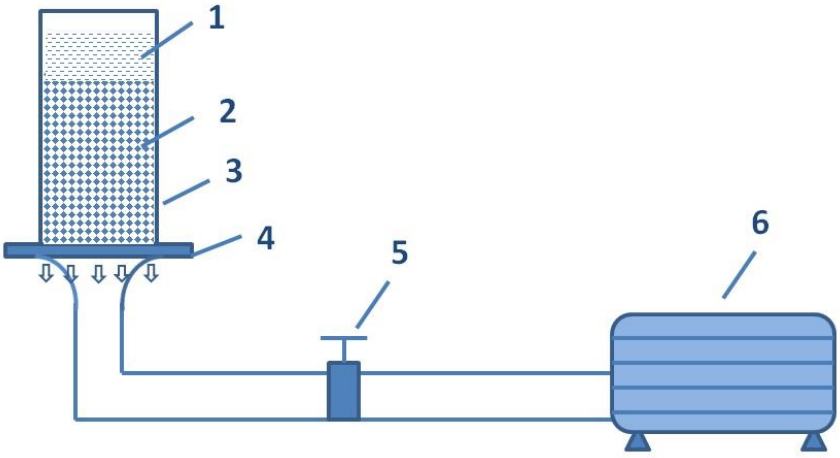

Figure 2.1 Schematic presentation of negative pressure casting process (1- Molten Aluminum, 2-Preform(salt particles), 3-Stainless steel mold, 4- Stainless steel cup, 5-Valve, 6- Vacuum pump)

2.2.1 Equipment of manufacturing

In the infiltration casting method, the foam structure of aluminum foam is based on the preform. The shape and size of the pores in aluminum foam are the copy of the particles. In order to control the shape and size of the cells in the aluminum foam, the soluble particles are grouped according to their diameters by a vibrating sieve. This vibrating sieving machine AS 200 basic Retsch® is composed of seven sieves of different sizes. It is therefore possible to separate the particles into seven different sizes according to the following diameters: 1.9, 1.6, 1.25, 1.0, 0.8, 0.58 and 0.365 mm.

After sieving, the particles of the same size are filled into a cylindrical stainless steel mold and slightly compacted to ensure a correct porosity. And then it is necessary to preheat the preform in order to avoid the solidification of aluminum at the beginning of infiltration. This process is realized by a chamber furnace, Labotherm N61/H of NabertherThe temperature rise during preheating must be relatively slow in order to prevent the particles from cracking or rupturing by the temperature. When a predefined temperature value is reached (620 °C), it must be maintained for at least one hour to ensure homogeneity within the preform.

The aluminum alloy is melted using a furnace, Nabertherm Labotherm K4 / 10. This furnace is characterized by its rapid temperature rise, by its bidirectional heating and its simplicity of using. Moreover, the rapid temperature rise could reduce the potential oxidation of the aluminum and thus preserves the quality of the aluminum.

Once the aluminum alloy is melted, the mold is placed over a suction stainless steel support. Then the liquid aluminum flows into the mold under the effect of negative pressure. This negative pressure is produced by a vacuum pump, controlled by a valve.

Due to the high corrosion of the salt, the mold is made of stainless steel, and its melting point (about 1500 °C) is much higher than that of aluminum (about 615 °C).

2.2.2 Materials and their physical properties

The choice of particles takes into account the following factors: the particles must be soluble in water, economical, and a higher melting point than that of aluminum alloy. In addition, this material should not have compatibility problem with aluminum such as chemical reaction, and these particles should not be too expensive. In this research, the salt particles were chosen as a preform whose properties are shown in Table 2-1.

Table 2-1 Properties of salt particles

ρ (25℃) [10^3kg/m^3]	ρ (600℃) [10^3kg/m^3]	Température de fusion [°C]	Conductivité thermique (600 ℃) [W/(m°C))]	Chaleur spécifique (600 ℃) [J/(kg°C)]	Coef. d'expansion thermique (-50 à 200 °C) [10^6K^{-1}]
2,165	2,158	801	4,6	1030	44

For aluminum foams, the main characteristic depends on the porous structure. In principle, there is no particular requirement for the chosen metal. Therefore, it was the mechanical properties of the metal and the cost price that guided our choice of material. In this study, the aluminum alloy AS7G was selected as the base metal. Physical and mechanical properties of AS7G are summarized in Table 2-2.

Table 2-2 Physical and mechanical properties of aluminum alloy AS7G

ρ solide (10^3kg/m^3)	ρ liquide (10^3kg/m^3)	Coef. de la dilatation α (10^{-6} /°C)	Chaleur spécifique [J/(kg) • °C)]	Température de solidification (°C)	Température de fusion (°C)
2,68	2,38	21,5	879	555	615
Contrainte d'élasticité (MPa)	Déformation à la rupture (%)	Module D'Yong (GPa)	Contrainte à la rupture (MPa)(traction)	Coef. de Poisson	Coef. d'expansion thermique (10^6K^{-1}) (20 à 100 °C)
165	2	70	140	0,33	23

2.2.3 Problems in traditional manufacturing method

During the fabrication of aluminum foam with traditional method, we found several problems, such as the seal of equipment, stability of negative pressure, the adjustability of negative pressure and so on. These problems are caused by many reasons.

-Seal of equipment: after many years of use, many air leakage points appear in the iron pipe joints. Since salt is used to make foam aluminum, salt corrosion reduces the seal of the system.

-Stability of negative pressure: the volume of pipe is not big enough to provide a stable negative pressure. At the beginning of the application of negative pressure, the negative pressure value is the preset value, but the negative pressure value continues to weaken with the negative pressure in the tube is released.

- Adjustability of negative pressure: because of the two above problems, the adjustability of negative pressure cannot be accurate enough during the infiltration. The negative pressure can only reach –0.8atm.

All the above problems need to be resolved in order to achieve a better performance of the system.

2.3 Improvement and upgrading of manufacturing process of the aluminum foam

2.3.1 Improvement and upgrading of experimental equipment

According to the experimental requirements and the above mentioned problems, we have several solutions to choose. The best solution is the improvement and upgrading base on the existed equipment.

The optimized equipment is shown in Figure 2.2. Compared to the old equipment, a grand vacuum tank, a manometer and a extra valve are added in the optimized equipment. These improvements are described below.

- Vacuum tank: a vacuum tank is connected to the vacuum pump and the mold in order to store negative pressure. The volume of the vacuum tank is about forty times more than the volume of the mold. A sufficiently large volume allows the negative pressure to maintain a steady state during pressure release.

- Manometer: In order to obtain an accurate pressure output value, we need to monitor the pressure in the tank. A manometer is added to the vacuum tank, its range is from 0 to −0.1Mpa. Its measurement accuracy is 0.002 MPa.

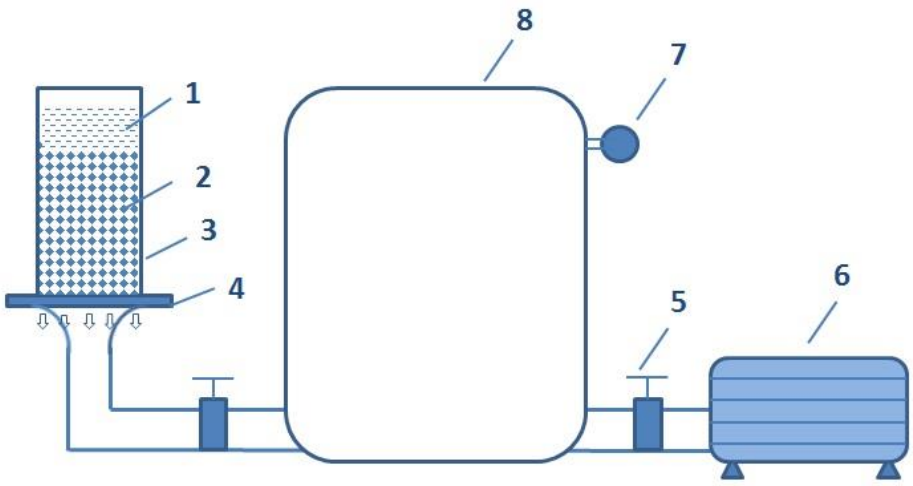

Figure 2.2 Schematic presentation of optimized equipment (1- Molten Aluminum, 2- Preform(salt particles), 3-Stainless steel mold, 4- Stainless steel cup, 5- Valve, 6- Vacuum pump, 7 - Manometer, 8- Vacuum tank)

-Valve: the second valve is added to the experimental equipment to control the opening and closure between the vacuum pump and the vacuum tank. This valve is opened when the vacuum pump is working, and it is closed when the negetive pressure reaches the preset value.

Beside the additions of vaccum tank, manometer and valve, other upgrades are also achieved: all the joints of pipe are sealed with silicone, and a seal verification was done. When the mold is placed on the platform,

2.3.2 Foam aluminium structure control

With this manufacturing method, the arrangement irregularity of the particles results from the stacking technique, therefore it is difficult to define the arrangement of the pores. Since the shape of the particles and the stacking technique are invariant in our study, the influence of the shape and the stacking of the particles on their mechanical and thermal behaviors can be considered as invariable and therefore they are not taken into account in our consideration. Thus the adjustable parameters of the elaboration are the pore size and the porosity of aluminum foam.

During the preparation, the following parameters directly influence the quality of the foams: temperature, pressing time, preheating, geometry and preparation of the mold, negative pressure etc.

1. Control of the pore size

During the casting process, the molten aluminum is filled into the space which is left by the salt particles. Therefore the shape and size of the cells duplicate those of the particles. After the solidification process, the aluminum contracts so that the volume and diameter of the cells increase. Then, once the soluble particles are dissolved in water, the pores form and take the form of the particles. Thus, in order

to simplify the approach, the diameter of the pores will be considered as equal to that of the particles.

2. Control of the porosity

According the process of manufacturing, the volume of pore could be divided into three parts.

1) The biggest part is the volume of the particles, called 'volume of preform V_p'.

2) The second part is called 'additional volume V_a', it is formed due to the surface tension of the liquid aluminum.

3) The third volume is called 'volume of shrinkage V_s', it is formed due to the shrinkage of aluminum during the solidification.

In the end, we obtain the volume of pores by the following relation, as shown in Figure 2.3.

$$V = V_p + V_a + V_s \tag{2-1}$$

The porosity P_{pore} is directly deduced from this volume:

$$P_{pore} = (V_p + V_a + V_s)/V_{Total} \tag{2-2}$$

V_{Total} is the volume of each salt particle which is shown in Figure 2.3.

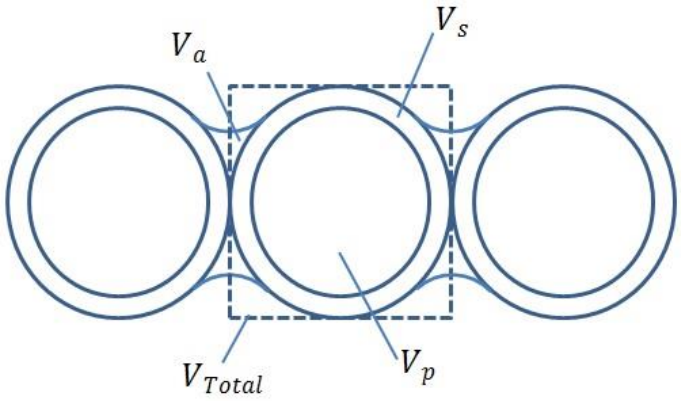

Figure 2.3 Description of the different volumes

The mechanical and thermal behavior of aluminum foam depends largely to its porosity. It can be controlled by adjusting the stack of the particles in the mold and by changing the negative pressure etc. According to other researches about the stack of the salt particles (He, 2004; Liu, 2007b; Wang, 2010), it is known that the arrangement of salt particles could largely influents the porosity of aluminum foam, such as the time of vibration of salt particles.

Due to the improvement and upgrading of manufacturing process of the aluminum foam, we focus on the influence of negative pressure to the porosity of aluminum foam.

In order to study and analyze the effect of negative pressure to the porosity of aluminum foam, the infiltration process must be firstly studied. The infiltration process of molten aluminum through the stacked salt particles is a complex process because it involves multi-phase flow (including air and liquid) in porous media. In addition, the infiltration process may also be affected by several factors:

preform size, temperature, pressure and surface tension. Until now, the infiltration process with common conditions could be well explained (Masur et al., 1989; Mortensen et al., 1989; Mortensen and Wong, 1990). These research works are mainly based on the capillary law and Darcy's law, which are two useful and important theories of the infiltration process. The detail discussions of these two laws are following.

Capillary law

During the infiltration process, the liquid aluminum is non-wetting for the salt particles, so there will be a force F (shown in Figure 2.4) this force is caused by the surface tension. This force F prevents the liquid aluminum from filling into the void space by gravity, as shown in Figure 2.4.

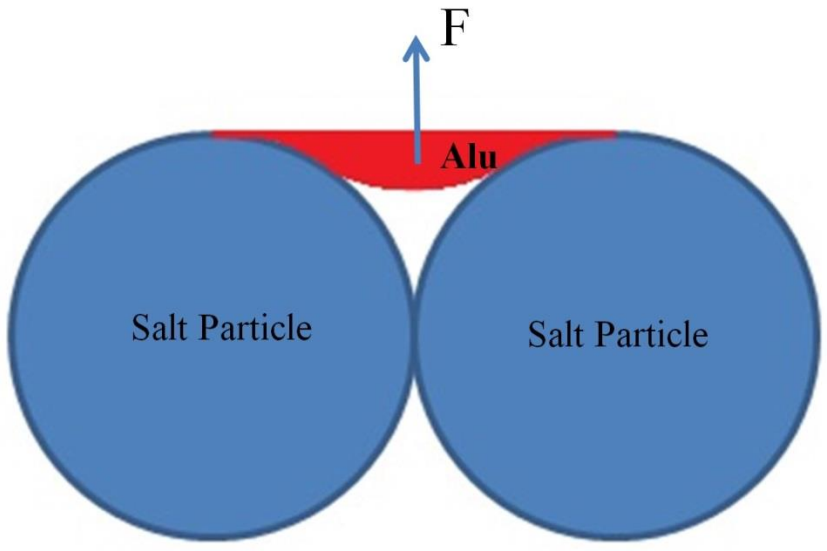

Figure 2.4 Schematic of the non-wetting phenomenon between liquid aluminum and salt particles

Therefore, in order to overcome the surface tension of liquid aluminum, a minimum pressure which is called the threshold pressure (P_0) should be obtained. This threshold pressure P_0 is determined by Garcia et al. (Garcia-Cordovilla et al., 1999). If the preform particles are approximated as spheres, the threshold pressure is shown as follows:

$$P_0 = 6\gamma \cos\theta \frac{V_p}{D\left(1-V_p\right)} \qquad (2\text{-}3)$$

Where, γ is the surface tension of liquid aluminum; θ is called the contact angel at liquid and solid interface; V_p is the particle volume; D is the average diameter of salt particles.

Before the infiltration process, the threshold pressure should be estimated firstly, and the negative pressure which is applied during the infiltration process should be larger than this threshold pressure. For our experiment, we found that the value of V_p has no relationship to the particle size, and this value is always about 0.52 without vibration and compaction. If *Vp* is always a constant value, the threshold pressure is the function of pore size. The value of surface tension γ and value of contact angel could be found in other researches, they are 0.85 N m-1 (Goicoechea et al., 1992) and 152 ° (Berchem et al., 2002), respectively. The results of P_0 are shown in Figure 2.5 (Zhu, 2017). It is observed that the threshold pressure reduces as the increase of the salt particle size. Thus, for the small particle, a large negative pressure should be applied to make the liquid aluminum penetrate into the void of salt particles.

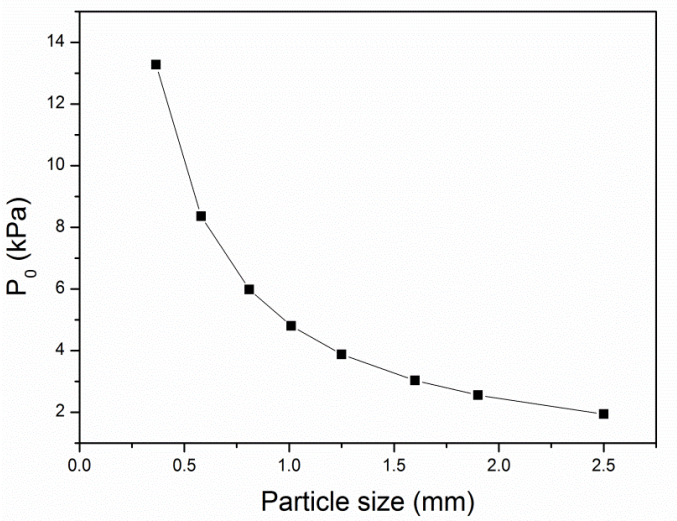

Figure 2.5 Threshold pressure (P_0) as the function of the salt particle size

Darcy's Law

In order to describe the relationship between pressure drop and velocity during the infiltration process in the porous media, the Darcy's law is always used. But the classical form of Darcy ś law, as shown in equation (2-4), should be deduced in the condition that the porous zone is full filled by liquid.

$$u = \frac{K}{\mu}(-\frac{dP}{dx}) \tag{2-4}$$

Where, u is the velocity; μ is the viscosity; P is the pressure; K is the permeability. In fact, the infiltration process could be seen as the process that the liquid aluminum takes the position of air in the porous zone. The movement of two-phase flow in the preform is essential for the infiltration process. Because of the non-wetting phenomenon and the surface tension of liquid, the void space could not be filled totally by liquid. In order to study and analyze the infiltration process

of the non-saturated flow, the relative permeability is presented in the Darcy ́s law(Molina et al., 2005) and the new equation is obtained, it is called Extended Darcy's law, shown in equation (2-5).

$$\mathbf{v} = -\frac{K_s K_r}{\mu} \nabla P \tag{2-5}$$

where, K_s is the permeability of a specific preform and it is also a physical property of material; K_r is the relative permeability. The relative permeability is a value between 0 and 1, and it depends on the saturation of two flows. The relationship between relative permeability and saturation could be expressed by equation (2-6).

$$K_r = As^B \tag{2-6}$$

where, A and B are constants and s is the value of saturation which is equal to the ratio of the liquid volume to the void space of preform. The infiltration process of metal-matrix composite was studied by T. Dopler et.al (Dopler et al., 2000) and they found that the numerical results have the best agreement with experimental ones when the values of A and B equal to 1. In addition, for the saturation, S.Y, HE (He, 2004) considered the surface tension of the liquid aluminum will prevent the liquid from filling all the void space. He established a model which could be used to calculate the volume of air, as presented in Figure 2.6 Geometry model of the air position between two particles. Finally, he found that the air fraction depends on two values, the particle size (d_s) and negative pressure (P).

$$V_{air} = \int_0^a \pi(kY^2 + d)^2 dY - \int_0^a \pi\left[R^2 - (Y-R)^2\right] dY \tag{2-7}$$

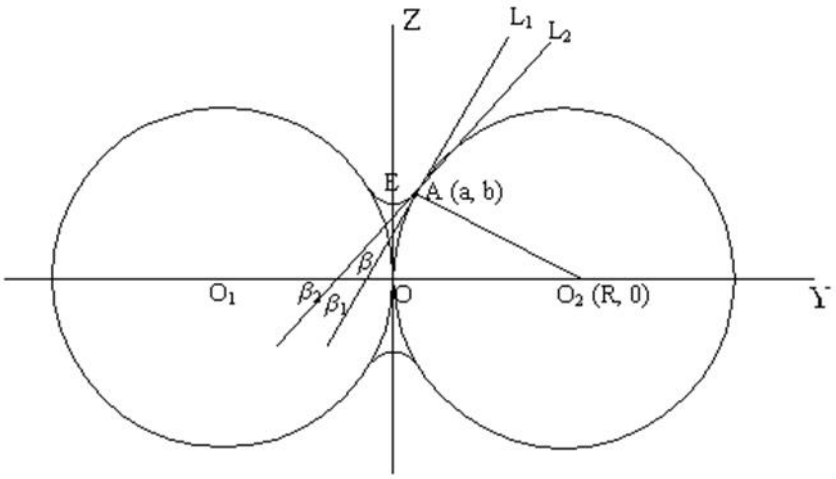

Figure 2.6 Geometry model of the air position between two particles

On the basis of other researches and theories above, we found more phenomena from our experiments, such as the effect of turbulent flow, the capillary phenomenon on the lower surface, non-uniform pressure distribution etc. These effects and phenomena will be discussed as follow.

Effects of turbulent flow

First of all, the Reynolds number (R_e) needs to be determined in order to define the flow of liquid aluminum is turbulent flow regimes or not. The equation of Reynolds number is defined as:

$$R_e = \frac{\rho v D}{\mu} \tag{2-8}$$

Where, ρ is the density of the fluid, v is a characteristic velocity of the fluid with respect to the object, D is a characteristic linear dimension and μ is the dynamic viscosity of the fluid. However, for the Reynolds number of flow in porous media should be expressed as:

$$R_{ep} = \frac{\rho v d}{\mu} \tag{2-9}$$

Where, the d replaces the D in equation (2-8), it is the average dimension of voids among the salt particles in this research.

In order to define the velocity of the flow (v), the permeability should be calculated according to the equation:

$$K = \frac{d_p^2 \varepsilon^3}{150(1-\varepsilon)} \tag{2-10}$$

Where, d_p is the average diameter of particle and ε is the porosity of packed bed. It is found that this correlation could be applied in the low porosity metal foam. Since the permeability K is obtained, the velocity (v) could be calculated according to equation (2-5).

It is well known that the flows of high-velocity in porous zones generate turbulence in the pores when the pore-Reynolds (R_{ep}) number is greater than 300 (Alvarez et al., 2003), which is much smaller than the limit value of R_e=2000. Two main differences between flow in porous zones and turbulent of free-stream flow are the dimension of eddies is limited by the size of pores and the additional

force effects which are caused by viscous and form of the porous solid matrix. In our research, the R_{ep} of our aluminum foam sample is about 2000 which is much greater than the limit value, 300. So it could be confirmed that the flow of liquid aluminum through porous media is turbulent flow.

The infiltration process is a very fast process, the velocity of flow could reach 0.82m/s and the pore-Reynolds reaches 2000, so there must be swirls and holes in the process of infiltration. Marcos H et al. (Marcos H. J. Pedras, 2001) simulated the flow in porous media and obtained the vector plots for different porosities, as shown in Figure 2.7(Marcos H. J. Pedras, 2001). From this simulation, it is obviously that a number of swirls are produced in porous media, and the air will be left into the liquid aluminum due to these swirls. It can be seen that these swirls are bigger if the porous size is smaller. The porous size of our samples is much smaller than that of the Figure 2.7(c) (the porous size of our samples is 2mm and the porous size of Figure 2.7(c) is 30mm), the arrangement is more compact and the shape of pores is more complicated. Therefore, the swirls in liquid aluminum during the infiltration process are more complicated and countless.

According to equation (2-5) and (2-9), when the pressure applied is greater, the velocity of flow is greater and the pores-Reynolds number is increased. If the pores-Reynolds number is increased, the turbulent kinetic energy is also increased, as shown in Figure 2.8 (Kuwahara et al., 2006). Finally, it can be concluded that the turbulent kinetic energy increases with the increase of negative pressure.

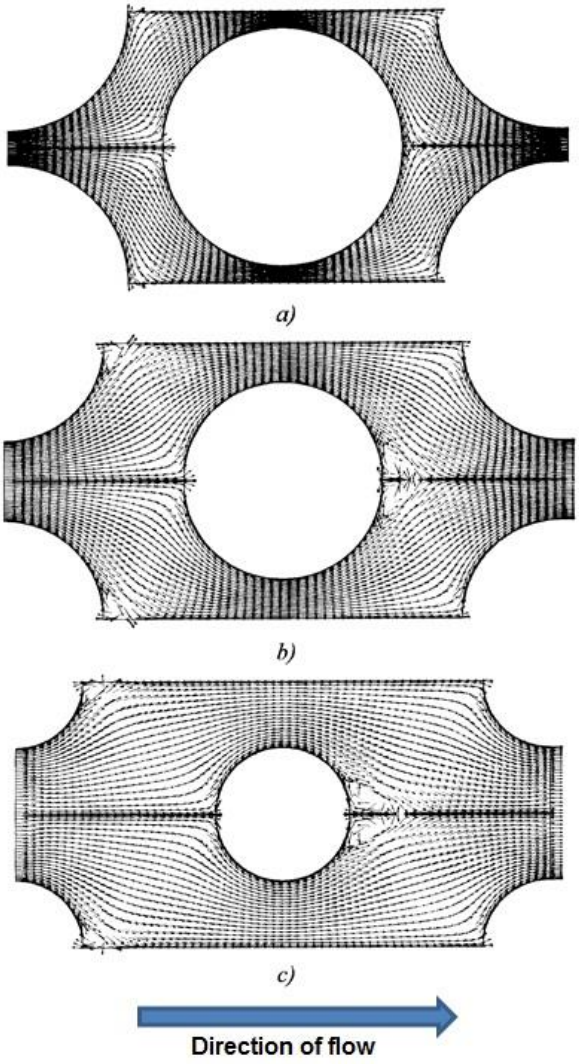

Figure 2.7 Vector plots, (a) ε=0.4; (b) ε=0.6; (c) ε=0.8

These strong swirls will keep more air in liquid aluminum, and the most of air remains under the salt particles, that is to say, a greater negative pressure will keep more air in the behind of the salt particles.

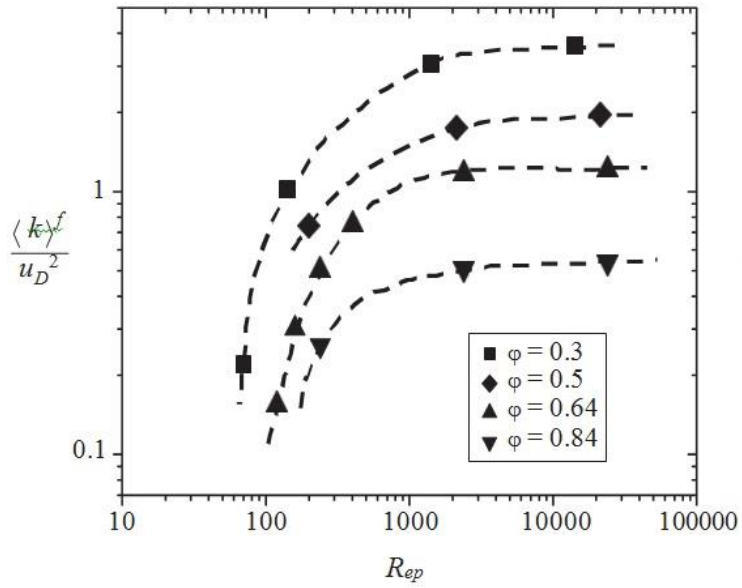

Figure 2.8 Macroscopic turbulent kinetic energy

Effects of non-uniform pressure distribution

Due to the complex structure of salt particles preform, the pressure during the infiltration process is not uniform. Marcos H et al. (Marcos H. J. Pedras, 2001) simulated also the pressure distribution of the flow in porous media for different porosities, as shown in Figure 2.9. From the contours of pressure distribution, it is obvious that the pressure in small voids is much higher than the left and right sides of salt particles, and the pressure of left side is higher than the right side, it means that the side facing to the liquid flow bears a greater pressure than the other side. Therefore, the liquid aluminum in the small voids is affected by several forces, such as gravity, surface tension and the force caused by high-speed liquid flow. The force analysis diagram of liquid aluminum in small voids is shown in Figure 2.10. This diagram is modified based on Figure 2.4, the gravity and the forces of flow are considered. For the molten aluminum on the top, F_1 is the surface tension

and F_2 is the resultant force of all downward forces (gravity and force of flow), because of the volume of liquid aluminum entering the voids becomes larger, which is shown by dashed lines in Figure 2.10. For the molten aluminum on the bottom, F_3 is the force of flow and F_4 is the resultant force of all downward forces (gravity and surface tension). F_3 is much smaller than F_2 and F_4 is much greater than F_1, so the upper liquid volume is much greater than the lower volume.

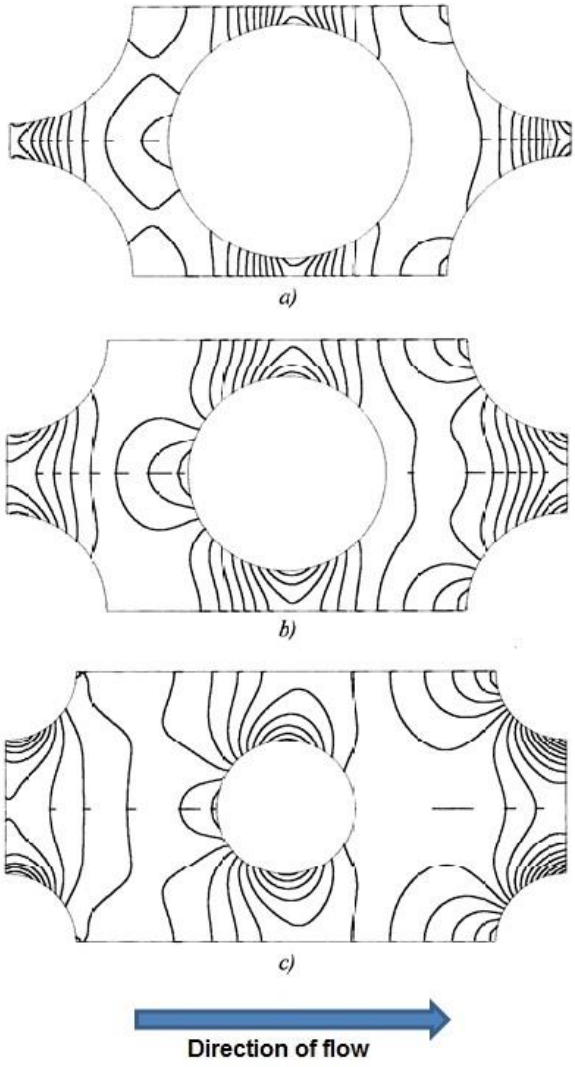

Figure 2.9 Pressure contours (a) ε=0.4; (b) ε=0.6; (c) ε=0.8

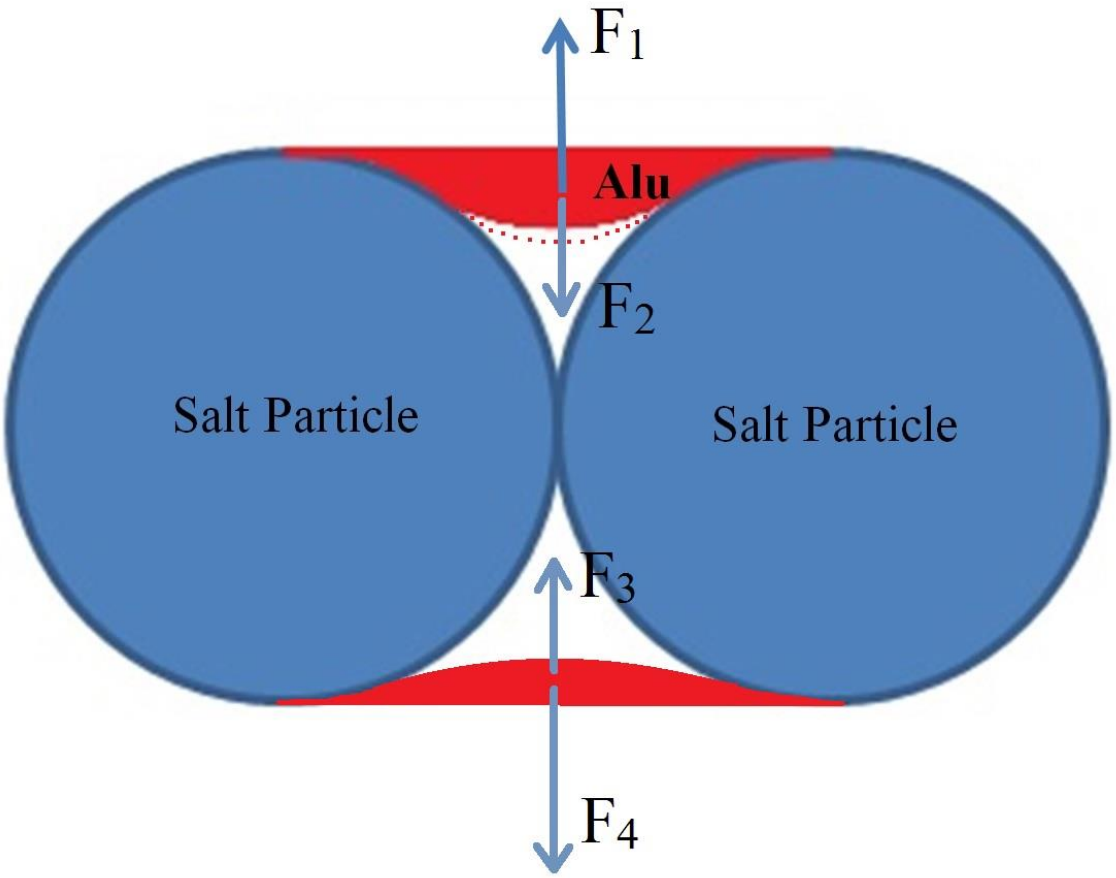

Figure 2.10 Force analysis diagram of liquid aluminum in small voids

According to all above effects, there is no doubt that the air will be left under salt particles. A simulation of liquid aluminum movement during its flow around particles (Wang, 2010) could be a good explanation. In Figure 2.11, the red part represents the liquid aluminum, and the blue part represents the air. It is obvious that the air is left under the salt particles even at the end of the process.

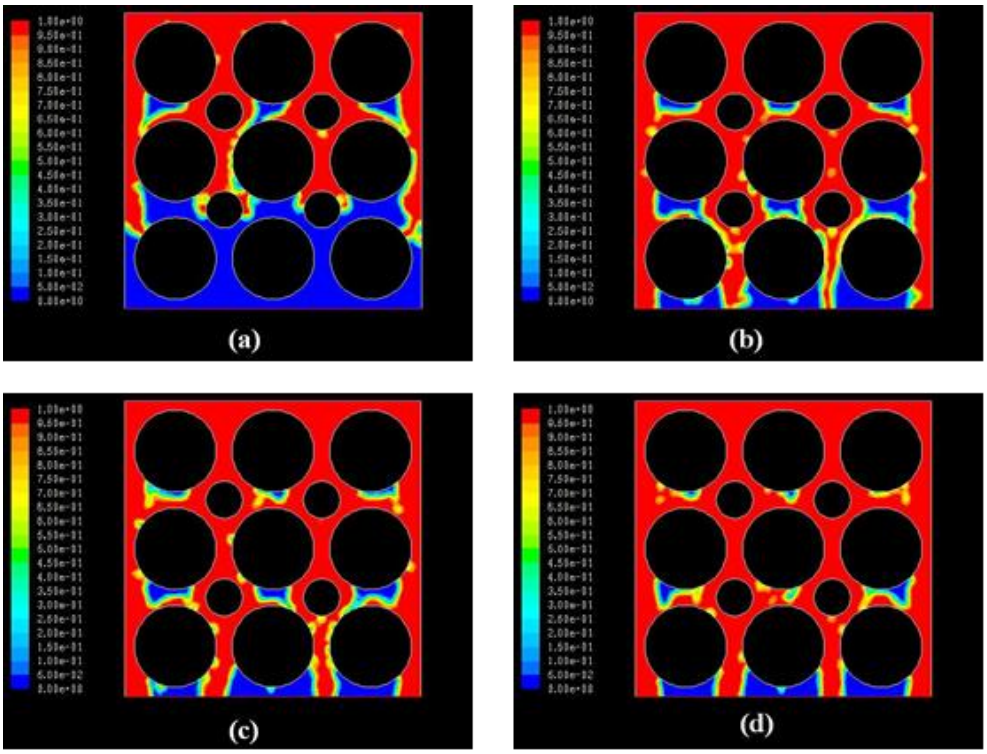

Figure 2.11 Liquid aluminum movement during its flow around particles; (a) temps=0,005 s ; (b) temps=0,01 s ; (c) temps=0,02 s ; (d) temps=0,05 s

2.3.3 Experimental results of aluminum foam manufactured under different negative pressures

In order to study the effect of negative pressure to the porosity of aluminum foam, several samples are manufactured under different negative pressures. Four different negative pressures are applied for comparison, the pressures are set at -0.03MPa, -0.05MPa, -0.07MPa, -0.09MPa. Thanks to the optimized and upgraded manufacturing process of the aluminum foam, the negative pressures are very stable and fluctuate in a very small range (-0.002MPa). For each negative pressure, five cube samples are obtained to be measured, and their dimensions are

20*20*20mm. In order to ensure the comparability of the experimental results, the positions of cube samples of each negative pressure in the cylindrical samples are the same.

In order to better observe the relationship between negative pressure and porosity of aluminum foam, we choose the salt particles as big as possible. Therefore, the size of salt particles for this comparison is 2mm.

The porosity of aluminum foam manufactured under different negative pressures is shown in Figure 2.12. From Figure 2.12, it is obvious that the porosity of aluminum foam decreases as the negative pressure decreases. The experimental results are consistent well with the previous theoretical explanation.

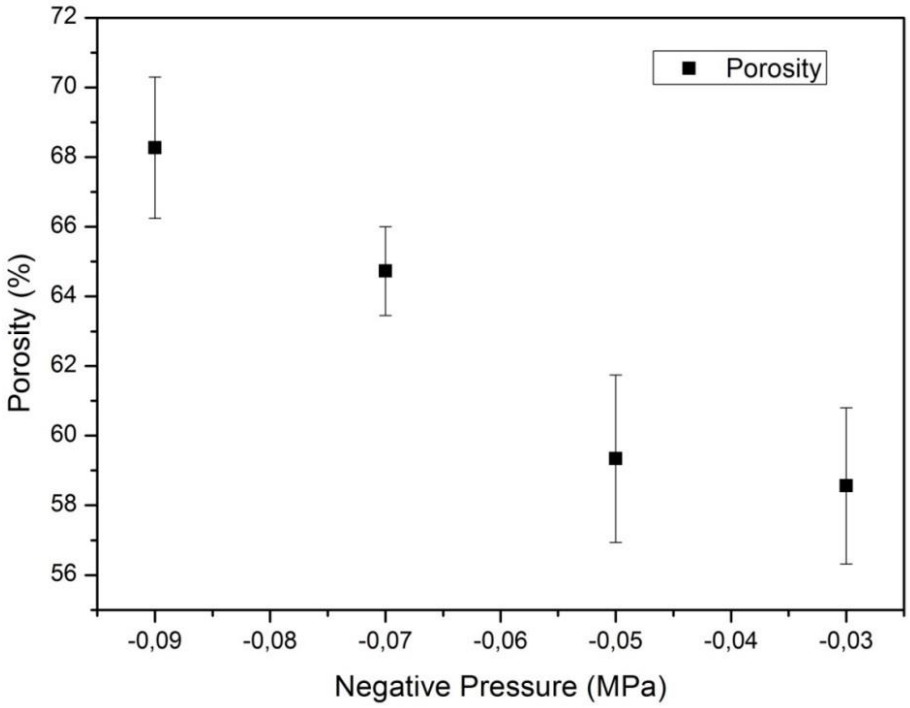

Figure 2.12 Porosity of aluminum foam manufactured under different negative pressures

The porosity of metal foam could be controlled by changing the negative pressure in order to meet different applications. There is no vibration for the preform of salt particles used in this comparison, so the porosity could be further increased. According the experimental results of J. WANG (Wang, 2010), the best vibration time is about 20 minutes.

On the basis of the first experiment, we did the second experiment with the vibration process of preform. In this experiment, the vibration time is set at 20 minutes. The number and size of the test samples and other parameters are the

same as the previous experiment. The results of metal foam porosity manufactured under different negative pressure with vibration are shown in Figure 2.13.

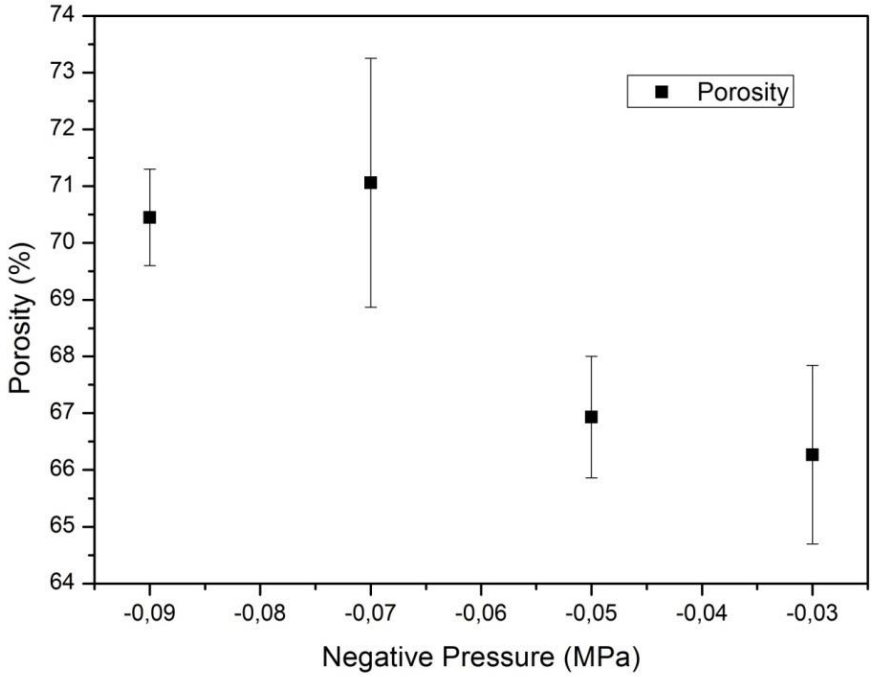

Figure 2.13 Metal foam porosity manufactured under different negative pressure with vibration

It can be seen from Figure 2.13 that the general trend of aluminum foam porosity is still reduced with the decrease of negative pressure, just as the previous experimental results. After the vibration of preform, the porosity of aluminum foam with different negative pressure was increased by about 6%.

2.4 Conclusion

The improvement and upgrading of the traditional manufacturing method are proposed and achieved. After the improvement and upgrading methods, the value of the negative pressure which is applied during the manufacturing process is steady and accurately controlled. The results show that the value of the negative pressure affects the porosities of the aluminum foam simples.

The porosities of aluminum foams under different negative pressures are compared. The porosity of aluminum foam decreases as the negative pressure decreases. The experimental results are consistent well with the previous theoretical explanation.

After the vibration of the preform, the experimental results show that the general trend of aluminum foam porosity is still reduced with the decrease of the negative pressure, just as the experimental results without vibration. The porosity of aluminum foam with different negative pressure was increased by about 6%.

After the improvement and upgrading, the porosity of aluminum foams could be controlled within a certain range by adjusting the negative pressure and vibration. The aluminum foams with different porosities could benefit different application conditions, which greatly expands the application domains.

Chapter 3 Experimental and numerical investigation of thermal performance of LPAF/PCM and HPAF/PCM composite

3.1 Introduction

Phase change materials (PCMs) can be widely used in many thermal management systems and thermal energy storage systems due to their large latent heat. However, PCMs always suffer from the low thermal conductivities, which reduce greatly the energy storage and release efficiency. In order to solve this problem, many researchers have added many kinds of high thermal conductivity materials in PCMs to improve the energy transfer efficiency of systems, such as metal fins, metal meshes and metal foam structures. Among these materials, open-cell metal foams have been widely investigated because of its high surface area to volume ratio which can greatly increase the energy storage efficiency. So far, the researchers focused often on high porosity metal foams (Baby and Balaji, 2013b; Sundarram and Li, 2014). However, the low mechanical properties of these metal foams can't satisfy the requirements of many applications, such as energy efficient buildings(Tyagi and Buddhi, 2007). Therefore, it is needed to reduce their porosities to produce metal foams with high mechanical property. However, few works have concentrated on the heat transfer in low porosity metal foams.

In this section, a model of the high mechanical property open-cell metal foam is proposed and validated by comparing with the experimental results. The melting processes of paraffin in two models are both simulated and the results are compared and discussed.

3.2 Thermal performance of materials

3.2.1 Thermal property of pure paraffin

Paraffin is a common organic phase change material (PCM), thanks to its low cost, large latent heat and other advantages; it is widely used in thermal storage field. Paraffin is consists of a mixture of mostly straight-chain n-alkanes, $CH3-(CH2)_n-CH3$(He and Setterwall, 2002). The thermal properties of paraffin depend on the length of the hydrocarbon chain. For example, if the chain length increases, the melting temperature and latent heat of paraffin will increase as well. According to the number of carbon atoms in the chain, the paraffin can be divided into several kinds, such as C18, C20-C33, C21-C50, etc. The melting temperature could be also a parameter to divide the paraffin, such as R54, R56, R58, etc. Many researches on the thermal properties of many kinds of paraffin have been done (Inaba and Tu, 1997; Kousksou et al., 2010; Ukrainczyk et al., 2010). Therefore, the paraffin could be chosen according these parameters to match different applications.

The type of paraffin used in our study is R56-58 (produced in Malaysia, by Merck Millipore). In order to obtain the detail thermal parameters of this type paraffin, we use the differential scanning calorimeter (DSC). The thermal parameters, such as latent heat and melting point of paraffin, are measured and obtained. The heat and cooling rate is 5℃/min. The curve of DSC result is shown in Figure 3.1 DSC result of paraffin.

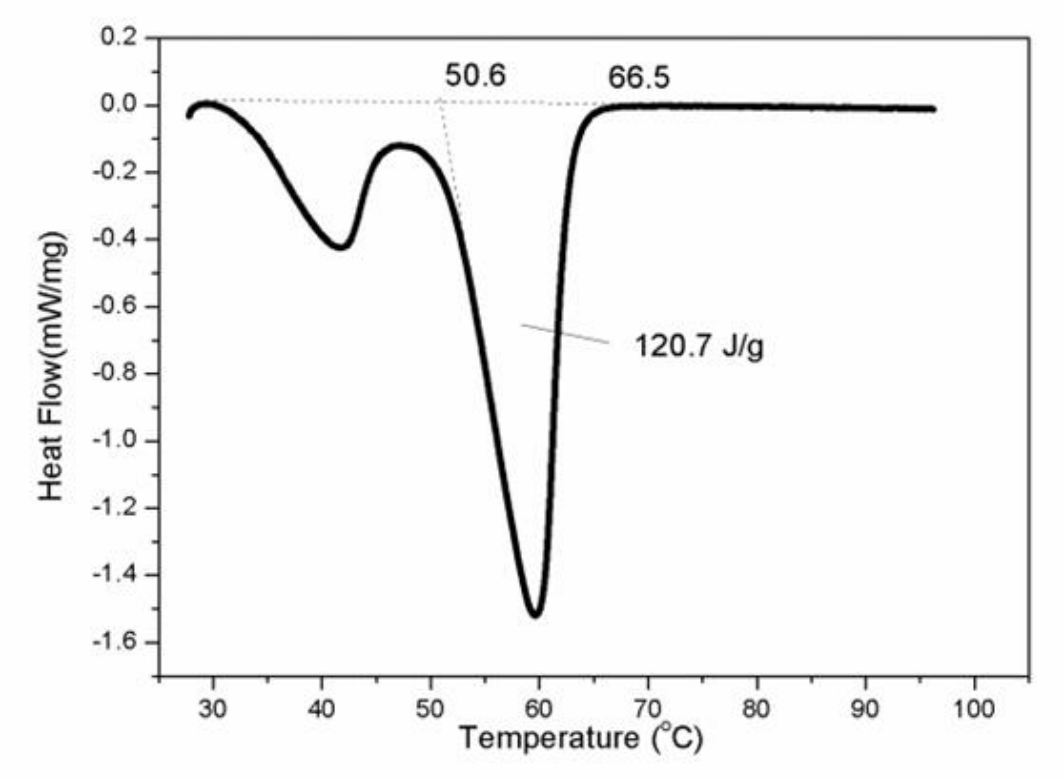

Figure 3.1 DSC result of paraffin

From Figure 3.1, it could be observed that the small peak represents the phase transition of solid-solid, and the greater peak is the phase transition of solid-liquid. It is obviously that the melting process of paraffin happens within a temperature range, not at constant temperature. In order to obtain the melting range of paraffin and the latent heat, the boundary and area of the greater peak is analyzed. The result is that the melting range of paraffin is 50.6-66.5℃ and the latent heat is 120.7 J g-1. There are also other thermal parameters and other physical parameters of the paraffin are listed in Table 3-1 Thermal and physical properties of paraffin. All these parameters are applied in the following numerical investigation.

Table 3-1 Thermal and physical properties of paraffin

Property	Value
Density,ρ (kg m^{-3})	840
Specific heat, C (J kg^{-1} K^{-1})	2100
Thermal conductivity, λ (W m^{-1} K^{-1})	0.2
Viscosity, μ (kg m^{-1} s^{-1})	0.003
Thermal expansion coefficient, γ (K^{-1})	0.0004
Latent heat, L (kJ kg^{-1})	120.7
Solidus temperature, T_{m1} (K)	323.6
Liquidus temperature, T_{m2}(K)	339.5

3.2.2 Thermal property of aluminum alloy

Aluminum alloy is a common metal material in the using of heat dissipation, heat storage systems and heat recovery systems. For example, the automobile radiator, CPU heatsink, Led heatsink and other cooling parts, they are usually made of aluminum alloy as shown in Figure 3.2 Various radiators and heatsinks made of aluminum alloys The reason why these parts are made of aluminum alloy is due to the good thermal conductivity of aluminum alloy. The thermal and physical properties of aluminum alloy are shown in Table 3-2.

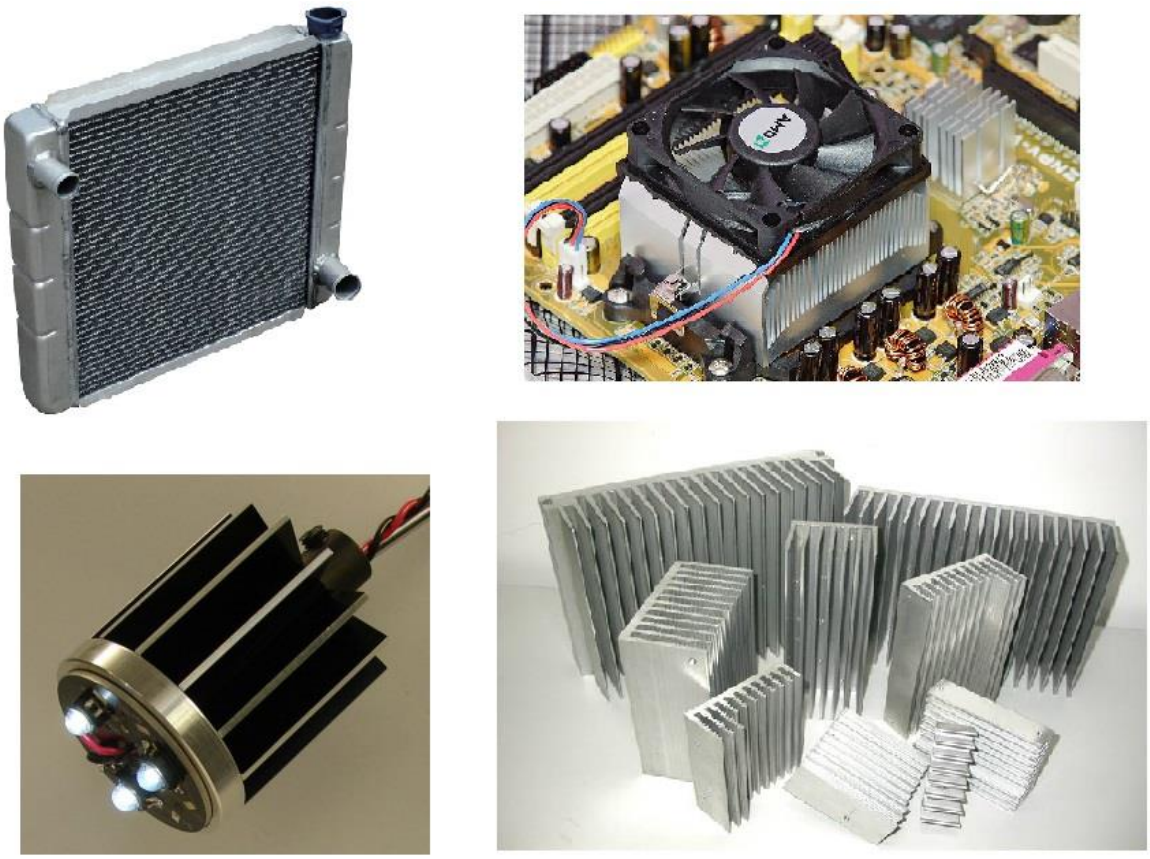

Figure 3.2 Various radiators and heatsinks made of aluminum alloys

From Table 3-2 and Table 3-1, it is easy to notice that the thermal conductivity of aluminum alloy (160 W m^{-1} K^{-1}) is much greater than that of paraffin (0.2 W m^{-1} K^{-1}), about 800 times greater. Through this great different, we can boldly assume that the aluminum foam could largely improve the thermal conductivity of aluminum/paraffin composite and the percentage of aluminum could affect the thermal conductivity of aluminum/paraffin composite. We will then carry out numerical and experimental analysis and research to prove our hypothesis.

Table 3-2 Thermal and physical properties of aluminum alloy

Property	Value	Unit
Density of liquid	2380	kg m^{-3}
Specific heat	963	J kg^{-1} K^{-1}
Thermal conductivity	160	W m^{-1} K^{-1}
Latent heat	389	kJ kg^{-1}
Solidus temperature	828	K
Liquidus temperature	888	K

3.3 Modeling Method

3.3.1 Modified Kelvin Model for High Mechanical Property Open-cell Metal Foam

The first step of the analysis is to create a model to represent the microstructure of metal foams and the aluminum/paraffin composite. With this model, we could do a variety of simulations and compare with the experimental results.

In order to describe the microstructure of metal foams, many models have been proposed by other researchers. The spherical cell model, the cubical cell model, the dodecahedron model (shown in Figure 3.3 Structure and characteristic lengths involved in the dodecahedron geometry. Left: “slim” dodecahedron made of prismatic struts. Right: “fat” dodecahedron made of rounded windows) (Huu et al., 2009) and the Kelvin (tetrakaidecahedron) model (shown in Figure 3.4) (Bamorovat Abadi and Kim, 2017; Peng et al., 2017; Yang et al., 2017) are widely used to represent the porous forms of metal foams in the research of metal foam

simulation. Among these models, the Kelvin model corresponds mostly to the real structure of metal foams whose porosity is more than 90% (High porosity aluminum foam/ HPAF).

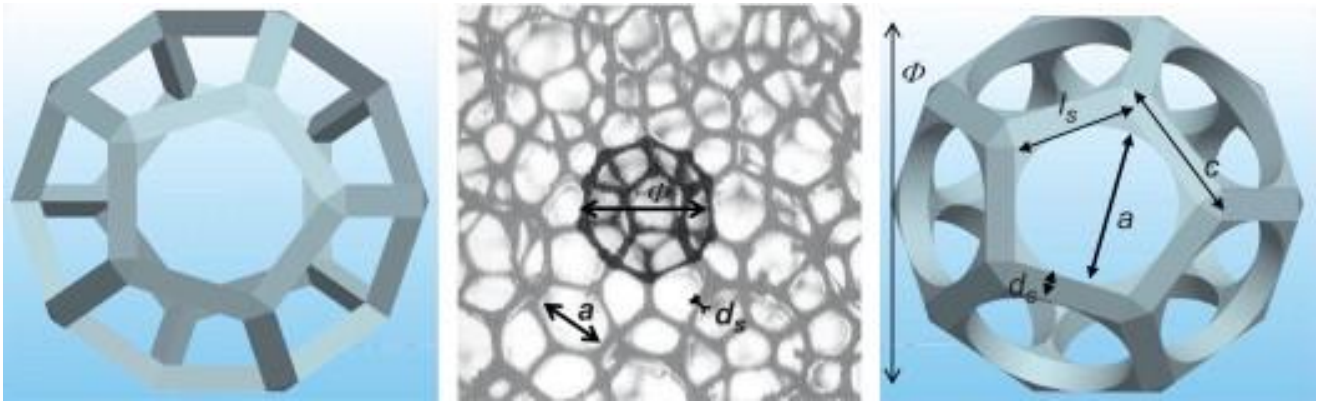

Figure 3.3 Structure and characteristic lengths involved in the dodecahedron geometry. Left: “slim” dodecahedron made of prismatic struts. Right: “fat” dodecahedron made of rounded windows

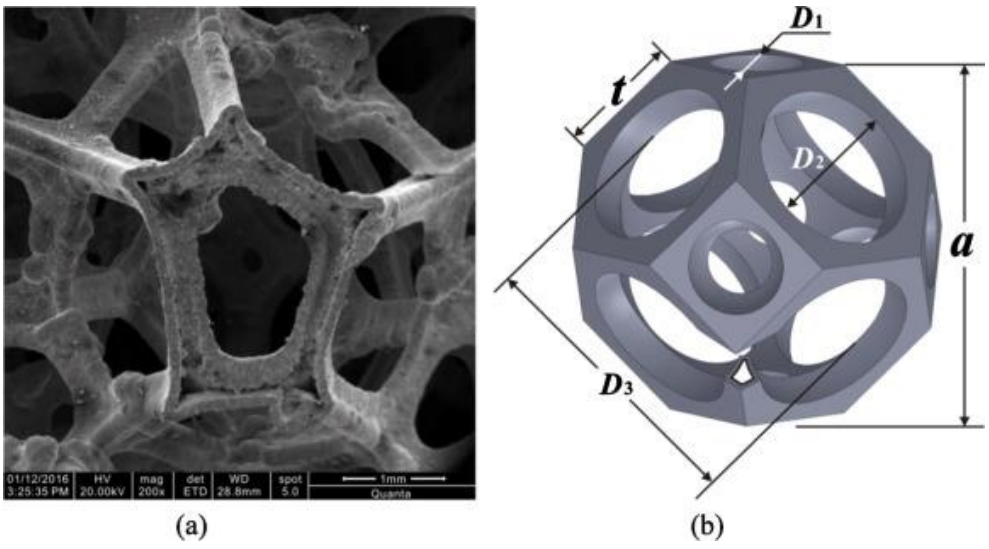

Figure 3.4 (a) SEM image of open-cell copper foam and (b) idealized tetrakaidecahedron unit cell model.

However, the high mechanical property aluminum foam, which is also called Low porosity aluminum foam (LPAF) prepared by infiltration casting method as described above, whose porosity is 50-70%, has a different structure compared to high porosity foams, as shown in Figure 3.5 SEM image of the low porosity aluminum foam structure.

Because of the casting fabrication method, the aluminum has complex structure instead of the simple fiber form, and its pore form depends on the preform structure. In this case, the modified Kelvin model is proposed to represent the high mechanical property metal foam (LPAF), as shown in Figure 3.6 Modified Kelvin model (65%), (a) metal part and (b) pore part (tetrakaidecahedron). The modified Kelvin model consists of a tetrakaidecahedron part and a solid porous unit, which represent respectively the pore and the aluminum. The porosity of the model could be adjusted by changing the square area in the tetrakaidecahedron.

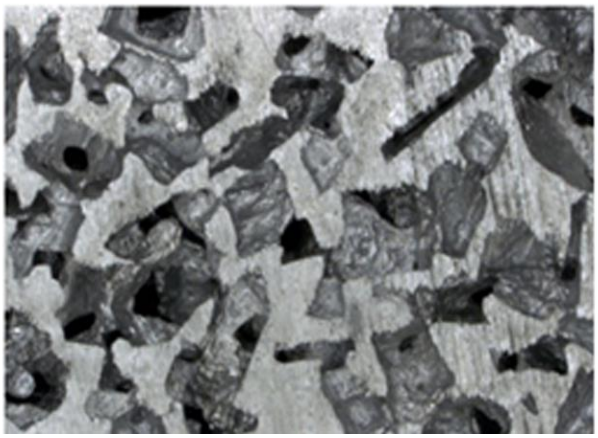

Figure 3.5 SEM image of the low porosity aluminum foam structure

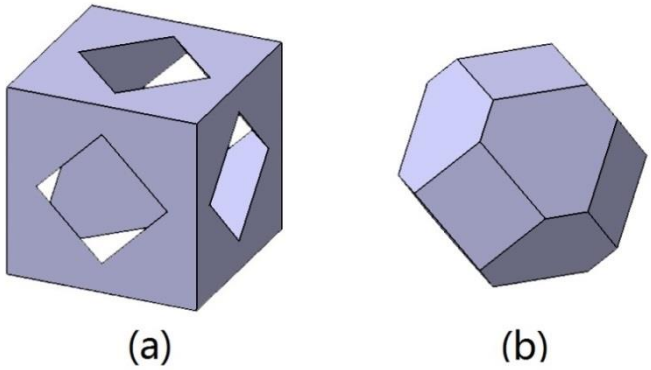

Figure 3.6 Modified Kelvin model (65%), (a) metal part and (b) pore part (tetrakaidecahedron)

3.3.2 Simulation of the Thermal Conductivity

For high mechanical property metal foams (LPAF), the thermal conductivity is very important because the heat conduct is the main form of the heat transfer in the foam/PCM composite. The investigate method of foam thermal conductivity is according to the reference(Moeini Sedeh and Khodadadi, 2013). The model is placed in the condition that the temperature gradient is 1K. The heat flux density will approach a constant number when the system arrives at steady state. Therefore, by using the Fourier law, the thermal conductivity could be obtained. The model grid used in this analysis is the tetrahedral mesh. In order to confirm the grid number, the model with different grid numbers is simulated at the condition discussed above. The heat flux density of middle surface is detected during the process.

Figure 3.7 Heat flux as function of number of cells shows the heat flux density as a function of grid number. It obvious that the value of the heat flux become steady

as the grid number increasing. The simulation results could approach the experimental results if the grid number is much greater.

In order to reduce the calculate time, the grid number should be as small as possible. However, a great precision needs a greater grid number. We should chose a proper grid number for the simulation which could balance the calculate time and accuracy. As a result, considering both the precision and calculate time, the grid number is set to 785257.

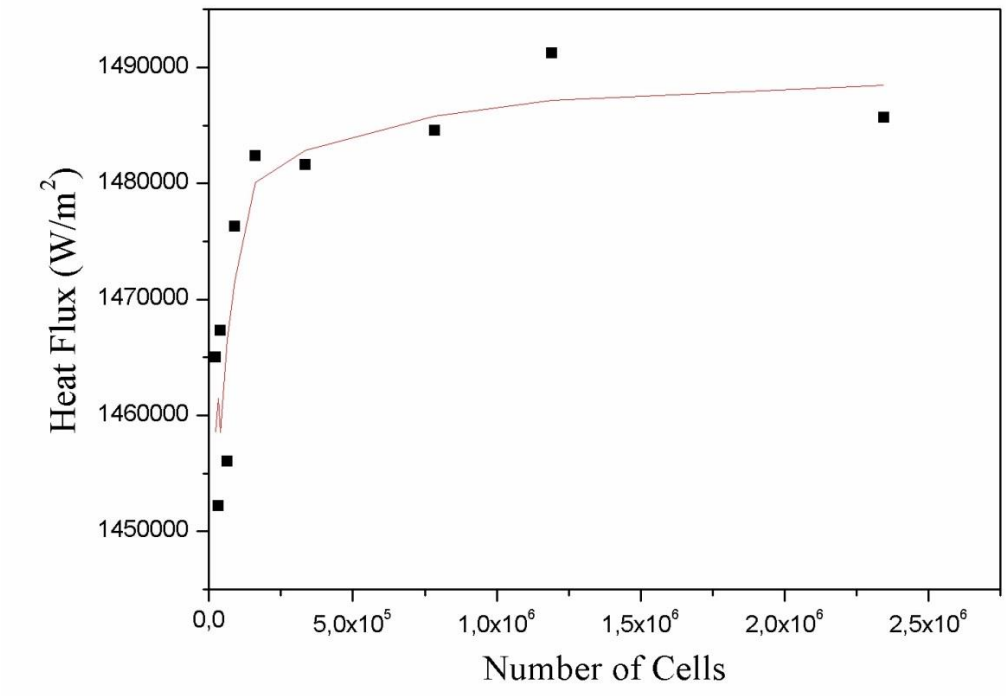

Figure 3.7 Heat flux as function of number of cells

3.3.3 Validation of the modified Kelvin Model and Kelvin Model

To verify the modified Kelvin model, the thermal conductivities of metal foams are simulated and compared with the experimental results (JINZHU SONG, 2008). The aluminum alloys is A356 and their porosities are from 57% to 69%. Figure 3.8 presents the comparison results. It is obvious that the thermal conductivity decreases as the foam porosity increases. This phenomena is due to the huge different of the thermal conductivity of the aluminum and air. So, the increase of the air volume could lead to the thermal conductivity decrease. Besides, in the compare results, the simulation results are consistent with the experimental ones. Therefore, the modified Kelvin model could be applied in thermal simulations of high mechanical property metal foams.

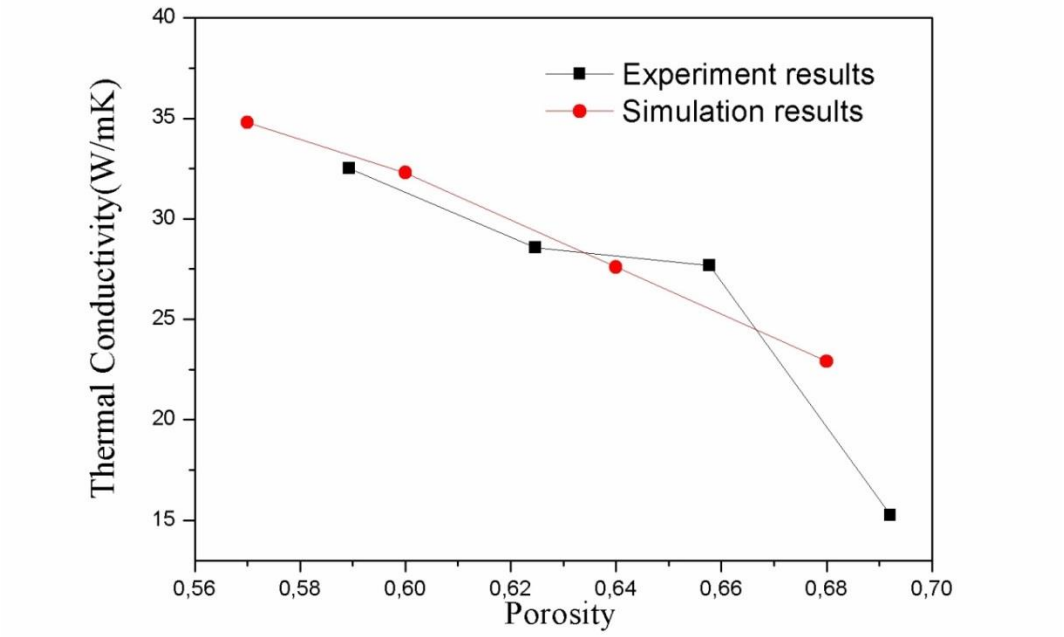

Figure 3.8 Comparison of experimental and numerical thermal conductivities

Since the Kelvin model has been used to represent the structure of HPAF for a long time in thermal simulation by other researchers (Kumar and Topin, 2014), the validation method in his study is shown in Figure 3.9. In fact, this validation method is the same as the method above. Prashant Kumar et al. obtained a good agreement between the numerical and experimental results by using the Kelvin model, just as the validation result of modified Kelvin model.

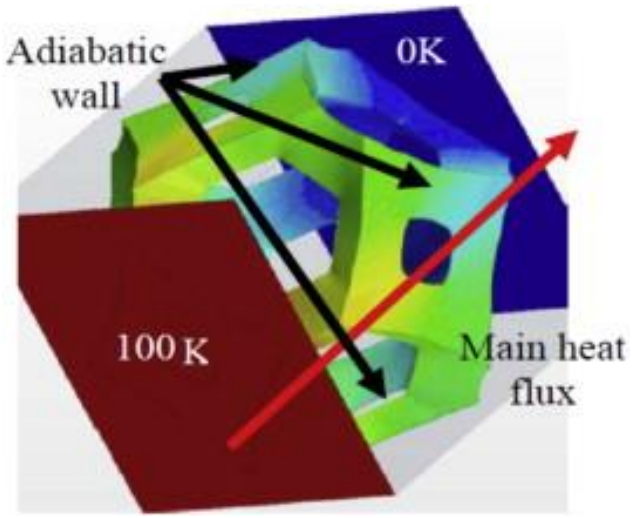

Figure 3.9 Boundary conditions and unit cell model: Heat flux in the main direction, no fluxes in other direction (adiabatic walls). Temperature difference is imposed in heat flux direction.

3.3.4 Finite Element Model

In our work, the finite element model consists of four units which represent the thickness of a layer energy storage system, as shown in Figure 3.10. The simulations are achieved by ANSYS Fluent® and the heat conduction is solved by the simple algorithm according to the energy conservation equation. The mesh type is tetrahedral and its size is uniform. The dimension of each unit is one

millimeter. The aluminum foam is made of AS7G, which is filled by paraffin. Their thermal properties are based on reference (Jie et al., 2014; Liu et al., 2013). The temperature of the heat surface is 350K which is higher than the paraffin melting temperature (321K-335K). The other surfaces are insulated. The initial temperature of models is 300K which makes paraffin in solid state.

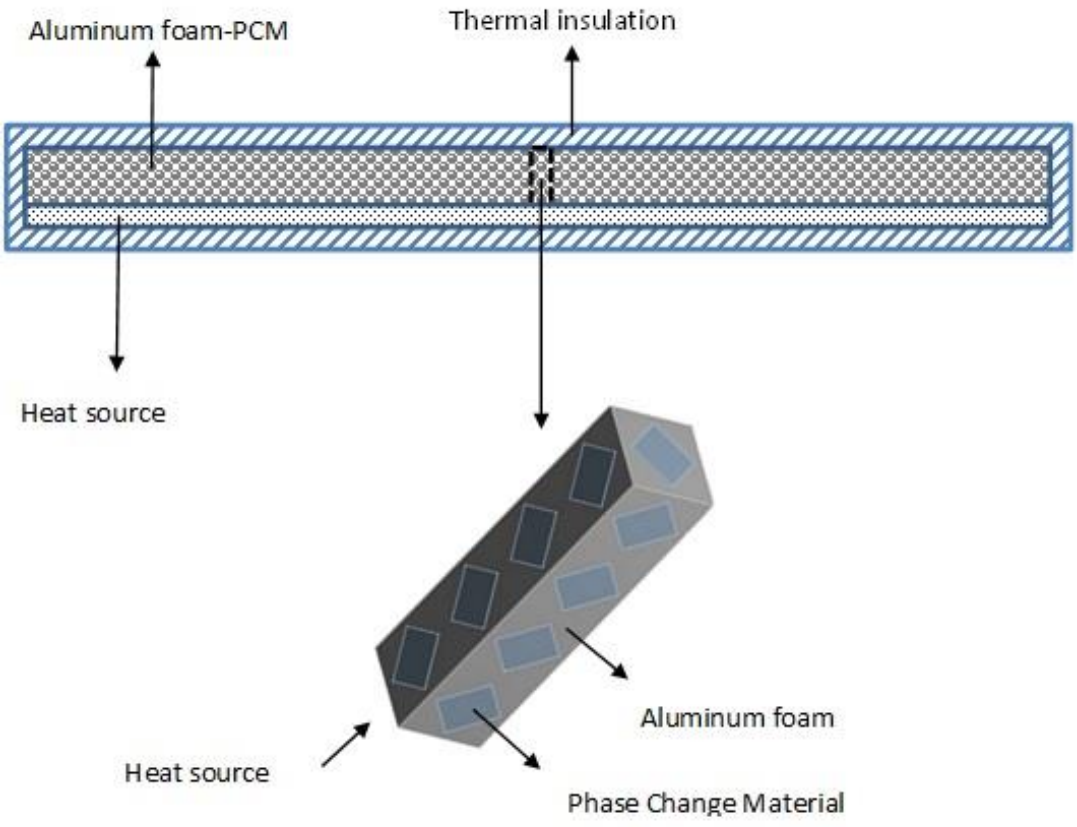

Figure 3.10 Layer energy storage system and its representative model

3.4 Results and Discussions

3.4.1 Melting process

To observe the paraffin melting process, a cross section in the middle of model is selected as observation surface for each model, which is shown in Figure 3.11. The results of high mechanical property model indicate that the paraffin melts from the interfaces to the center. A similar phenomenon can be observed in the high porosity model, the paraffin begins to melt from the interfaces. Moreover, the temperature of aluminum is always higher than the paraffin. This phenomenon could be explained that the paraffin is not only heated by heat surface, but also heated by the interfaces thanks to the high thermal conductivity of aluminum.

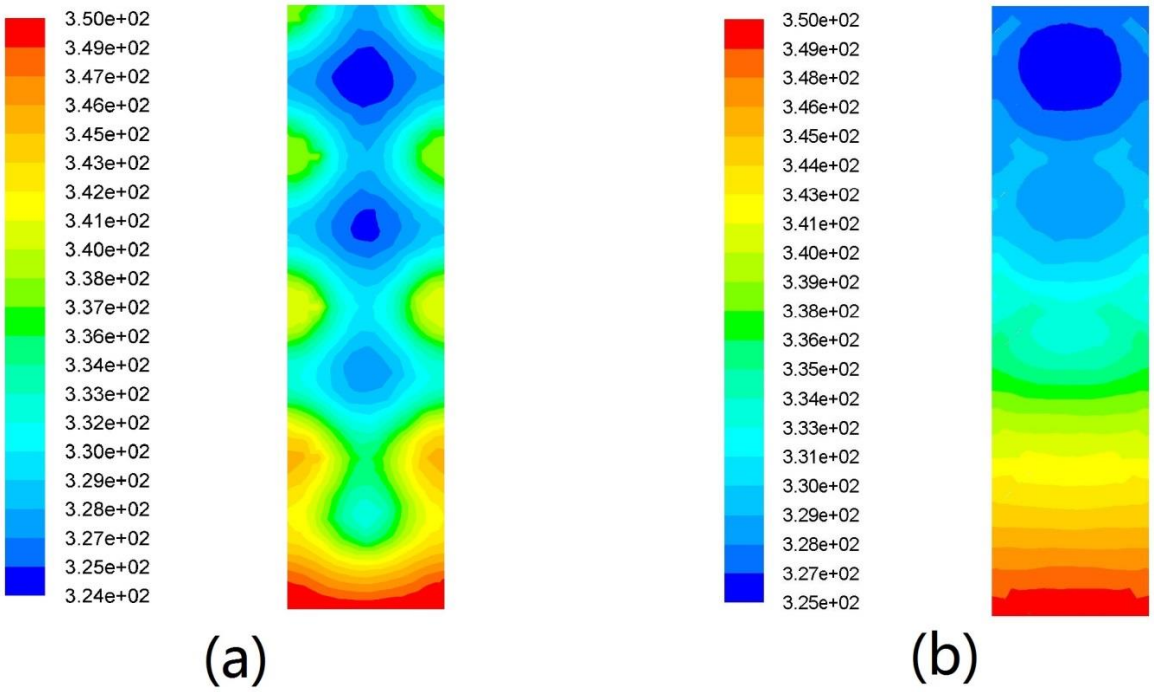

Figure 3.11 Temperature fields of two models, (a) modified Kelvin model (65% porosity) and (b) Kelvin model (96% porosity)

In order to compare the melting process in different units, four representative points (F1, F2, F4 and F5) of 70% porosity model and four points (P1, P2, P3 and P4) of pure paraffin are chosen as observation points who are located in the center of each cube unit. Their temperature curves are shown in Figure 3.12. The point F4 which is farthest from the heat surface is heated in the beginning. The temperature curves of all four points of 70% model are very similar. However, the curves of pure paraffin are different. The point P4 which located in the same position as F4 is much more difficult to be heated. The complete melting times of 70% model and pure paraffin model are 5.8 and 337 seconds. The comparison shows that the aluminum can greatly enhance the melting rate of systems, thereby reducing the time of energy storage and release.

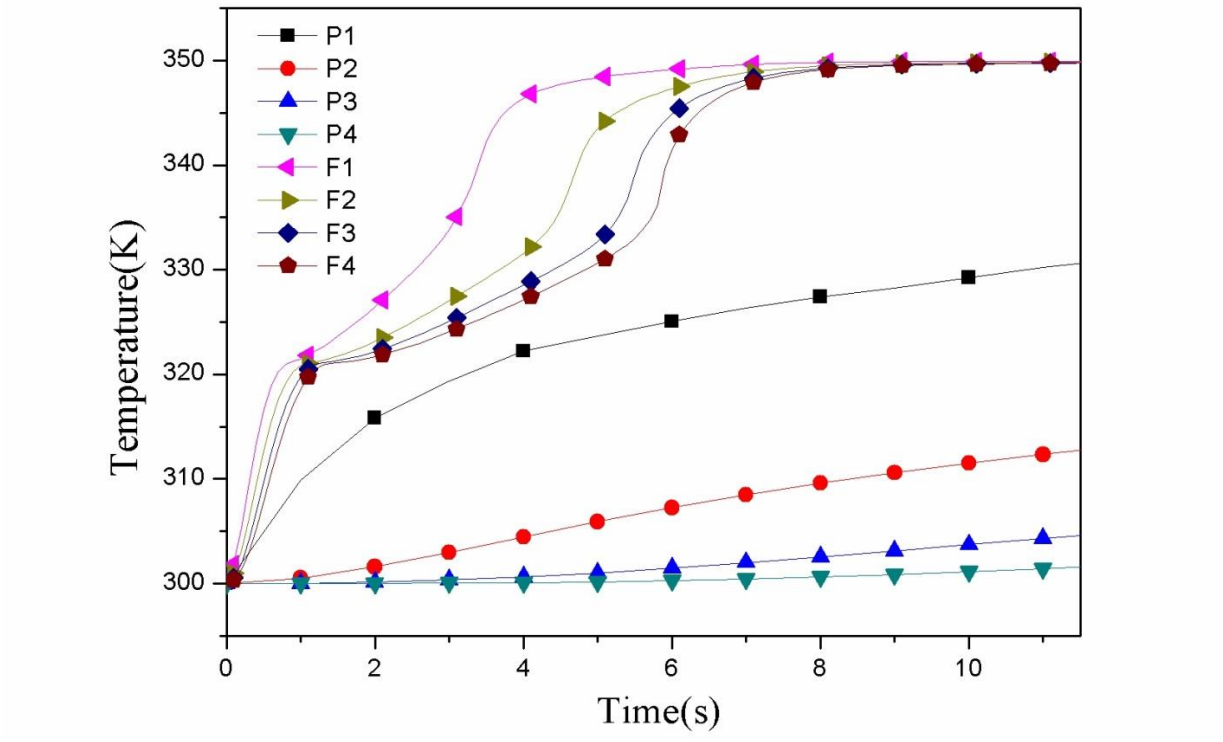

Figure 3.12 Temperature variations of eight center points of modified model and pure paraffin

3.4.2 Comparison of Different Structural Models

For each type model, modified Kelvin model (70% porosity) and Kelvin model (96% porosity) are selected to analyze the effect of structure. Two liquid fraction curves of paraffin are shown in Figure 3.13. The paraffin in modified Kelvin model melts completely in 5.8 seconds which is much shorter than the melting process of high porosity model. The melting rate of modified Kelvin model is largely higher than the one of Kelvin model. Firstly, the increased volume of metal helps to accelerate the heat transfer. Secondly, the high mechanical property foams have more contact surface which can heat efficiently the paraffin, so that the paraffin melts faster.

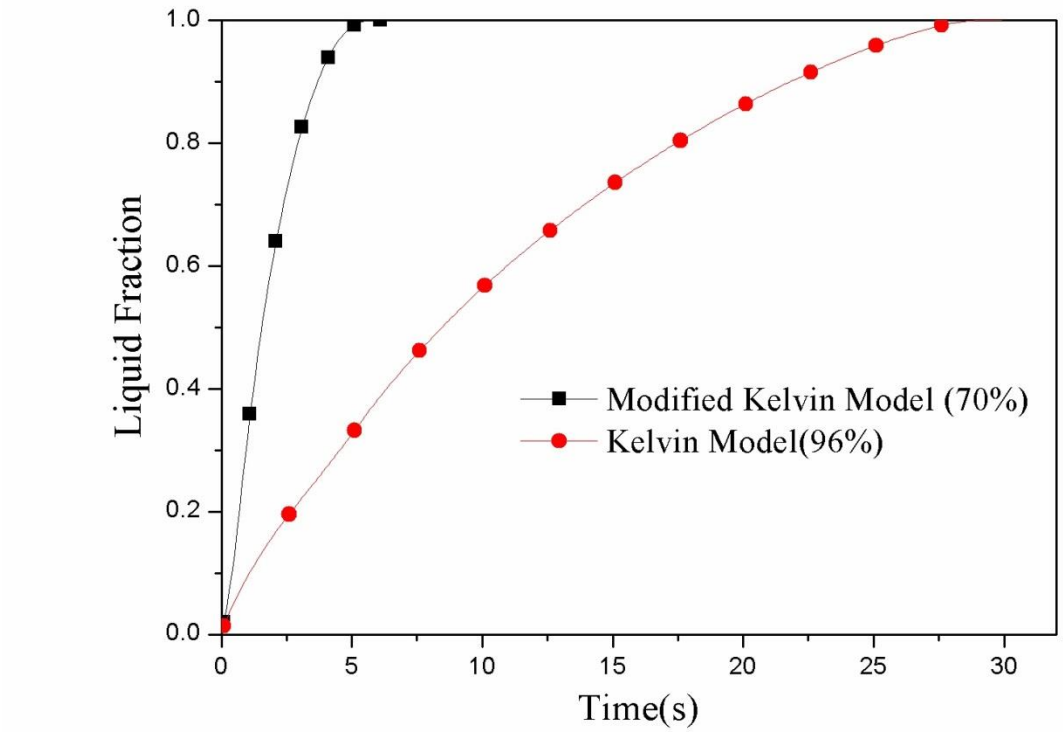

Figure 3.13 Comparison of liquid fraction between modified model and Kelvin model

3.4.3 Effect of Porosity

Because high mechanical foams have a better performance in energy storage systems than high porosity foams, three different porosities (65%, 70% and 75%) of high mechanical property foams are analyzed. Their liquid fraction curves of different porosities are shown in Figure 3.14. From these three curves, the different melting times can be easily observed. The melting time increases with the increase of foam porosity. Therefore, for lower foam porosity, the extra aluminum helps transfer the heat from heat resource to the paraffin, but the heat storage amount reduces as a consequence of the decreased volume fraction of paraffin.

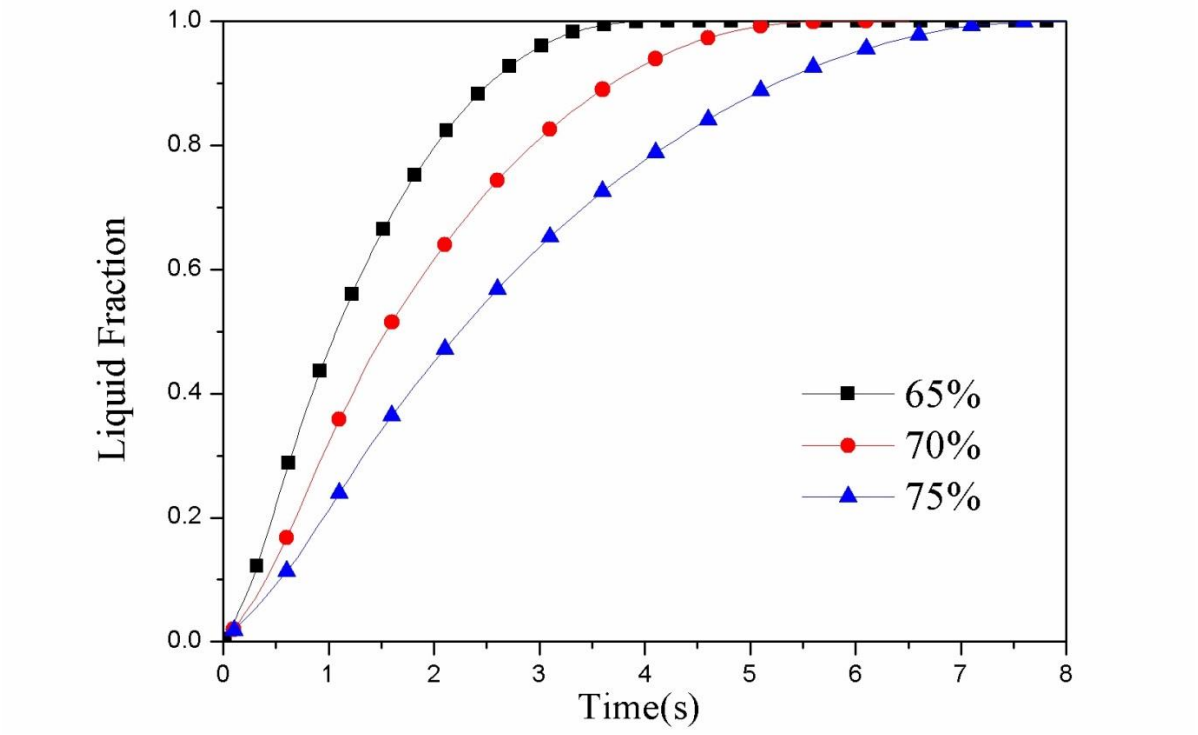

Figure 3.14 Liquid fraction variations of paraffin in three different porosity models of modified Kelvin model

3.5 Conclusion

In this chapter, a modified Kelvin model is developed to represent high mechanical property metal foams by comparing with experimental results. The melting processes of paraffin in high mechanical property and high porosity metal foams are studied. Metal foam plays an important role in the melting process of PCMs by separating PCMs in very small pieces and heating separately them, thereby reducing largely the melting time. For high mechanical property metal foams, even though the heat storage amount of systems is less, the melting process becomes much shorter than high porosity metal foams. As a result, the energy storage systems which are made by high mechanical property metal foams could store effectively the heat in a very short time.

Chapter 4 Thermal behavior analysis of open-cell metal foams manufactured by rapid tooling

4.1 Introduction

This study focuses on the methodology of periodic open-cell composite foams manufacturing by rapid tooling as well as the thermal analysis of the obtained structure. A composite is prepared by introducing a phase change material (paraffin wax) into metal foam. The aim is to provide structural composite foam to study its thermal behavior for the energy storage and achieve an adapted geometry with the help of the rapid tooling by Three-Dimensional Printing (3DP). Concretely, the composite melting process is experimentally studied in order to determine thermal behavior. In this study temperature variations and distributions of composite are analyzed and compared with the results of pure paraffin. Moreover, the effect of natural convection is analyzed and discussed. The results show that the periodic open-cell metal foam could be a potential solution to the problem of storage and recovery of energy.

Open-cell metal foams have many excellent properties such as high mechanical strength, high permeability, high porosity and large specific surface area. Therefore, Reay (2013) considered that metal foam could be more and more used in a variety of fields, especially the applications in the energy storage and other energy management systems. For example, Mohammadian et al. (2015) investigated the application of metal foam in thermal management of high-power lithium-ion battery; Chen et al. (2016) found that the metal foam has the potential to expand its applications for different solar thermal energy storage. Recently, the thermal performance of energy storage systems using phase change materials (PCMs) and open-cell metal foams is largely experimentally and numerically investigated. Baby and Balaji (2013a) experimentally investigated the thermal

performance enhancement and effect of orientation on porous matrix filled PCM based heat sink. Sundarram and Li (2014) analyzed the thermal management performance of PCM infiltrated in microcellular metal foams. Chen et al. (2014) experimentally and numerically studied the melting of phase change materials in metal foams.

Reticulated open-cell metal foams are constituted by a number of irregular cells which are enclosed by several metal ligaments. According to Twigg and Richardson (2007), the open-cell metal foams can be described by their morphological parameters, such as pore size, window size, ligament diameter and porosity. These parameters are always studied by researchers because the structures of metal foam are critical for the mechanical and thermal performances, Bekoz and Oktay (2013) studied the effect of the porosity and pore size of alloy steel foam on its mechanical properties; Ambrosio et al. (2016) found that the convection heat transfer coefficient decreases with porosity. Different geometrical models were discussed by Thomson (1970), such as tetrahedral model, cubic model and tetrakaidecahedra model. They are often presented to study the mechanical and thermal properties of foams in many literatures.

However, the morphological and geometrical parameters of traditional reticulated open-cell metal foams cannot be accurately controlled and obtained for different applications, which greatly limits their developments. In order to solve this problem, Additive Manufacturing (AM) technologies and rapid tooling are attractive and promising methods, e.g. selective laser sintering (SLS), selective electron beam melting (SEBM) and 3DP. In them, the metal foam manufactured with SEBM is experimentally and numerically investigated by Inayat et al. (2011).

In this work, a fabrication method of periodic open-cell metal foams will be presented, combining the traditional casting method and the 3D printing by plaster and binder jetting. Thanks to J.GARDAN, who provides us with the mold prepared by 3d impression in EPF. With the help of this method, the morphological and geometrical parameters of open-cell metal foam could be designed and controlled according to the manufacturing constraints.

After manufacturing the metal foam based on tetrakaidecahedron geometry, the thermal performance of energy storage system is investigated. A phase change material (paraffin wax) is introduced in this open-cell metal foam to prepare a composite. The melting process of composite is observed and the temperature variation is recorded by infrared camera in order to understand the thermal behavior. The temperature variations of pure paraffin and composite are measured by thermocouples. The natural convection and heat transfer process in the composite during the melting process is also discussed.

4.2 Materials and method

4.2.1 Preparation of mold

This mold is prepared in EPF with the help of J. GARDAN, we have studied and produced these molds together.

(1) Rapid tooling by binder jetting

In the context of structured aluminum foam achievement, the AM technologies allow different possibilities to study a complex shape in order to realize adequate aluminum foam. They are most commonly used for modeling, prototyping, tooling through an exclusive machine or 3D printer. In order to reduce the time and cost of molds fabrication, AM technologies are used to develop and manufacture systems of rapid tooling. They are not only largely used for manufacturing short-term prototypes but also involved for small-scale series production and tooling applications (Rapid tooling) (Stampfl and Hatzenbichler, 2014). Laser technologies on metal powder bed (SLS, SEBM or DMLS - Direct Metal Laser Sintering) are of expensive manufacturing processes and the research environment guides the work towards aluminum casting. Based on the study of Maeda and Childs (2004), a metal powder product through an AM laser technology keeps a granular structure which is not desirable in this thermal behavior study of metal foam. Therefore, the 3DP technology shows the advantages to realize rapid tooling intended for aluminum foam by casting.

(2) 3DP Technology

3DP (Three-Dimensional Printing) also known as CJP (Color Jet Printing), combines raw powder and binder jetting. 3DP was invented in the late 1980s by an MIT student named Paul Williams and his advisor Professor Eli Sachs, which was recorded in the book by Lipson and Kurman (2013). The main advances of this process are the time and cost reduction, human interaction, and consequently the product cycle management (Ashley, 1995). In the 3D printer, each layer is created

by spreading a thin powder layer with a roller inside a manufacturing tray and the powder is selectively linked by a printing head containing an array of binder fluid jets, as shown in Figure 4.1.

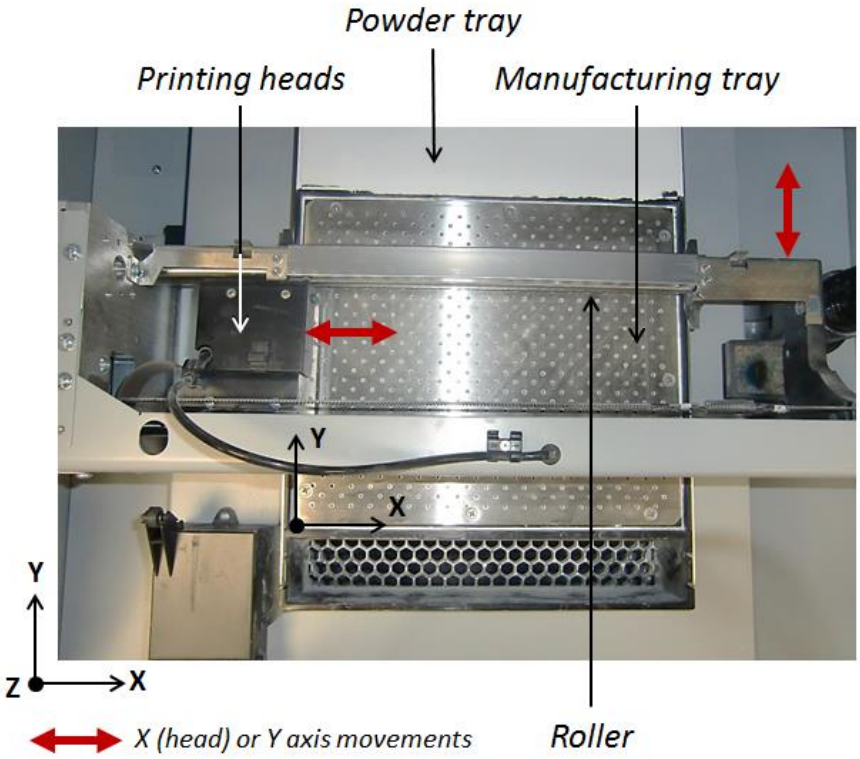

Figure 4.1 3D Printer manufacturing chamber

The manufacturing tray goes down of one layer thickness and a new layer of powder is spread and this layer is then printed by the printing nozzles. This procedure is repeated until the 3D part is accomplished. After the process, the powder is linked together by the binder. The prototype is removed from the powder bed because the part is surrounded powder Lu et al. (2009). This process has been used to fabricate numerous metal, ceramic, silica and polymeric components of any geometry for a wide array of applications.

In the study, we use the ProJet® 460 Plus (3D Systems, formerly ZCoporation) to produce some molds for casting. A powder hopper provides the manufacturing tray in hydraulic powder by spreading through a roller. The powder is a white powder consisting mostly or entirely of Calcium Sulfate Hemihydrate (plaster or gypsum) which is used in making casts, molds, and sculpture. The commercial name of powder is VisiJet® PXL Core used into the 3D ZPrinter®. In order to integrate the available technology, the approach defined a manufacturing process to produce the foam structure that corresponds to the cavities of plaster mold.

(3) Rapid tooling process

The process begins with a 3D model in CAD software before converting it in STL format file. This format is treated by specific software own to the AM technology which cuts the piece in slices to get a new file containing the information for each layer. The specific software generates the hold to maintain the complex geometries automatically with sometimes the possibility to choose some parameters. In the study, supports were not necessary because the models have a flat base. The engineering and manufacturing cycle involved to AM process is describe below according to the method proposed by Gardan (2015):

Part design in CAD;

Conversion of part geometry in exchange format (STL…);

Exchange file implementation into the specific software of the AM machine (3DPrint™);

Configuration and orientation of the set (parts and supports);

Slicing of the part by the specific software;

Computation and layers manufacturing;

Post-processing.

The geometry of 3D model of lattices has been chosen according to the geometry of tetrakaidecahedra model which was proposed by Thomson (1970).

Then the powder mold is produced by binder jetting on powder bed which requires finally a fine cleaning in order to extract the non-hardened powder inside the mold, see Figure 4.2. Indeed, the procedure needs to determine a density of the lattice conducive to a good extraction of the remaining powder. After some empiric experimentations, the results have shown that the higher density is more difficult to manage in order to extract the powder inside channels and gaps. The density range which can be extracted is about 90%. The final mold in plaster is used like a lost tool through a casting process in order to shape the aluminum foam.

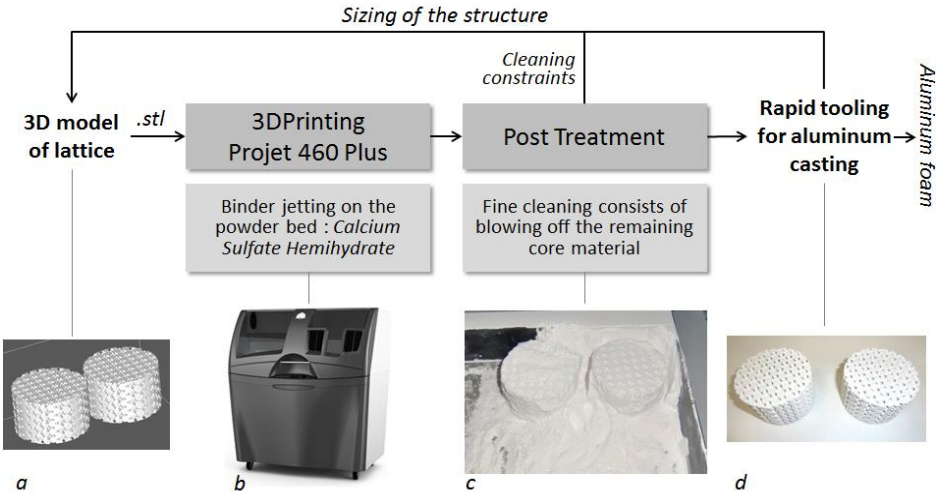

Figure 4.2 Manufacturing process of rapid tooling using 3D Printing: a. 3D model in stl format, b. 3D Printer Projet 460+, c. Parts into the powder, d. Final model (mold cavities)

4.2.2 Preparation of metal foam

The preparation process concludes three steps: (i) pretreatment, (ii) casting and (iii) post treatment. Once the plaster mold has been manufactured, the pretreatment methods should be performed to obtain a plaster mold more suitable for next steps. The negative pressure casting method is used to fulfill the molten aluminum into the plaster mold. Finally, the post treatment is carried out to remove all plaster remained in the aluminum foam.

(1) Pretreatment methods

In the manufacturing process of plaster mold, the moisture will exist in the matrix, which will evaporate during casting process and affect the infiltration of molten aluminum. In order to reduce these defects in samples, the moisture in plaster must be removed as much as possible before casting process.

The viscosity of molten aluminum will increase if the mold temperature is too low regarding the temperature of melting aluminum. A high viscosity is not efficient to make the molten aluminum fill all cavities of plaster molds. Hence, a high temperature preheating of plaster molds should certainly be used before casting process.

According to the chemical properties of plaster and the results of several pretests, the pretreatment methods with two steps are proposed to improve the quality of the samples of metal foam

- Heating plaster molds four hours with 200℃,

- Heating plaster molds 20 minutes before casting with 400℃ in order to avoid the reduction of the liquidity of melting aluminum,

After these two pretreatment steps, the plaster mold will be standby for negative pressure casting.

(2) Negative pressure casting

Due to the surface tension of melting aluminum and the small dimensions of the passages, melting aluminum could not completely fill the cavities with a conventional gravity casting method. To overcome this problem, a negative pressure must be used to increase the difference of pressure to make melting aluminum entirely fill the plaster mold. The pressure difference is 80 KPa between the atmosphere side and the negative pressure side. A schematic representation of negative pressure casting is given in Figure 4.3.

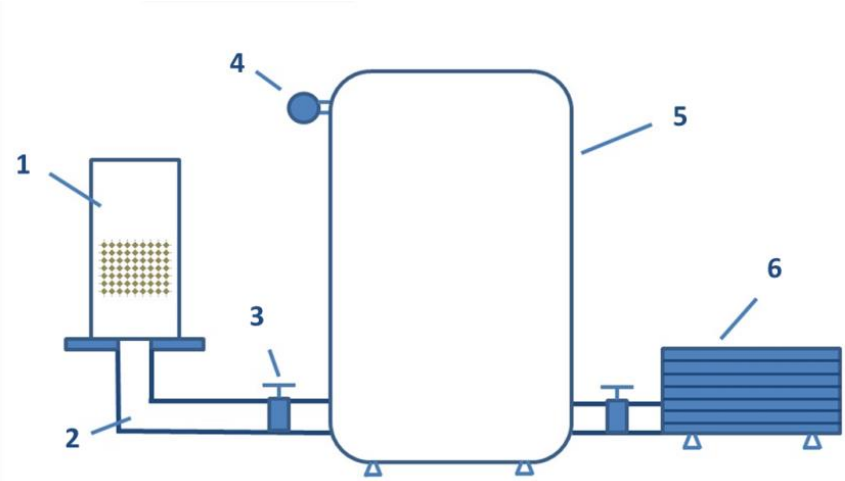

Figure 4.3 Schematic presentation of negative pressure casting process (1- Mold, 2- Vacuum pipe, 3- Valve, 4- Manometer, 5- Vacuum tank, 6- Vacuum pump)

(3) Removing the plaster

After the process of casting, the plaster remained should be removed from the aluminum foam. However, due to the stability of the plaster and the complex internal structure of plaster molds, the plaster becomes very hard and difficult to be removed after cooling.

Several methods have been tried to remove plaster molds, such as rinsing with water or weak acid, vibration, beating with hammer, heating with high temperature. Among these methods, by combining the vibration and heating with high temperature, the plaster could be removed easily and entirely. The plaster will become powder again if it is heated with 500℃ during 4 hours, and the powder could be removed by vibration. After repeating the process several times,

the plaster will be removed completely. The final aluminum foam sample obtained is shown in Figure 4.4.

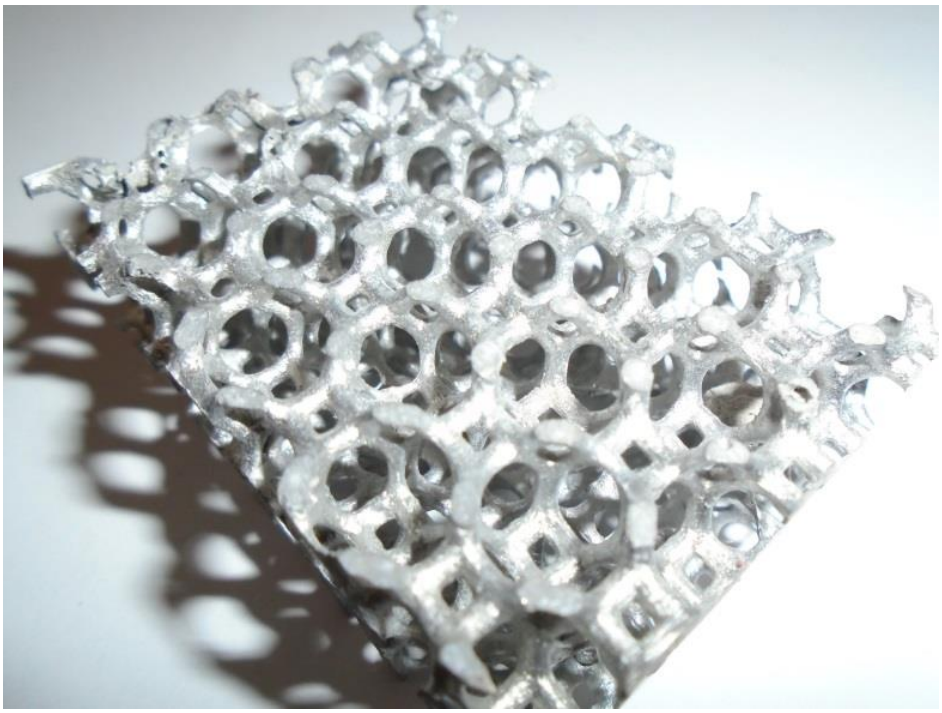

Figure 4.4 Periodic aluminum foam manufactured using 3D printing mold

4.2.3 Experimental setup and procedure

In order to study the energy storage system using metal foam, phase change materials are always introduced in metal foam as a composite. In this study, the paraffin is used as the phase change material and the open-cell aluminum foam obtained is used as metal foam. The thermal properties of pure paraffin wax and pure aluminum are shown in Table 4-1. This composite can be seen as a small energy storage system. The melting process and the temperature variation of the composite are investigated and compared with the pure paraffin.

Table 4-1 Properties of pure paraffin and pure aluminum

Property	Material	
	Paraffin	AS7G
Density (kg m^{-3})	840	2680
Specific heat (J kg^{-1} K^{-1})	2100	963
Thermal conductivity (W m^{-1} K^{-1})	0.2	160
Latent heat (kJ kg^{-1})	181	-
Solidus temperature (K)	323	828
Liquidus temperature (K)	339	888

Dimensions of the foam sample are about 60mm×45mm×20mm. This foam is immersed into melted liquid pure paraffin. After cooling, a composite sample is obtained by cutting away the extra paraffin wax. This sample is placed into a PMMA box whose bottom surface is heated by a heating film. This experimental equipment is shown in Figure 4.5. The power per unit area of the heating film is about 0.01 W/mm^2. All outer surfaces of the PMMA box are wrapped by insulation material except the observation surface. An infrared thermal imaging camera is used to record the temperature distribution of the observation surface. Three thermocouples are used inside the sample. The distances between the heating surface and thermocouple 1, 2 and 3 are 1cm, 2cm and 3cm. All temperature data is measured and recorded in the computer each second. All above conditions are used in the melting process of pure paraffin wax.

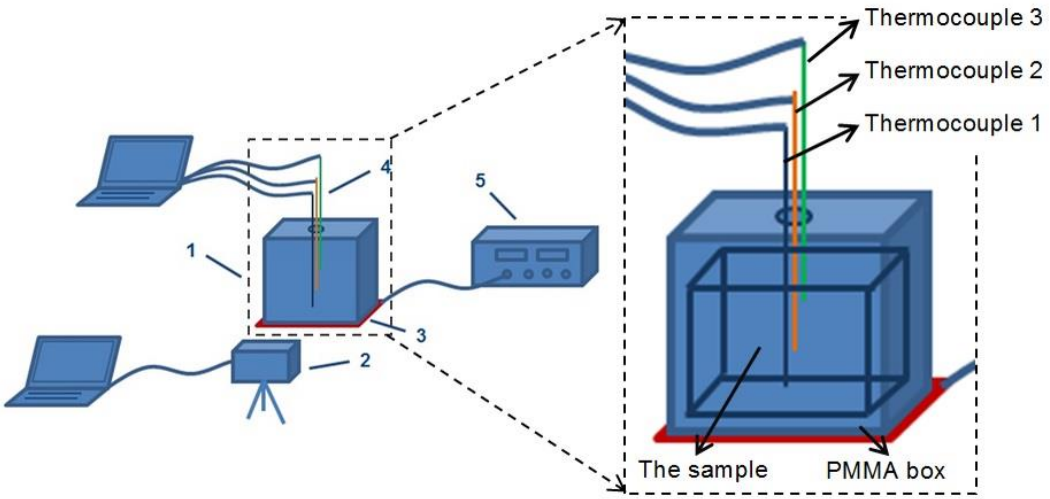

Figure 4.5 Schematic presentation of the experimental equipment (1- PMMA box and the sample, 2- infrared thermal imaging camera, 3- Heating film, 4- Thermocouples, 5- Power supply)

4.3 Results and Discussion

4.3.1 Effect of metal foam microstructures

The addition of metal foam has two main effects on the melting process of composite, the increase of the effective thermal conductivity and the suppression of natural convection. These two effects are largely determined by the microstructures and thermal properties of metal foam.

The aluminum foam can be considered as heat source because aluminum has a much higher thermal conductivity than the paraffin wax. As shown by the arrows in Figure 4.6, the paraffin begins to melt from the interface of paraffin wax and aluminum. Therefore, the paraffin wax which is far away from the heating film

could be heated by aluminum foam at the beginning of melting process. It can be also explained through a temperature distribution which is shown in Figure 4.7. These zones with higher temperature than surrounding in this figure are always aluminum. The aluminum foam can transfer heat flux more efficiently from the heating surface to paraffin through the foam skeleton. Moreover, the aluminum foam separates the paraffin wax into small parts and heats them separately. Thereby, the heat transfer efficiency of composite is greatly improved.

The natural convection plays an important role during the melting process of pure paraffin wax. When solid paraffin wax near the heating surface becomes liquid, the natural convection appears and dominates gradually the heat transfer. The liquid paraffin wax near heating film absorbs heat and becomes lighter than other liquid paraffin wax far away from the heating film, and then the hotter and lighter melted paraffin wax flows upward and the colder paraffin wax flows downward caused by buoyancy force. However, the addition of aluminum foam with low permeability greatly restricts the flow of liquid paraffin wax, which weakens the natural convection in composite. According the study of Sundarram and Li (2014), the influence of natural circulation could be ignored because of the small pore size of metal foam. However, the natural circulation must be considered in this study due to the big pore size and big windows between pores of aluminum foam.

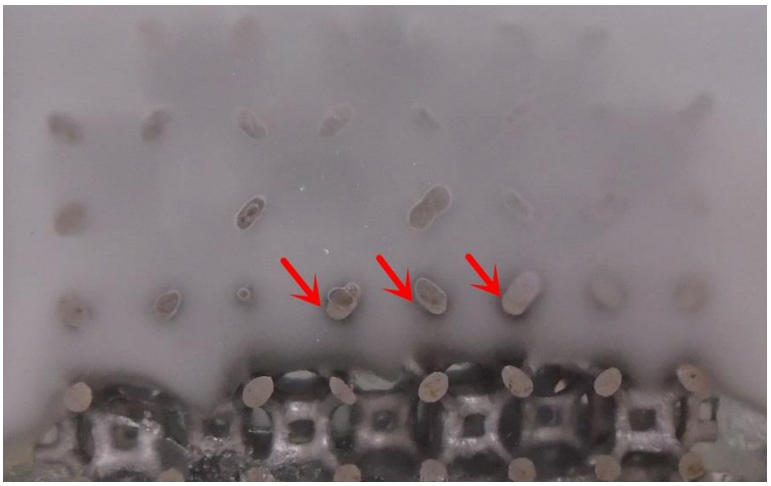

Figure 4.6 Taken picture of melting process at 2100 second

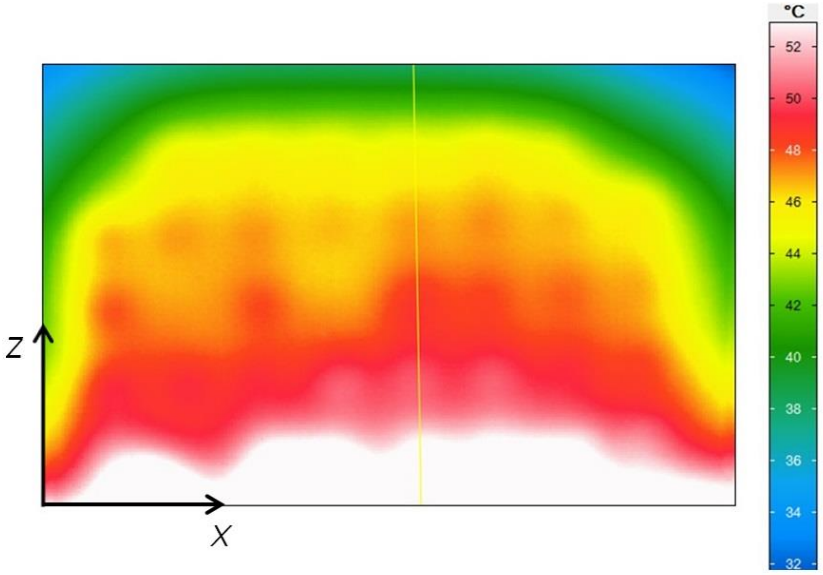

Figure 4.7 Temperature distribution obtained by infrared thermal imaging camera at 2100 second

4.3.2 Temperature variations of the detected points

Three curves (P1, P2 and P3) of temperature variation with time of pure paraffin wax are shown in Figure 4.8. The spatial locations of these detected points have

been shown in Figure 4.5. It can be seen that the temperature variations of these three different points are not uniform. The temperature of upper detected points is higher than the temperature of lower points. The heat is transferred from heating film to paraffin wax, hence the temperatures of detected points near the heating film increase faster than those far away from the heating film. Two factors can affect the heat transfer in the melting process of paraffin wax: thermal conduction and natural convection of liquid paraffin wax. In the initial period, the thermal conduction of solid paraffin wax plays a dominant role in heat transfer. Due to the low thermal conductivity of paraffin wax, the temperature increases slowly in this period. As the temperature increases, more and more solid paraffin melts and becomes liquid. Thereby, the natural convection dominates gradually the heat transfer of melting process as previously discussed. This phenomenon can be confirmed by the fluctuations of temperature variation curves above 60℃. These fluctuations show that liquid paraffin with different temperatures flows through each detected point. The natural convection of melted paraffin wax is more efficient than thermal conduction of solid paraffin wax, so the temperature increases in this period greatly faster than that in the period dominated by thermal conduction.

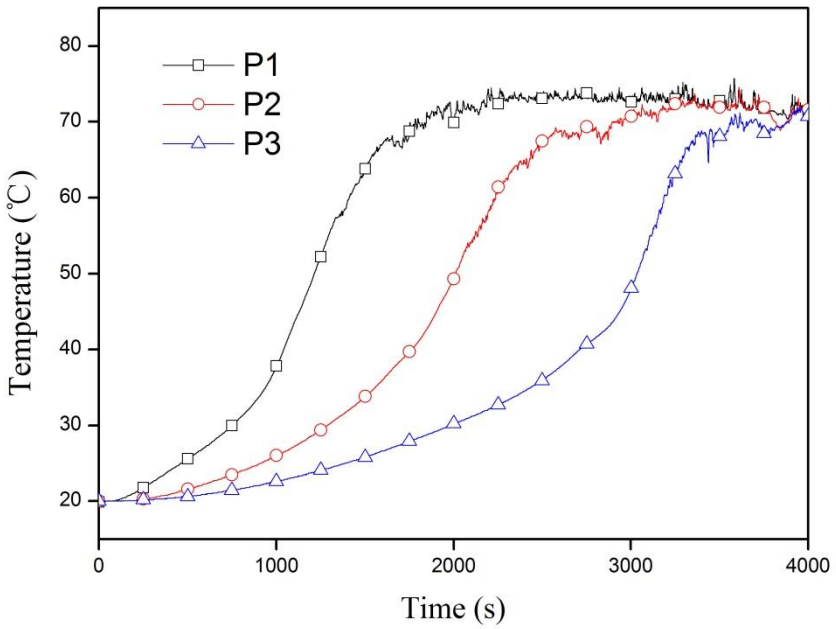

Figure 4.8 Temperature variations of Point 1, 2 and 3 during melting process for the pure paraffin

Figure 4.9 shows three curves (P4, P5 and P6) of the temperature variations with time of composite. The detected points have the same locations as P1, P2 and P3. Similar to the melting process of pure paraffin wax, the temperature of upper detected points is higher than the temperature of lower points. However, the curves of temperature variation shown in Figure 4.9 are much more synchronous. As previously explained, the metal foam increases largely the effective thermal conduction of composite, so at the same initial period, the temperatures of detected points all increase faster than the detected points in paraffin wax. Besides, an endothermic temperature span for latent heat can be clearly observed in Figure 4.9. But in pure paraffin wax, there is no clear endothermic temperature span because of the strong natural convection which mixes liquid paraffin wax with high and

low temperature. However, comparing to endothermic temperature span during the melting process of composite made by small pore size metal foam in the experimental study of Yang et al. (2016a), the endothermic temperature span in this study is not distinct. The liquid paraffin wax is restricted by the porous structure of metal foam, so the flow is weak. The big pore size and big window size of metal foam in this study lead to a significant permeability. Thereby, the natural convection still plays an important role in the melting process of composite. The curve fluctuations above 60℃ in Figure 4.9 also show that there are both thermal conduction and natural convection during the melting process of composite.

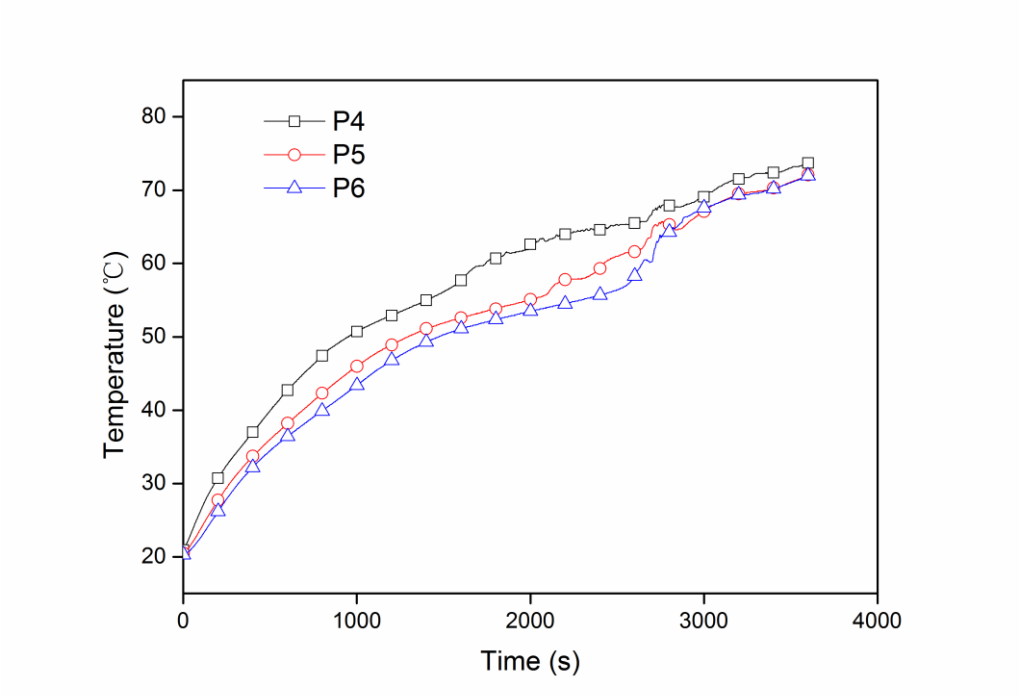

Figure 4.9 Temperature variations of Point 4, 5 and 6 during melting process for the composite

4.3.3 Difference of Temperature

As shown in Figure 4.8 and Figure 4.9, in the middle period of melting process, the temperature difference of composite is much smaller than that of pure paraffin, which demonstrates that the stratifications in temperature of composite is weak. To analyze quantitatively the temperature differences in two samples, two curves of temperature difference are shown in Figure 4.10. The temperature difference between point 1 and 3 has been compared with the temperature difference between point 4 and 6. It can be seen that the temperature difference of point 4 and 6 varies between 0℃ and 8℃. However, the temperature difference of point 1 and 3 reaches 32℃ which is 4 times more than that of point 4 and 6. The natural convection dominates the heat transfer in the liquid zone of pure paraffin wax sample, so the temperature of the liquid zone is more uniform and higher than that of solid zone. However, the low thermal conductivity of solid paraffin wax still affects the increment of temperature in solid zone. When the paraffin wax at point 1 begins to melt and the paraffin at point 3 is still solid, the temperature difference increases until 32 ℃ as shown in Fig 10. As shown in Figure8, when the temperature of point 1 stops the rapid increment around 1800s, the temperature rise rate of point 3 also begins to increase. Therefore, the temperature difference between point 1 and 3 begins to decrease after 1800s, as presented in Figure 4.10. The natural convection could lead to a uniform temperature distribution in the liquid zone, so when point 1 and 3 are both in the natural convection zone, the temperature difference between them become smaller and smaller, until reaching around zero. However, during the melting process of composite, the temperature difference between P4 and P6 varies in a small range. Comparing with the pure

paraffin wax sample, the effective thermal conductivity of composite is much higher and the natural convection in the liquid zone of composite is suppressed due to the addition of metal foam. Thus, the temperature distribution is much more uniform, and the variation of the temperature difference is relatively small.

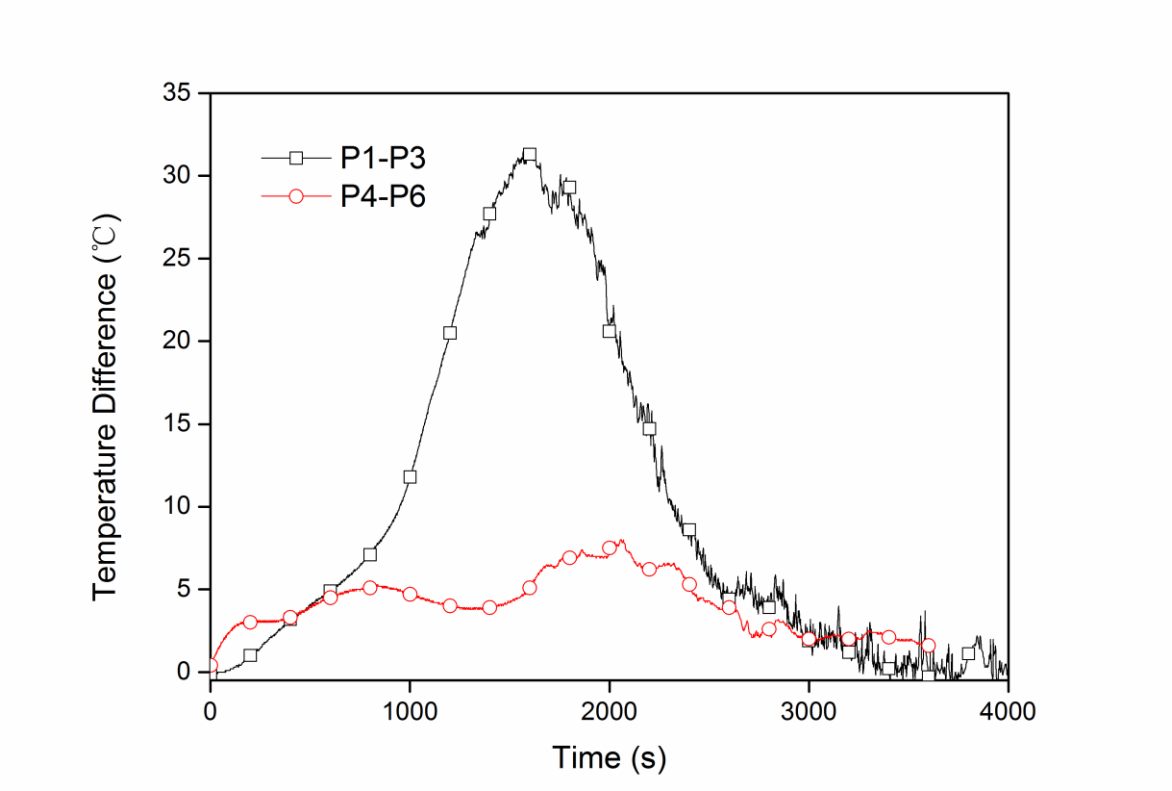

Figure 4.10 Temperature Difference between point 1 and 3, point 4 and 6

4.4 Conclusion

This study presents a manufacturing method of open-cell metal foams combining traditional casting process and advanced 3D printing technology. This method offers a possibility to manufacturing complex structures which can be designed and modified according to different constraints. The aim was to realize aluminum

foam with the help of a rapid tooling and a casting process in order to improve the thermal conductivity and the thermal storage of composite. The approach shows that the process efficiency through the generation of structural foam is able to manage some thermal exchanges. The thermal results show that the periodic open-cell aluminum foam not only improves greatly the effective thermal conductivity of composite, but also allow the effect of natural convection. There by improving significantly the thermal performance of systems. Moreover, the rapid tooling is developed with hope to improve the classical fabrication technologies through an alternative tooling. The rapid tooling opens perspectives in the realization of complex geometries through the AM technologies and precisely the 3DP into this study in order to realize a powder mold oriented casting.

Chapter 5 Conclusions and perspectives

5.1 Conclusion

This thesis mainly contains three parts, the improvement and upgrading of the manufacturing method, the pore-scale modeling of metal foams and manufacturing method of the periodic open-cell composite foams by combining the traditional manufacturing method and additive manufacturing technology.

In the chapter of bibliography, the microscopic structures of metal foams, the mechanical and thermal properties and the AM technology are generally introduced. After many years of manufacturing development, several manufacturing methods are already mature, which offers necessary experience for the improvement and upgrading. The numerical modeling of the porous structure makes the numerical simulations possible. Therefore, the comparison of porosities and structures could be achieved. The AM technology offers a possibility to obtain periodic aluminum foams with a designed structure.

In the second chapter, the improvement and upgrading of the traditional manufacturing method are achieved. The results show that the optimized and upgraded manufacturing method is effective. After the improvement and upgrading methods, the value of the negative pressure which is applied during the manufacturing process is steady and accurately controlled. The results show that the value of the negative pressure affects the porosities of the aluminum foam simples. The porosities of aluminum foams under different negative pressures are numerically compared. The results show that the porosity of aluminum foam decreases as the negative pressure decreases. The experimental results are consistent well with the previous theoretical explanation. After the vibration of the

preform, the experimental results show that the general trend of aluminum foam porosity is still reduced with the decrease of the negative pressure, just as the experimental results without vibration. The porosity of aluminum foam with different negative pressure was increased by about 6%. After the improvement and upgrading, the porosity of aluminum foams could be controlled within a certain range by adjusting the negative pressure and vibration. The aluminum foams with different porosities could benefit different application conditions, which greatly expands the application domains.

In the third chapter, a modified Kelvin model is developed to represent high mechanical property metal foams by comparing with experimental results. The melting processes of paraffin in high mechanical property and high porosity metal foams are studied. Metal foam plays an important role in the melting process of PCMs by separating PCMs in very small pieces and heating separately them, thereby reducing largely the melting time. For high mechanical property metal foams, even though the heat storage amount of systems is less, the melting process becomes much shorter than high porosity metal foams. As a result, the energy storage systems which are made by high mechanical property metal foams could store effectively the heat in a very short time.

In the fourth chapter, a manufacturing method of open-cell metal foams combining traditional casting process and advanced 3D printing technology is introduced. This method offers a possibility to manufacturing complex structures which can be designed and modified according to different constraints. The aim was to realize aluminum foam with the help of a rapid tooling and a casting process in order to improve the thermal conductivity and the thermal storage of composite. The

approach shows that the process efficiency through the generation of structural foam is able to manage some thermal exchanges. The thermal results show that the periodic open-cell aluminum foam not only improves greatly the effective thermal conductivity of composite, but also allow the effect of natural convection. There by improving significantly the thermal performance of systems. Moreover, the rapid tooling is developed with hope to improve the classical fabrication technologies through an alternative tooling. The rapid tooling opens perspectives in the realization of complex geometries through the AM technologies and precisely the 3DP into this study in order to realize a powder mold oriented casting.

5.2 Perspectives

This thesis focuses on the manufacturing method upgrading, the thermal performance of energy storage systems using aluminum foams/PCM composite and the novel manufacturing method based on AM technology. For the future research, some aspects are needed to be furtherly studied.

1. The preparation of aluminum foams with graded porosity or specific designed structures

Thanks to 3D printing technology, the mold with different porosities and different structures could be obtained. Combining these molds, the aluminum foams with graded porosity and different designed structures could be prepared by the novel manufacturing method. Besides, their thermal performance and other properties also need further investigation.

2. The effect of different kinds of PCMs on the energy storage systems.

According to various application conditions, the different kinds of PCMs should be applied. Thus, in order to ameliorate the performance of the composite, the melting processes of some other PCMs need to be analyzed experimentally.

3. The energy release of energy storage systems

The energy release process is an important performance of energy storage systems, and it could be also improved by aluminum foams. If we want to improve this process, some parameters of the aluminum foams need to be modified, such as container sharp, the material of cold wall or the structure of aluminum foams.

Chapter 6 Résumé en français

6.1 Introduction

Les mousses métalliques (tels que: les mousses d'aluminium, les mousses de nickel…) sont largement utilisées grâce aux propriétés intéressantes que leurs confèrent leurs microstructures. Ils ont une faible densité, une excellente capacité d'absorption d'énergie, une surface spécifique très étendue leur conférant de bonnes performances de transfert de chaleur, une bonne capacité d'absorption acoustique…Particulièrement les mousses d'aluminium à pores ouverts sont des matériaux fonctionnels prometteurs qui pourraient être largement utilisé dans le domaine de stockage d'énergie. Les propriétés mécaniques de ces mousses ont fait l'objet de nombreuses études depuis les années 90. Notamment au sein de l'équipe ICD-Lasmis, plusieurs travaux de recherches sur l'étude les mousses ont été réalisés (He, 2004; Liu, 2007b). Dans cette thèse l'étude est focalisée sur l'analyse de l'effet de l'utilisation des mousses composites d'aluminium et matériaux à changement de phase (MCP) sur l'amélioration des propriétés de transfert thermique.

Dans un premier temps, le procédé d'élaboration des mousses d'aluminium avec la méthode d'infiltration à pression négative est présenté. Les avantages et les limitations du procédé sont ensuite analysés. Ainsi, les méthodes d'amélioration sont proposées et réalisées. Après les méthodes d'amélioration, les propriétés des mousses d'aluminium pourraient être contrôlées précisément. Les porosités des mousses d'aluminium sous différentes pressions négatives sont comparées.

Dans un second temps, un modèle de mousse métallique à pores ouverts est proposé et validé par comparaison avec des résultats expérimentaux. Les processus de fusion de la paraffine dans deux modèles sont simulé numériques et les résultats sont comparés et discutés.

Finalement, le procédé d'élaboration des mousses d'aluminium à pores ouverts périodiques se basant sur les techniques d'impression 3D est présenté. Cette méthode d'élaboration originale a permis un meilleur contrôle paramètres morphologiques et géométriques des mousses d'aluminium à pores ouverts adapté aux besoins des applications. Les mousses ainsi obtenus sont caractérisés par des pores de forme tétrakaidécaèdrale, et leurs performances de stockage d'énergie thermique ont été étudiées.

6.2 Elaboration des mousses d'aluminium

6.2.1 Méthode d'élaboration classique des mousses d'aluminium

Dans le procédé classique de l'infiltration à pression négative, la structure des mousses d'aluminium est basée sur la préforme de sel. La forme et la taille des pores des mousses d'aluminium émanent directement de la forme géométrique non régulière des particules de sels. Afin de contrôler au mieux la dispersion la forme et la taille des cellules, les particules de sel qui sont triés par un système vibrant composé de 7 tamis de différentes tailles (AS 200 basic Retsch®). Il est donc

possible de séparer les particules en sept tailles différentes selon les diamètres suivants: 1.9mm, 1.6mm, 1.25mm, 1.0mm, 0.8mm, 0.58mm et 0.365mm.

Après tamisage, les particules solubles de sel ayant la même taille sont placées dans un moule de forme cylindrique en inox et un compactage léger est réalisé afin d'assurer une porosité homogène. Notons qu'un chauffage préalable de la préforme est nécessaire dans le but d'éviter la solidification de l'aluminium au début du processus d'infiltration. Ce procédé est réalisé dans un four à chambre, Labotherm N61/H de Nabertherm. La température pendant le préchauffage doit évoluer aussi lentement que possible jusqu'à 620 °C afin d'assurer une température le plus homogène que possible évitant ainsi la fissuration des particules favorisée par les gradients de température.

L'alliage d'aluminium fondu, est coulé en imposant une pression négative dans le moule placé sur un support en acier inoxydable. Comme le montre la Figure 6.1, l'aspiration de la coulée de l'aluminium est assurée par une pompe à vide qui est contrôlée par une vanne.

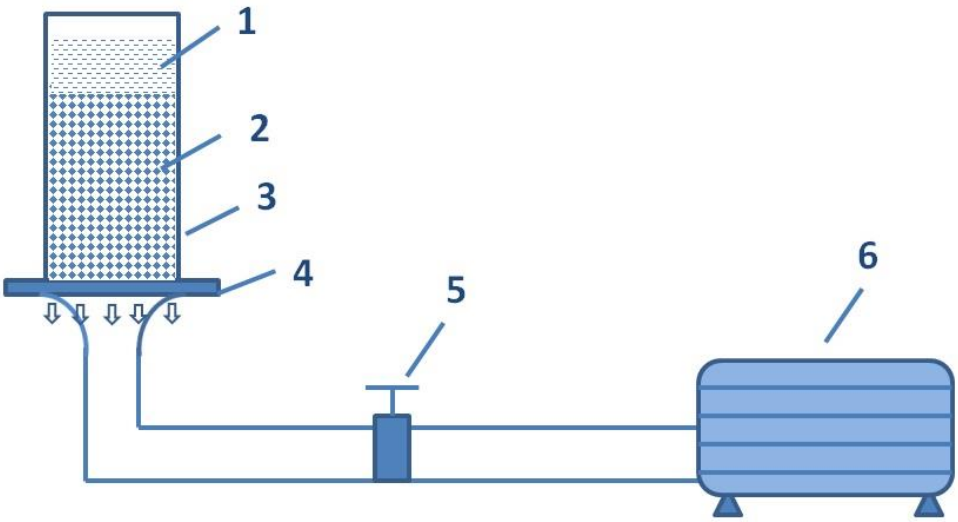

Figure 6.1 Principe d'élaboration des mousses d'aluminium à pores ouverts (1-aluminium fondu, 2-préforme (particules de sel), 3-moule en acier inoxydable, 4-plate-forme en acier inoxydable, 5-vanne, 6-pompe à vide)

6.2.2 Problèmes reliés à la méthode classique d'élaboration des mousses d'aluminium

Le processus classique d'élaboration des mousses d'aluminium relève plusieurs problèmes, tels que: le manque d'étanchéité, l'instabilité de la pression négative d'aspiration, le réglable de la pression négative, etc. Ces problèmes sont causés par les raisons suivante :

-L'étanchéité: après plusieurs cycles d'utilisation, des points de fuite d'air apparaissent dans les joints des tuyaux en fer. La corrosion par le sel réduit l'étanchéité du système.

-Stabilité de la pression négative d'aspiration: le volume de tuyau n'est pas assez grand pour fournir une pression négative stable pendant le processus d'élaboration.

-Réglable de la pression négative: en raison des deux problèmes ci-dessus, le réglable de la pression négative ne peut pas être suffisamment précis pendant l'infiltration. La pression négative ne peut qu'atteindre -0.8atm.

6.2.3 Amélioration du processus d'élaboration des mousses d'aluminium

L'élaboration améliorée des mousses d'aluminium est illustrée par la Figure 6.2. Un réservoir sous vide, un manomètre ainsi qu'une vanne supplémentaire sont ajoutés.

-Le réservoir sous ayant un volume 40 fois plus important que le volume du moule permet de maintenir la stabilité de la pression d'aspiration pendant le processus de l'élaboration,

-Le manomètre permet de contrôler la pression dans le réservoir sous vide,

-La vanne permet de contrôler l'ouverture et la fermeture de la conduite qui sépare la pompe et le réservoir sous vide.

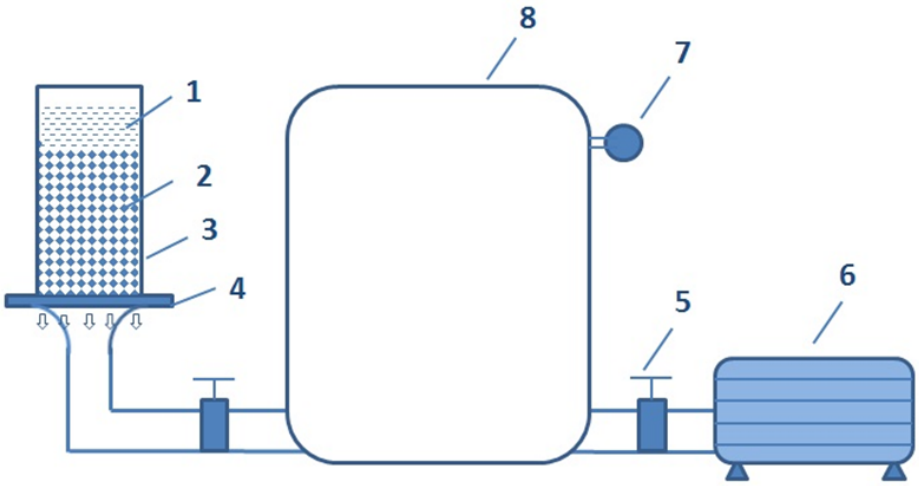

Figure 6.2 Principe d'élaboration améliorée des mousses d'aluminium (1-aluminium fondu, 2-préformes (particules de sel), 3-moule en acier inoxydable, 4-plate-forme en acier inoxydable, 5-vanne, 6-pompe à vide, 7-manomètres, 8-réservoir à vide)

6.2.4 Résultats expérimentaux des mousses d'aluminium élaborées sous différentes pressions négatives

Afin de mieux étudier la relation entre la pression négative d'aspiration et la porosité des mousses d'aluminium qui en résulte, nous avons choisi de mettre en œuvre la préforme avec les particules de sel le plus grandes taille possible (2 mm).

En considérant la taille de 2mm des particules de sel et en variant la pression négative d'aspiration, on constate une variation de la porosité des mousses. Dans la Figure 6.3 est donnée l'évolution de porosité en fonction de la pression négative qui montre clairement que la porosité décroit lorsque la pression tend vers la pression atmosphérique.

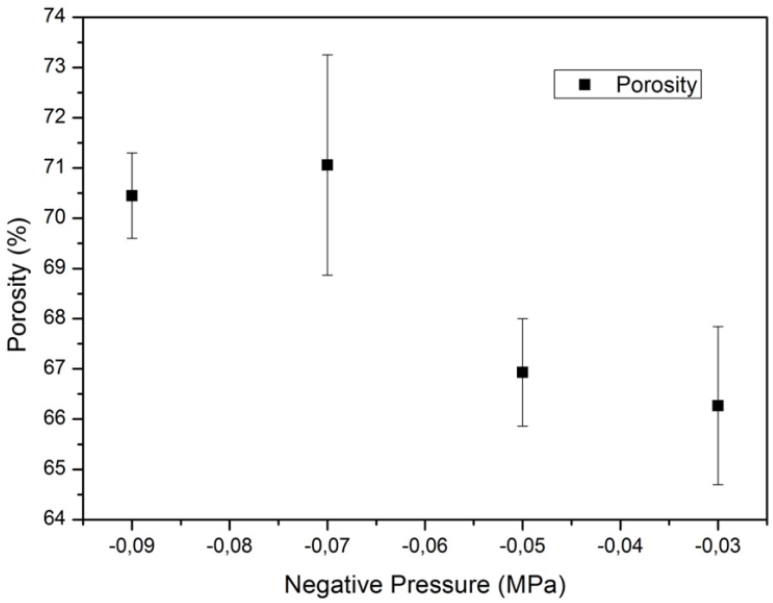

Figure 6.3 Porosités des mousses d'aluminium fabriquées sous différentes pressions négatives

L'ajout d'une vibration de la plaque de support pendant une durée de 20 minutes a permis de réduire les porosités d'une valeur moyenne de l'ordre de 6% comme le montre la Figure 6.4 avec une même tendance de la Figure 6.3.

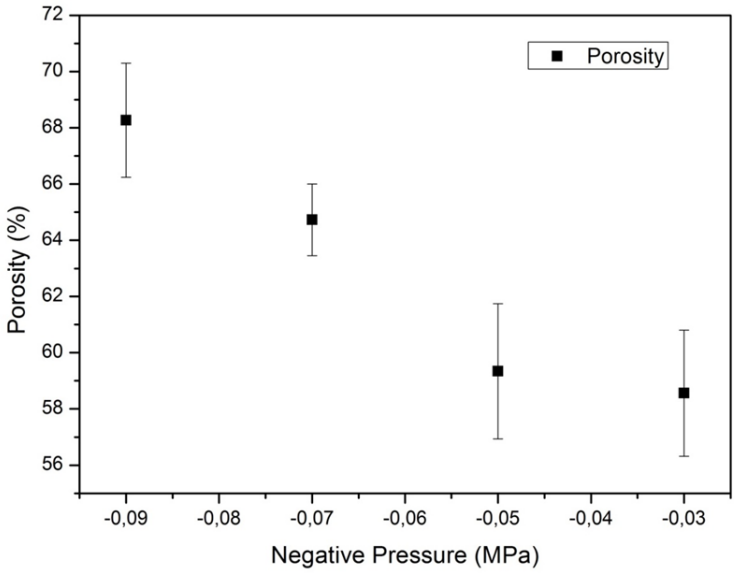

Figure 6.4 Porosités des mousses d'aluminium fabriquées sous différentes pressions négatives avec vibration

6.3 Modélisation et simulation numériques du comportement thermique des mousses composites

6.3.1 Méthodologie de modélisation

Le modèle de Kelvin (tétrakaidecaèdre) (Figure 6.5) est largement utilisé pour représenter les formes poreuses de mousses. Le modèle de Kelvin comme le montre la Figure 6.6 correspond à la structure réelle des mousses métalliques qui ont une porosité supérieure à 90% (Mousse d'aluminium à haute porosité / MAHP).

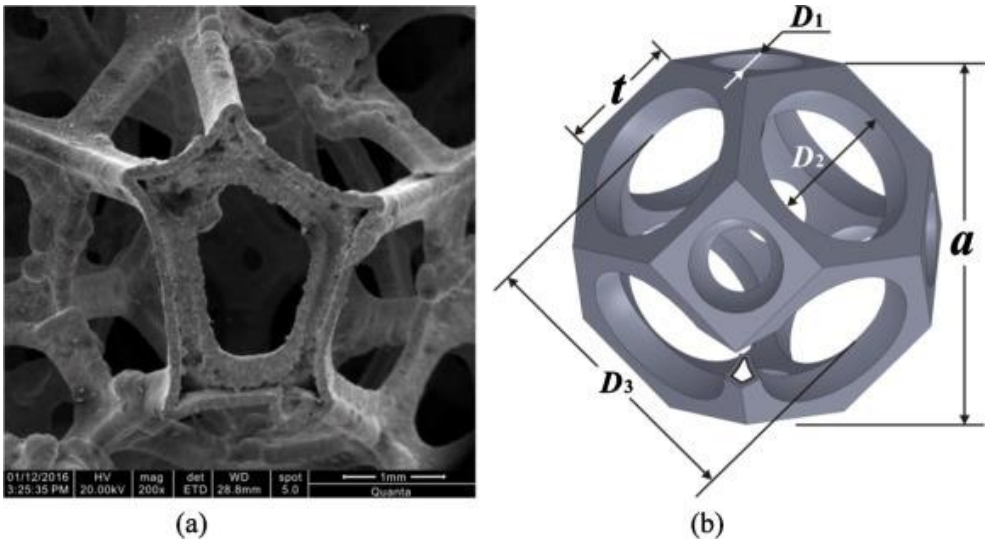

Figure 6.5 (a) SEM image de la mousse métallique à pore ouvert et (b) le modèle de Kelvin (tétrakaideca èdre)

Cependant, les mousses d'aluminium qui sont fabriqués par méthode d'infiltration à pression négative ne peuvent pas être représentées par le modèle de Kelvin (tétrakaideca èdre) vu qu'ils ont une structure différente comme indiqué dans Figure 6.6. De ce fait, un modèle de Kelvin modifié est proposé pour représenter les mousses d'aluminium à faible porosité (MAFP), comme le montre la Figure 6.7.

Figure 6.6 Observation de la structure de mousse d'aluminium à faible porosité (MAFP)

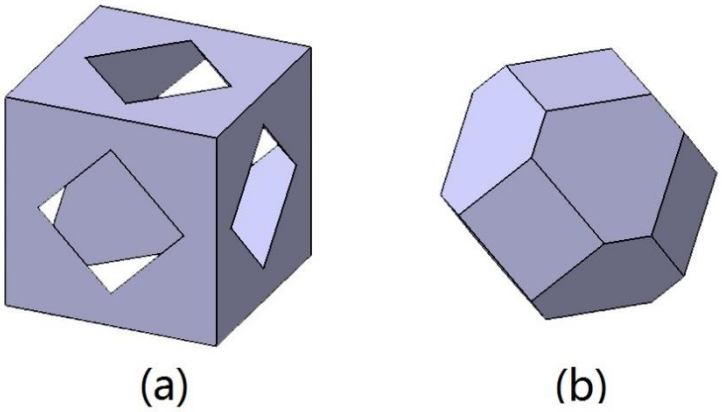

Figure 6.7 Modèle Kelvin modifié (porosité=65%), (a) partie métallique et (b) partie poreuse (tétrakaidécaèdre)

6.3.2 Modèle d'éléments finis

Le modèle d'éléments finis se compose de quatre unités qui représentent un système de stockage d'énergie comme le montre la Figure 6.8. Les simulations sont réalisées sur ANSYS Fluent®. La température de la surface de la chaleur est de 350K qui est supérieure à la température de fusion de paraffine (321K-335K). Les autres surfaces sont isolées. La température initiale des modèles est de 300K, ce qui rend la paraffine à l'état solide.

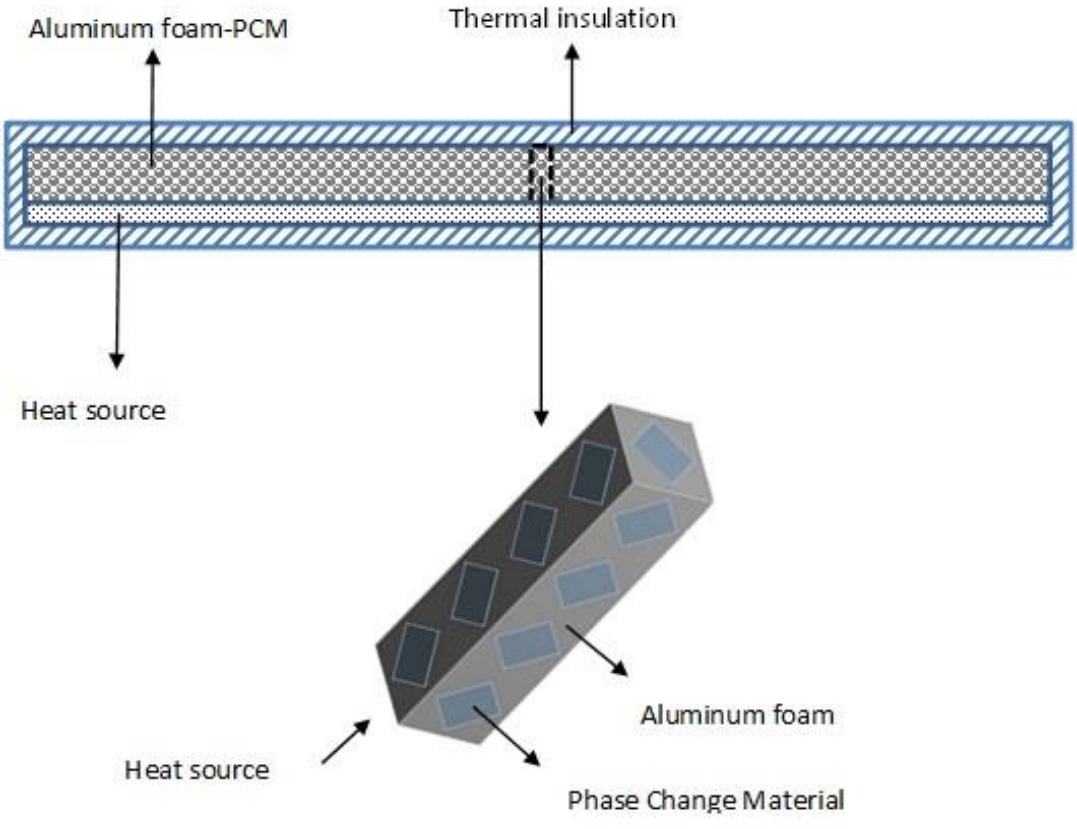

Figure 6.8 Système de stockage d'énergie de couche et son modèle représentatif

6.3.3 Résultats et discussions

-Comparaison de deux types de mousse d'aluminium

Pour observer le processus de transfert thermique entre la mousse et la paraffine, une section transversale au milieu du modèle est désignée comme surface d'observation pour chaque modèle. Les résultats des simulations en termes de cartes de température sont illustrés dans la Figure 6.9. Ces résultats montrent clairement l'effet de la porosité sur distribution de la température dans la mousse composite. On peut également constater que la paraffine change de phase (en

passant de l'état solide à l'état liquide) de l'interface avec les parois de la mousse vers le centre. La température qui règne dans les parois de la mousse d'aluminium est toujours plus élevée que la paraffine. Ce phénomène pourrait expliquer que la paraffine n'est pas seulement chauffée par la surface de la chaleur, mais aussi par les interfaces grâce à la haute conductivité thermique de l'aluminium.

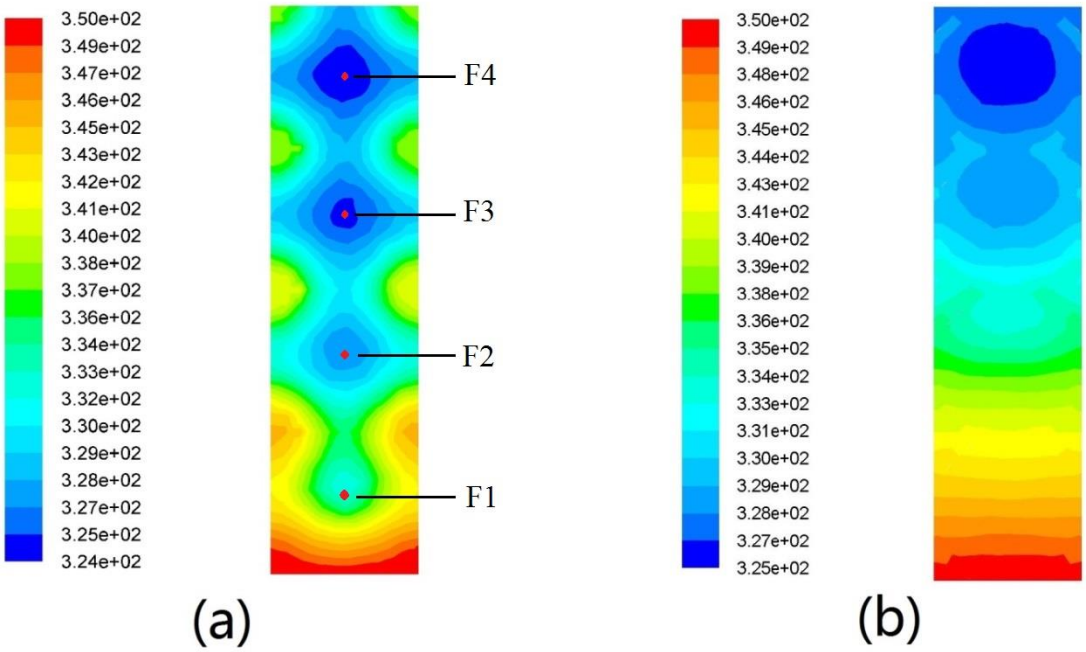

Figure 6.9 Les champs de température obtenus avec les deux modèles, (a) modèle modifié Kelvin (65% de porosité) et (b) modèle de Kelvin (porosité à 96%)

-Comparaison de mousse d'aluminium à faible porosité/pure paraffine composite (MAFP/PCM) et pure paraffine

Afin de comparer le processus de transfert thermique entre les parois de la mousse d'aluminium et la paraffine et notamment le changement de phase de la paraffine en différentes cellules du modèle , huit points représentatifs, F1, F2, F3 et F4 pour modèle modifié Kelvin (70% de porosité), P1, P2, P3 et P4 pour pure paraffine. Ils

se situent au centre de chaque unité de cube. La comparaison des évolutions de la température en fonction du temps dans les différents points considérés est donnée dans la Figure 6.10. Les courbes de température des quatre points du modèle de mousse composite à 70% de porosité sont comparables contrairement aux mêmes points dans la paraffine pure. Pour le cas de la mousse, le point F4 qui est le plus éloigné de la surface chauffée et dans lequel la température évolue le moins atteint néanmoins la température imposé au bout de 8 secondes de chauffage. Par contre, le même dans la paraffine pure (point P4) admet une évolution de la température beaucoup plus lente (1 °C au bout de 10 seconde). Notons que pour les deux cas les temps correspondant à la fusion complète de la paraffine sont respectivement de 5,8 secondes pour le cas de la mousse composite et de 337 secondes pour le cas de la paraffine pure. La comparaison montre que l'utilisation des mousses d'aluminium améliore considérablement le taux de fusion des systèmes de stockage d'énergie en réduisant ainsi les temps de stockage.

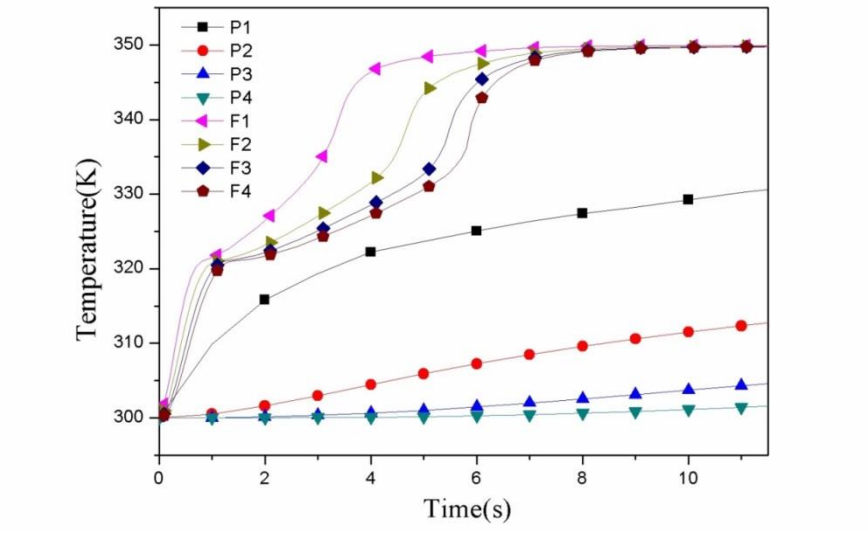

Figure 6.10 Variations de température de huit points dans la mousse composite MAFP/Paraffine et paraffine pure

-Comparaison de deux types de mousses composites

Le modèle de Kelvin modifié est adopté pour la mousse à (70% de porosité (MAFP/paraffine) et le modèle Kelvin est adopté pour la mousse à 96% de porosité (MAHP/paraffine). Dans la Figure 6.11 sont comparées les courbes d'évolution de fraction liquide de la paraffine des deux modèles. Pour le cas du modèle MAFP/paraffine, la fusion complète de paraffine survient au bout de 5,8 secondes, ce qui est beaucoup plus rapide que le cas du modèle (MAHP/paraffine) pour lequel la fusion complète survient après 28 secondes. L'étendu de la surface spécifique d'échange ainsi que quantité de matière métallique (ayant une plus grande inertie thermique) sont les facteurs le plus importants pour accélérer le transfert de chaleur.

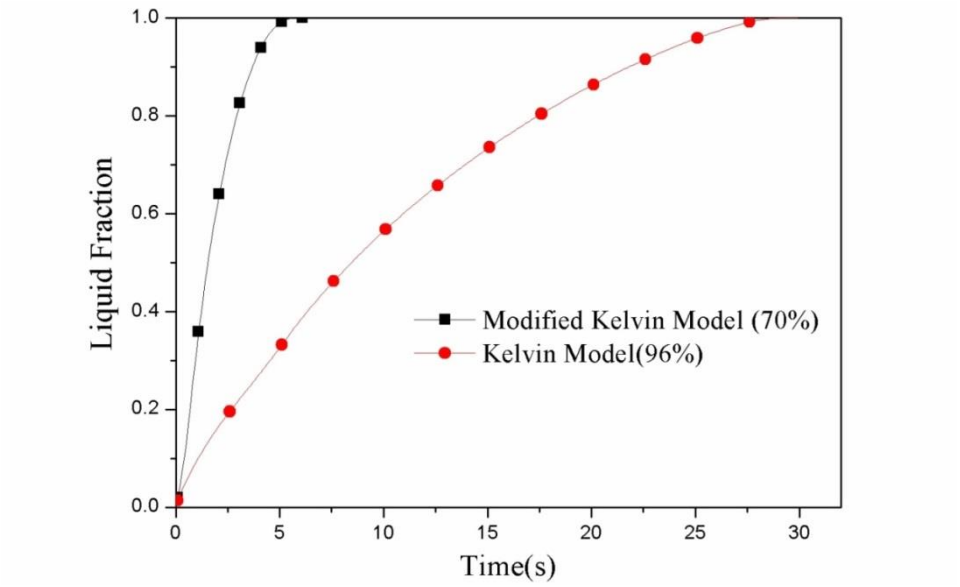

Figure 6.11 Comparaison en termes d'évolution de de la fraction liquide de paraffine obtenus avec les deux types de composites

-Effet de la porosité

D'après les résultats de la Figure 6.11 le modèle (MAFP/paraffine) présente des performances thermiques plus intéressantes pour l'utilisation dans les systèmes de stockage d'énergie. Pour voir de plus près l'effet de la porosité nous avons considéré avec le même modèle MAFP/paraffine trois porosités différentes (65%, 70% et 75%). Les courbes des évolutions de la fraction liquide des différentes porosités sont présentées dans la Figure 6.12. Dans cette figure on constate que le temps de fusion augmente avec l'augmentation de la porosité. Par conséquent, pour une faible porosité de la mousse, la masse excédante de l'aluminium favorise un transfert de chaleur plus rapide vers la paraffine, cependant la quantité de stockage de chaleur diminue en raison de la diminution de la fraction volumique de la paraffine.

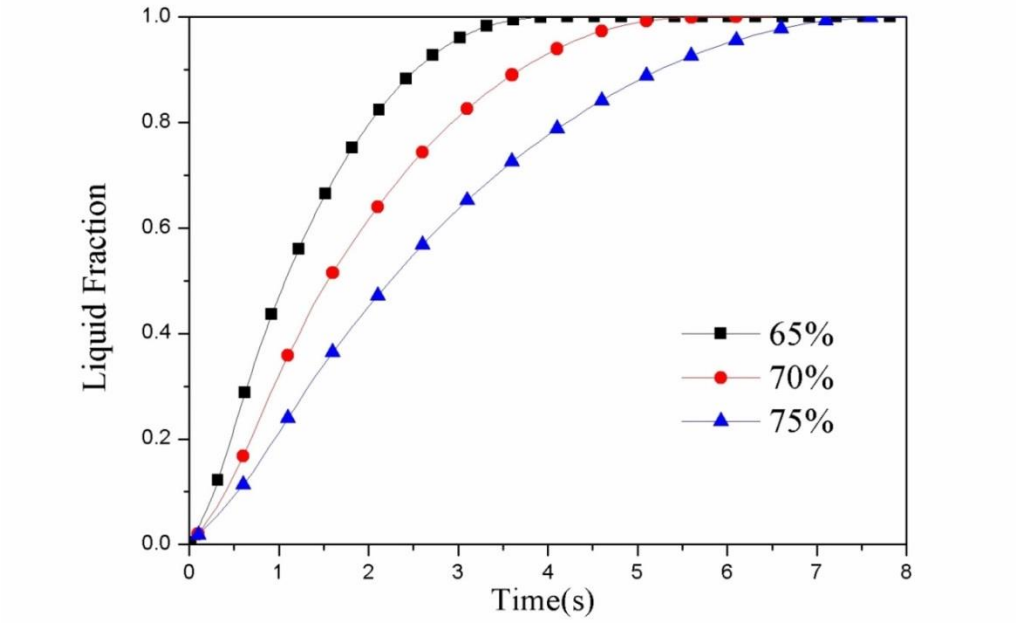

Figure 6.12 Variations de la fraction liquide de la paraffine pour les trois cas de porosité du modèle MAFP/Paraffine.

6.4 Etude du Comportement thermique des mousses d'aluminium dont le processus de fabrication est basé sur la technique d'impression 3D

6.4.1 Elaboration du moule par impression 3D du plâtre

Dans l'imprimante 3D (ProJet® 460 Plus, 3D Systems, formerly ZCoporation), chaque couche est créée en étalant une mince couche de plâtre avec un rouleau à l'intérieur d'un plateau de fabrication. La poudre est liée par une tête d'impression en jetant liquide de liaison, comme le montre la Figure 6.13.

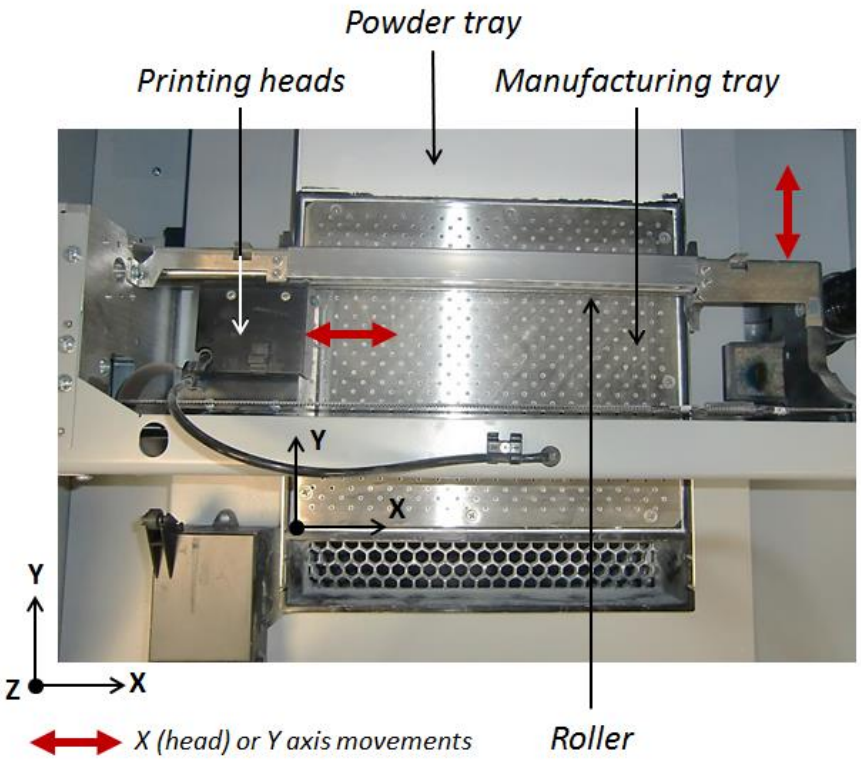

Figure 6.13 Chambre d'imprimante 3D

Le procédé d'élaboration des moules en plâtre est décrit par le graphe de la Figure 6.14, Dans ce procédé le moule imprimé en plâtre se substitue aux particules de sels dans le procédé classique.

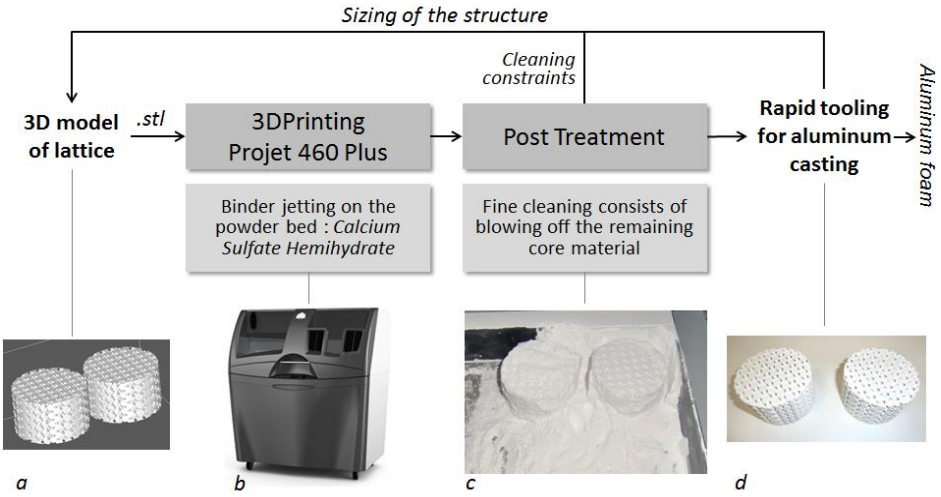

Figure 6.14 Processus de fabrication des moules à l'aide de l'impression 3D: a. Modèle 3D au format STL, b. 3D Printer Projet 460+, c. Pièces dans la poudre, d. Moules finals

Le moule de plâtre est placé dans le moule de la coulée d'aluminium pour réaliser le processus d'infiltration à pression négative. Comparé au procédé classique, ce procédé permet d'améliorer la stabilité de la préforme pour un meilleurs contrôle de la porosité des mousses d'aluminium obtenues. Ceci dit, après la coulée de l'aluminium le décrassement du plâtre emprisonné dans la mousse est une étape plus délicate que celle de l'élimination des particules de sel dans le procédé classique. Plusieurs méthodes ont été développées et testées pour enlever les moules en plâtre, tels que le rinçage avec de l'eau ou un acide faible, la vibration, le chauffage à haute température. Finalement la méthode adoptée consiste à

combiner les vibrations et le chauffage à haute température, qui permet d'enlever le plâtre facilement et entièrement. Dans Figure 6.15, l'illustrée l'échantillon final de mousse d'aluminium est obtenu.

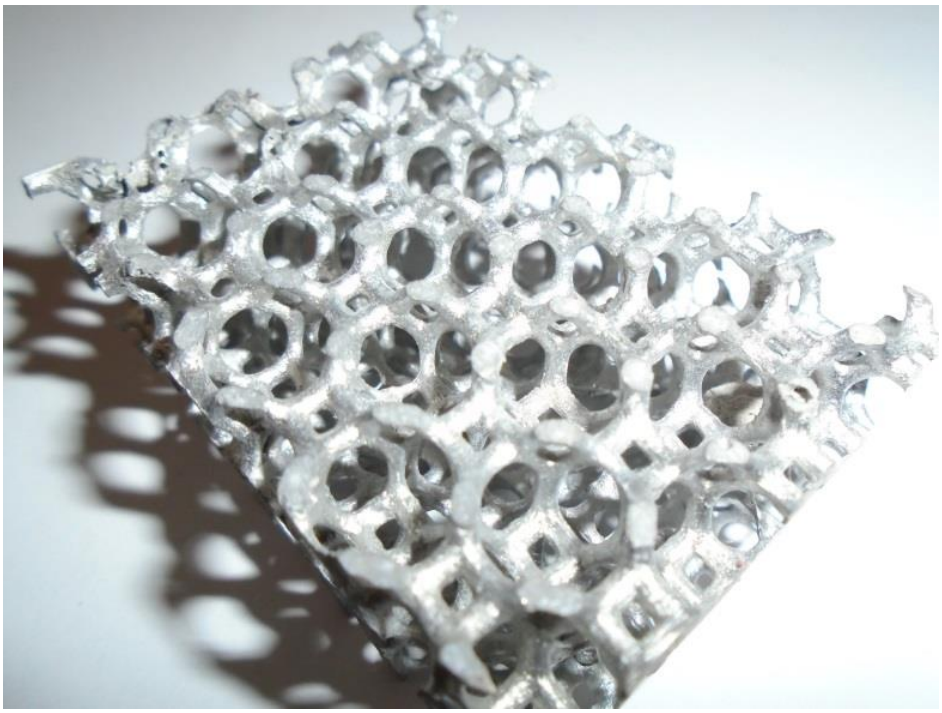

Figure 6.15 Mousse d'aluminium périodique fabriquée à l'aide d'un moule en plâtre issue de l''impression 3D

6.4.2 Dispositif et procédure d'étude expérimentale

Les dimensions des échantillons de mousse d'aluminium sont d'environ 60mm × 45mm × 20mm. Ces échantillons sont immergés dans paraffine liquide. Après refroidissement, on obtient un échantillon composite. Cet échantillon est placé dans une boîte en PMMA dont la surface inférieure est chauffée par un film chauffant. Le dispositif expérimental pour analyser le comportement thermique des mousses composite est illustré dans la Figure 6.16.

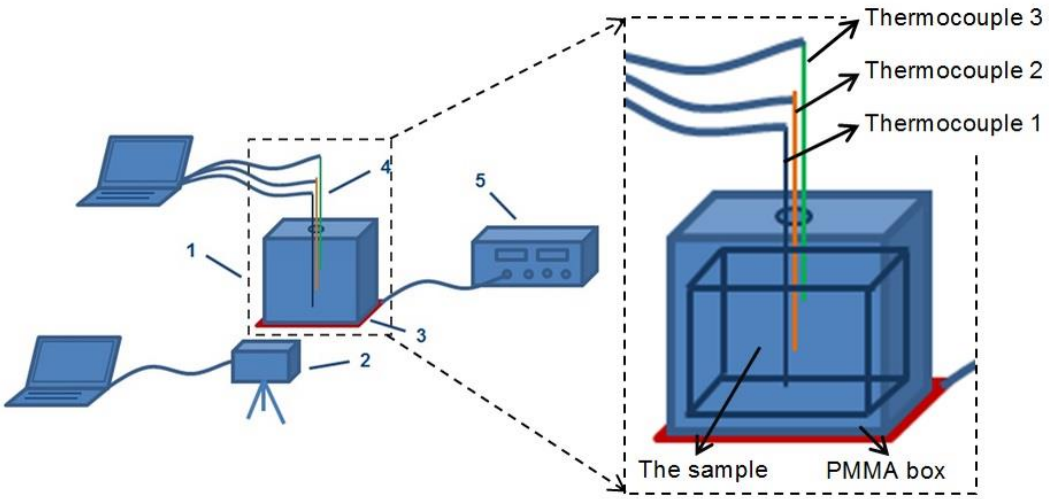

Figure 6.16 Présentation schématique de l'équipement expérimental (1-boîte PMMA et l'échantillon, 2-caméra infrarouge thermique, 3- film chauffant, 4-thermocouples, 5-alimentation)

6.4.3 Résultats et discussion

Comme le montrent les flèches dans la Figure 6.17, la paraffine commence à fondre à partir de l'interface avec les parois de la mousse d'aluminium. Par conséquent, la paraffine qui est trouvé loin du film chauffant perçoit la température de chauffage au bout d'un certain temps relativement faible que prendrait le processus de conduction thermique dans les parois de la mousse. Ceci est bien illustré dans la Figure 6.18 qui montre la distribution de la température obtenue par la caméra infrarouge après 2100 seconde sur une section longitudinale se trouvant au milieu de l'échantillon. Dans cette figure. Les zones ayant des températures plus élevées représentent toujours les parois de la mousse d'aluminium.

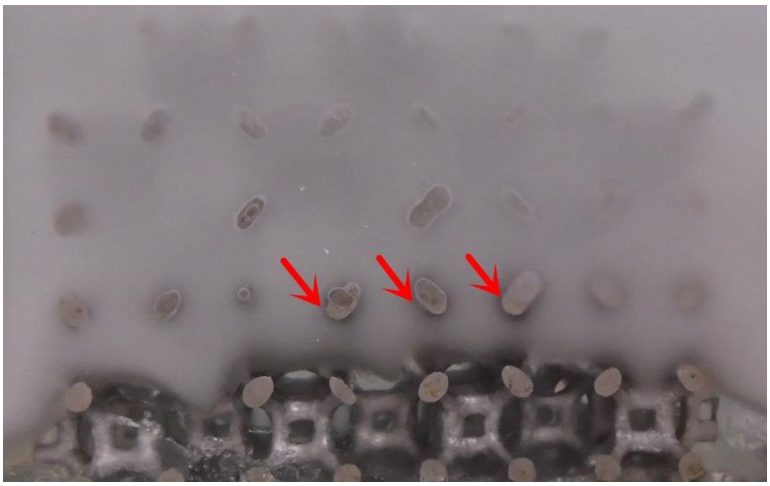

Figure 6.17 Image prise après 2100 secondes illustrant le processus de fusion de la paraffine dans la mousse d'aluminium.

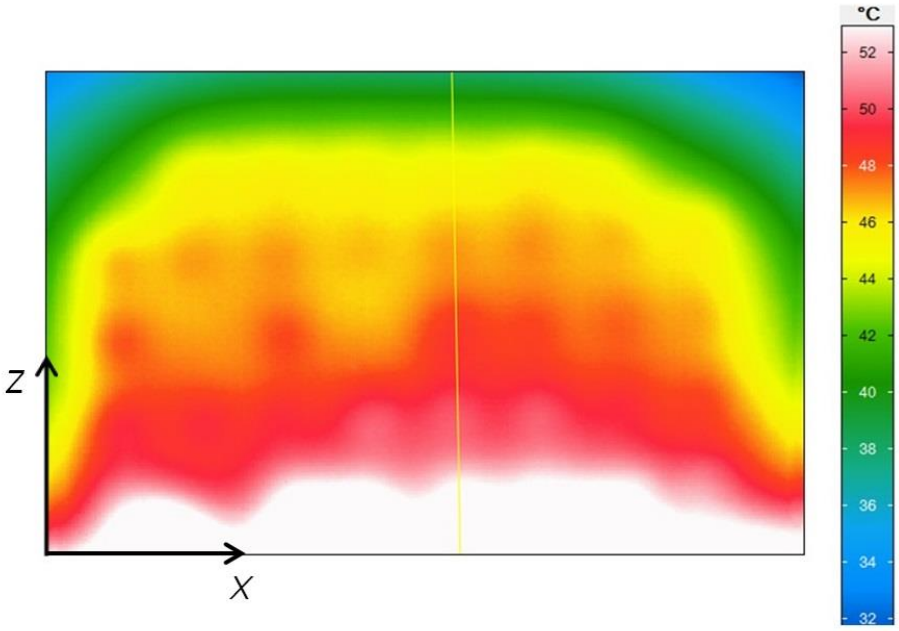

Figure 6.18 Distribution de la température obtenue par caméra infrarouge thermique après 2100 secondes

Dans la Figure 6.19 sont données les évolutions de la température pour le cas de paraffine pure dans les 3 points de mesure (P1, P2 et P3 illustrés dans la Figure 6.16). Les températures des points détectés au voisinage du film chauffant

évoluent plus rapidement que celles des points éloignés du film. Au début du processus, la conduction thermique de la paraffine solide joue un rôle dominant dans le transfert de chaleur. En raison de la faible conductivité thermique de la paraffine, la température évolue lentement pendant cette période.. Dès que la paraffine passe à l'état liquide la convection naturelle devient le phénomène dominant pour le transfert de chaleur et ainsi les évolutions de la température plus rapides.

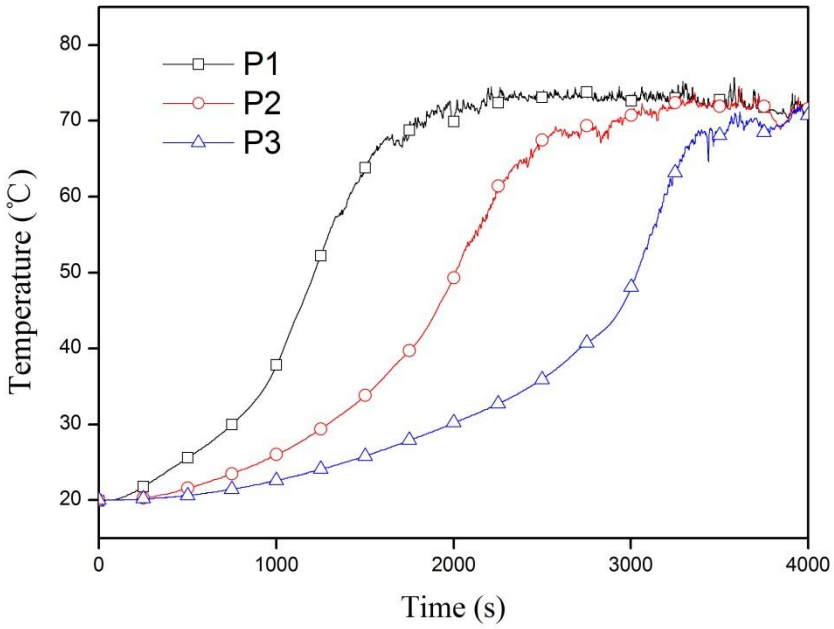

Figure 6.19 Variations de température dans les points de mesure P 1, P2 et P3 pendant le processus de fusion de la paraffine pure

Les résultats concernant l'échantillon en composite sont données dans la Figure 6.20 qui illustre la variation de la température des 3 points (P4, P5 et P6) qui se situent dans la phase paraffine et exactement aux mêmes positions que les points P1, P2 et P3. Les résultats montrent une réduction importante de la différence

entre les 3 mesures aux points P4, P5 et P6. Autrement dit, la température dans la phase paraffine devient plus homogène en présence de la mousse d'aluminium. . Cette dernière à cause de sa conductivité thermique importante et l'étendue de sa surface spécifique d'échange permet un meilleur transfert de chaleur de la source vers la paraffine.

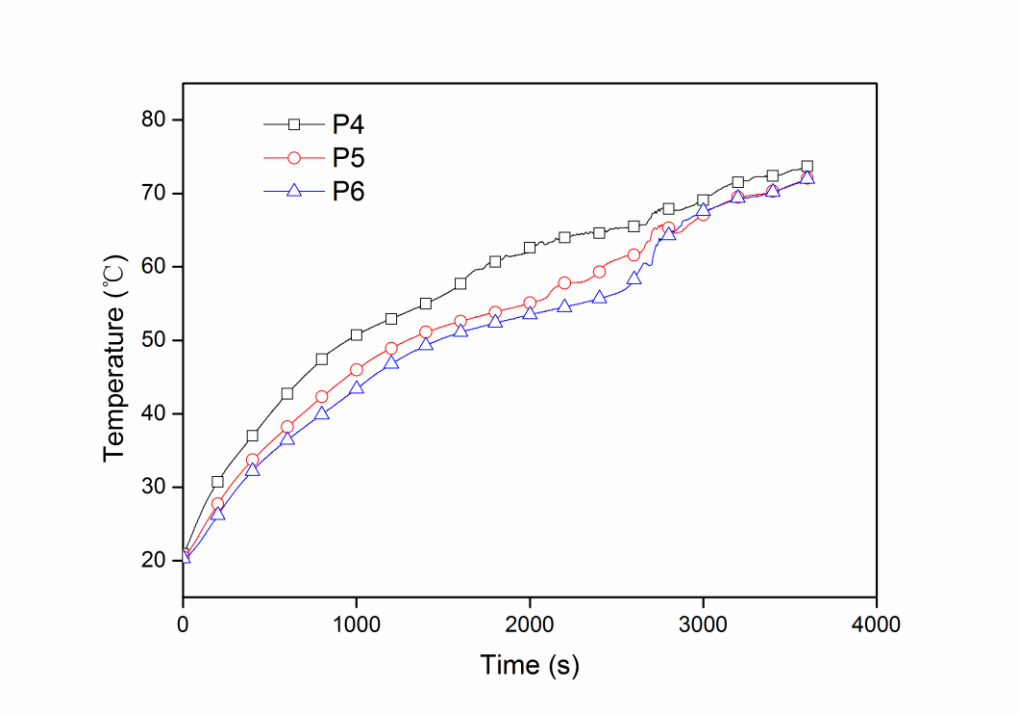

Figure 6.20 Variations de températures dans les points P4, P5 et P6 situés dans la phase paraffine.

Pour analyser quantitativement le gradient de température dans les deux échantillons (paraffine pure et composite), nous avons tracé dans la Figure 6.21. L'évolution de la différence de température entre deux points extrêmes de chaque échantillon les points P1 et P3 pour la paraffine pure et les points P4 et P6 pour le composite. A partir des courbes on constate que le gradient de température est beaucoup plus important dans la paraffine pure et qu'il atteint son maximum au

moment de la fusion de la paraffine pour atteindre une valeur de l'ordre de 6 fois plus importante que le cas du composite.. Ainsi, la distribution de la température est beaucoup plus homogène et la variation de la différence de température est relativement faible dans le composite.

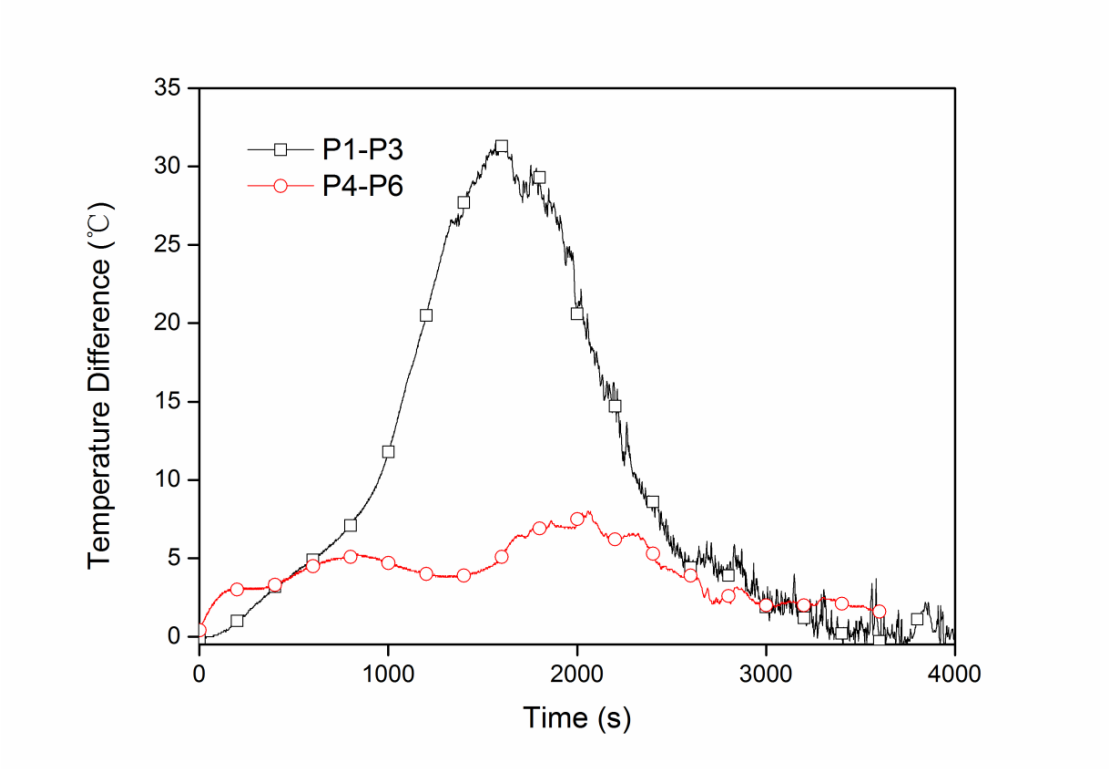

Figure 6.21 Différence de température entre les points 1 et 3, point 4 et 6

On a présenté une méthode de fabrication de mousses métalliques à pores ouverts en combinant la méthode classique et la technologie d'impression 3D. Cette méthode offre la possibilité d'élaborer r des structures complexes qui peuvent être conçues et modifiées selon les différents besoins d'application. Les résultats de l'étude thermiques montrent que les mousses d'aluminium à pores ouverts périodique améliorent les propriétés thermiques.

6.5 Conclusions

Cette thèse est composée principalement trois parties : l'amélioration de la méthode d'élaboration des mousses d'aluminium, la modélisation de la structure des mousses d'aluminium et enfin le développement de la méthode d'élaboration des mousses d'aluminium à ports ouverts périodiques en combinant la méthode classique et les techniques d'impression 3D.

L'amélioration de la méthodologie d'élaboration classique est réalisée. Les résultats montrent que les améliorations apportées l'amélioration ont concluants. Ces améliorations ont permis notamment de mieux contrôler la valeur de la pression négative appliquée pendant le processus de fabrication. Il importe de rappeler que la valeur de la pression négative affecte fortement les porosités des mousses d'aluminium. Les porosités des mousses d'aluminium sous différentes pressions négatives ont été comparées numériquement. Les résultats ont montés que les porosités décroissent avec la décroissance de la pression négative. Après la vibration de la préforme, la porosité de la mousse d'aluminium augmente d'environ 6%. Les mousses d'aluminium avec différentes porosités pourraient bénéficier à différentes conditions d'application, ce qui élargit les domaines d'application.

Un modèle Kelvin modifié est développé pour représenter des mousses d'aluminium à faible porosité en comparant les résultats expérimentaux. La mousse métallique joue un rôle important dans le processus de fusion de PCM en séparant le PCM en très petits morceaux et en les chauffant séparément, ce qui réduit considérablement le temps de fusion.

On a présenté une méthode de fabrication de mousses métalliques à pores ouverts en combinant la méthode classique et la technologie d'impression 3D. Cette méthode offre la possibilité de fabriquer des structures complexes qui peuvent être désignées et modifiées selon différentes demandes d'applications. Les résultats thermiques montrent que la mousse d'aluminium périodique à pore ouvert améliore la conductivité thermique de composite

References

Abhat, A., Low temperature latent heat thermal energy storage: Heat storage materials, Solar Energy, vol. 30, pp. 313-332, 1983.

Alvarez, G., Bournet, P.-E., Flick, D., Two-dimensional simulation of turbulent flow and transfer through stacked spheres, Int. J. Heat Mass Transfer, vol. 46, pp. 2459-2469, 2003.

Ambrosio, G., Bianco, N., Chiu, W.K.S., Iasiello, M., Naso, V., Oliviero, M., The effect of open-cell metal foams strut shape on convection heat transfer and pressure drop, Appl. Therm. Eng., vol. 103, pp. 333-343, 2016.

Andersen, O., Waag, U., Schneider, L., Stephani, G., Kieback, B., Novel metallic hollow sphere structures, Adv. Eng. Mater., vol. 2, pp. 192-195, 2000.

Antohe, B., Lage, J., Price, D., Weber, R.M., Numerical characterization of micro heat exchangers using experimentally tested porous aluminum layers, Int. J. Heat Fluid Flow, vol. 17, pp. 594-603, 1996.

Ashby, M.F., Evans, A.G., Fleck, N.A., Gibson, L.J., Hutchinson, J.W., Wadley, H.N.G., List of contributors, Metal Foams. Butterworth-Heinemann, Burlington, pp. xi-xii, 2000.

Ashley, S., Rapid prototyping is coming of age, Mech. Eng., vol. 117, pp. 62, 1995.

Baby, R., Balaji, C., Experimental investigations on thermal performance enhancement and effect of orientation on porous matrix filled PCM based heat sink, Int. Commun. Heat Mass, vol. 46, pp. 27-30, 2013a.

Baby, R., Balaji, C., Experimental investigations on thermal performance enhancement and effect of orientation on porous matrix filled PCM based heat sink, Int. Commun. Heat Mass, vol. 46, pp. 27-30, 2013b.

Bamorovat Abadi, G., Kim, K.C., Experimental heat transfer and pressure drop in a metal-foam-filled tube heat exchanger, Exp. Therm Fluid Sci., vol. 82, pp. 42-49, 2017.

Banhart, J., Manufacture, characterisation and application of cellular metals and metal foams, Prog. Mater Sci., vol. 46, pp. 559-632, 2001.

Beaman, J.J., Barlow, J.W., Bourell, D.L., Crawford, R.H., Marcus, H.L., McAlea, K.P., Solid freeform fabrication: a new direction in manufacturing, Kluwer Academic Publishers, Norwell, MA, vol. 2061, pp. 25-49, 1997.

Bekoz, N., Oktay, E., Mechanical properties of low alloy steel foams: Dependency on porosity and pore size, Mater. Sci. Eng., A, vol. 576, pp. 82-90, 2013.

Berchem, K., Mohr, U., Bleck, W., Controlling the degree of pore opening of metal sponges, prepared by the infiltration preparation method, Materials Science and Engineering: A, vol. 323, pp. 52-57, 2002.

Bhattacharya, A., Calmidi, V., Mahajan, R., Thermophysical properties of high porosity metal foams, Int. J. Heat Mass Transfer, vol. 45, pp. 1017-1031, 2002.

Boomsma, K., Poulikakos, D., Zwick, F., Metal foams as compact high performance heat exchangers, Mech. Mater., vol. 35, pp. 1161-1176, 2003.

Brezny, R., Green, D.J., The effect of cell size on the mechanical behavior of cellular materials, Acta metallurgica et materialia, vol. 38, pp. 2517-2526, 1990.

Chen, C., Lakes, R., Analysis of the structure-property relations of foam materials, Cell. Polym., vol. 14, pp. 186-202, 1995.

Chen, P., Gao, X., Wang, Y., Xu, T., Fang, Y., Zhang, Z., Metal foam embedded in SEBS/paraffin/HDPE form-stable PCMs for thermal energy storage, Sol. Energy Mater. Sol. Cells, vol. 149, pp. 60-65, 2016.

Chen, Z., Gao, D., Shi, J., Experimental and numerical study on melting of phase change materials in metal foams at pore scale, Int. J. Heat Mass Transfer, vol. 72, pp. 646-655, 2014.

Comb, J.W., Priedeman, W.R., Turley, P.W., FDM technology process improvements, Proceedings of Solid Freeform Fabrication Symposium. DTIC Document, pp. 42-49.

Deshpande, V., Fleck, N., Isotropic constitutive models for metallic foams, J. Mech. Phys. Solids, vol. 48, pp. 1253-1283, 2000.

Dopler, T., Modaressi, A., Michaud, V., Simulation of metal-matrix composite isothermal infiltration processing, Metallurgical and Materials Transactions B, vol. 31, pp. 225-234, 2000.

Excell, J., Nathan, S., The rise of additive manufacturing, The engineer, vol. 24, pp., 2010.

Garcia-Cordovilla, C., Louis, E., Narciso, J., Pressure infiltration of packed ceramic particulates by liquid metals, Acta Mater., vol. 47, pp. 4461-4479, 1999.

Gardan, J., Additive manufacturing technologies: state of the art and trends, Int. J. Prod. Res., vol., pp. 1-15, 2015.

Gibson, I., Rosen, D., Stucker, B., Additive manufacturing technologies: 3D printing, rapid prototyping, and direct digital manufacturing. Springer, 2014.

Gibson, I., Rosen, D.W., Stucker, B., Additive manufacturing technologies. Springer, 2010.

Gibson, L.J., Ashby, M.F., Cellular solids: structure and properties. Cambridge university press, 1999.

Goicoechea, J., Garcia-Cordovilla, C., Louis, E., Pamies, A., Surface tension of binary and ternary aluminium alloys of the systems Al-Si-Mg and Al-Zn-Mg, Journal of Materials Science, vol. 27, pp. 5247-5252, 1992.

Grenestedt, J.L., Bassinet, F., Influence of cell wall thickness variations on elastic stiffness of closed-cell cellular solids, International Journal of Mechanical Sciences, vol. 42, pp. 1327-1338, 2000.

Hasnain, S.M., Review on sustainable thermal energy storage technologies, part I: Heat storage materials and techniques, Energy Convers. Manage., vol. 39, pp. 1127-1138, 1998.

He, B., Setterwall, F., Technical grade paraffin waxes as phase change materials for cool thermal storage and cool storage systems capital cost estimation, Energy Convers. Manage., vol. 43, pp. 1709-1723, 2002.

He, S., Metallci foam and metal porou polymer composite (MPPC): manufacture and mechanical behavior, LASMIS. Universitt of Technology of Troyes, Troyes, France.

Huu, T.T., Lacroix, M., Pham Huu, C., Schweich, D., Edouard, D., Towards a more realistic modeling of solid foam: Use of the pentagonal dodecahedron geometry, Chem. Eng. Sci., vol. 64, pp. 5131-5142, 2009.

Inaba, H., Tu, P., Evaluation of thermophysical characteristics on shape-stabilized paraffin as a solid-liquid phase change material, Heat Mass Transfer., vol. 32, pp. 307-312, 1997.

Inayat, A., Schwerdtfeger, J., Freund, H., Körner, C., Singer, R.F., Schwieger, W., Periodic open-cell foams: Pressure drop measurements and modeling of an ideal tetrakaidecahedra packing, Chem. Eng. Sci., vol. 66, pp. 2758-2763, 2011.

Jacobs, P.F., Rapid prototyping & manufacturing: fundamentals of stereolithography. Society of Manufacturing Engineers, 1992.

Jie, Z., Dongqi, Z., Pengwei, W., Gang, W., Feng, L., Penglong, D., Numerical Simulation Research of Investment Casting for TiB2/A356 Aluminum Base Composite, Rare Metal Materials and Engineering, vol. 43, pp. 47-51, 2014.

JINZHU SONG, S.H., The heat transfer perfomance of porous aluminum foam, Jiangsu Metallurgy, vol. 36, pp. 28-30, 2008.

Kaviany, M., Laminar flow through a porous channel bounded by isothermal parallel plates, Int. J. Heat Mass Transfer, vol. 28, pp. 851-858, 1985.

Kousksou, T., Jamil, A., Rhafiki, T.E., Zeraouli, Y., Paraffin wax mixtures as phase change materials, Sol. Energy Mater. Sol. Cells, vol. 94, pp. 2158-2165, 2010.

Kumar, P., Topin, F., Simultaneous determination of intrinsic solid phase conductivity and effective thermal conductivity of Kelvin like foams, Appl. Therm. Eng., vol. 71, pp. 536-547, 2014.

Kuwahara, F., Yamane, T., Nakayama, A., Large eddy simulation of turbulent flow in porous media, Int. Commun. Heat Mass, vol. 33, pp. 411-418, 2006.

Lim, T.-J., Smith, B., McDowell, D., Behavior of a random hollow sphere metal foam, Acta Mater., vol. 50, pp. 2867-2879, 2002.

Lipson, H., Kurman, M., Fabricated: The New World of 3D Printing. Wiley, 2013.

Liu, Y., Elaboration et étude des propriétés mécaniques des mousses d'aluminium et des métaux poreux polymères composites. Troyes.

Liu, Y., Manufacture and Machanical Properties of Aluminium Foams and Metal Porous Polymeric Composites, Lasmis. Universty of Technology of Troyes, Troyes, France.

Liu, Z., Yao, Y., Wu, H., Numerical modeling for solid–liquid phase change phenomena in porous media: Shell-and-tube type latent heat thermal energy storage, Appl. Energy, vol. 112, pp. 1222-1232, 2013.

Lu, K., Hiser, M., Wu, W., Effect of particle size on three dimensional printed mesh structures, Powder Technol., vol. 192, pp. 178-183, 2009.

Lu, T., Stone, H., Ashby, M., Heat transfer in open-cell metal foams, Acta Mater., vol. 46, pp. 3619-3635, 1998.

Ma, L., Song, Z., He, D., Cellular structure controllable aluminium foams produced by high pressure infiltration process, Scripta Mater., vol. 41, pp. 785-789, 1999.

Maeda, K., Childs, T.H.C., Laser sintering (SLS) of hard metal powders for abrasion resistant coatings, J. Mater. Process. Technol., vol. 149, pp. 609-615, 2004.

Marcos H. J. Pedras, M.J.S.d.L., SIMULATION OF TURBULENT FLOW IN POROUS MEDIA USING A SPATIALLY PERIODIC ARRAY AND A LOW RE TWO-EQUATION CLOSURE, Numerical Heat Transfer, Part A: Applications, vol. 39, pp. 35-59, 2001.

Masur, L.J., Mortensen, A., Cornie, J.A., Flemings, M.C., Infiltration of fibrous preforms by a pure metal: Part II. Experiment, Metall. Trans. A, vol. 20, pp. 2549-2557, 1989.

Mazumder, J., Schifferer, A., Choi, J., Direct materials deposition: designed macro and microstructure, Mater. Res. Innovations, vol. 3, pp. 118-131, 1999.

Mellouli, S., Dhaou, H., Askri, F., Jemni, A., Nasrallah, S.B., Hydrogen storage in metal hydride tanks equipped with metal foam heat exchanger, Int. J. Hydrogen Energy, vol. 34, pp. 9393-9401, 2009.

Moeini Sedeh, M., Khodadadi, J.M., Thermal conductivity improvement of phase change materials/graphite foam composites, Carbon, vol. 60, pp. 117-128, 2013.

Mohammadian, S.K., Rassoulinejad-Mousavi, S.M., Zhang, Y., Thermal management improvement of an air-cooled high-power lithium-ion battery by embedding metal foam, J. Power Sources, vol. 296, pp. 305-313, 2015.

Molina, J.M., Piñero, E., Narciso, J., García-Cordovilla, C., Louis, E., Liquid metal infiltration into ceramic particle preforms with bimodal size distributions, Curr. Opin. Solid State Mater. Sci., vol. 9, pp. 202-210, 2005.

Mortensen, A., Masur, L.J., Cornie, J.A., Flemings, M.C., Infiltration of fibrous preforms by a pure metal: Part I. Theory, Metall. Trans. A, vol. 20, pp. 2535-2547, 1989.

Mortensen, A., Wong, T., Infiltration of fibrous preforms by a pure metal: Part III. capillary phenomena, Metall. Trans. A, vol. 21, pp. 2257-2263, 1990.

Mueller, B., Kochan, D., Laminated object manufacturing for rapid tooling and patternmaking in foundry industry, Computers in Industry, vol. 39, pp. 47-53, 1999.

Narayana, A., Research and Reviews: Journal of Chemistry, vol., pp.,

Nieh, T., Kinney, J., Wadsworth, J., Ladd, A., Morphology and elastic properties of aluminum foams produced by a casting technique, Scripta Mater., vol. 38, pp. 1487-1494, 1998.

Niu, X.P., Hu, B.H., Pinwill, I., Li, H., Vacuum assisted high pressure die casting of aluminium alloys, J. Mater. Process. Technol., vol. 105, pp. 119-127, 2000.

Peng, W., Xu, M., Li, X., Huai, X., Liu, Z., Wang, H., CFD study on thermal transport in open-cell metal foams with and without a washcoat: Effective thermal conductivity and gas-solid interfacial heat transfer, Chem. Eng. Sci., vol. 161, pp. 92-108, 2017.

Rabiei, A., O'Neill, A.T., A study on processing of a composite metal foam via casting, Materials Science and Engineering: A, vol. 404, pp. 159-164, 2005.

Reay, D., Metal Foams: Fundamentals and Applications, Appl. Therm. Eng., vol. 61, pp. 1, 2013.

Sachs, E.M., Haggerty, J.S., Cima, M.J., Williams, P.A., Three-dimensional printing techniques. Google Patents.

San Marchi, C., Mortensen, A., Deformation of open-cell aluminum foam, Acta Mater., vol. 49, pp. 3959-3969, 2001.

Stampfl, J., Hatzenbichler, M., Additive Manufacturing Technologies, In: Laperrière, L., Reinhart, G. (Eds.), CIRP Encyclopedia of Production Engineering. Springer Berlin Heidelberg, Berlin, Heidelberg, pp. 20-27, 2014.

Sundarram, S.S., Li, W., The effect of pore size and porosity on thermal management performance of phase change material infiltrated microcellular metal foams, Appl. Therm. Eng., vol. 64, pp. 147-154, 2014.

Thomson, W., On the division of space with minimum partitional area, Acta Math., vol. 11, pp. 121-134, 1970.

Twigg, M.V., Richardson, J.T., Fundamentals and Applications of Structured Ceramic Foam Catalysts, Ind. Eng. Chem. Res, vol. 46, pp. 4166-4177, 2007.

Tyagi, V.V., Buddhi, D., PCM thermal storage in buildings: A state of art, Renewable and Sustainable Energy Reviews, vol. 11, pp. 1146-1166, 2007.

Ukrainczyk, N., Kurajica, S., Šipušić, J., Thermophysical comparison of five commercial paraffin waxes as latent heat storage materials, Chem. Biochem. Eng. Q., vol. 24, pp. 129-137, 2010.

Vendra, L.J., Rabiei, A., A study on aluminum–steel composite metal foam processed by casting, Materials Science and Engineering: A, vol. 465, pp. 59-67, 2007.

Wadley, H.N., Cellular metals manufacturing, Adv. Eng. Mater., vol. 4, pp. 726-733, 2002.

Wang, J., Modelling and Numerical Simulation of a Manufacturing Process of Aluminium Foams and MPPC Materials, Lasmis. Universitt of Technology of Troyes, Troyes, France.

Weaire, D., Coughlan, S., Fortes, A., The modeling of liquid and solid foams, J. Mater. Process. Technol., vol. 55, pp. 178-185, 1995.

Weaire, D., Drenckhan, W., Structure and dynamics of confined foams: A review of recent progress, Adv. Colloid Interface Sci., vol. 137, pp. 20-26, 2008.

Weaire, D., Phelan, R., A counter-example to Kelvin's conjecture on minimal surfaces, Philos. Mag. Lett., vol. 69, pp. 107-110, 1994.

Yamada, Y., Shimojima, K., Sakaguchi, Y., Mabuchi, M., Nakamura, M., Asahina, T., Mukai, T., Kanahashi, H., Higashi, K., Effects of heat treatment on compressive properties of AZ91 Mg and SG91A Al foams with open-cell structure, Materials Science and Engineering: A, vol. 280, pp. 225-228, 2000.

Yang, J., Yang, L., Xu, C., Du, X., Experimental study on enhancement of thermal energy storage with phase-change material, Appl. Energy, vol. 169, pp. 164-176, 2016a.

Yang, X., Feng, S., Zhang, Q., Chai, Y., Jin, L., Lu, T.J., The role of porous metal foam on the unidirectional solidification of saturating fluid for cold storage, Appl. Energy, vol. 194, pp. 508-521, 2017.

Yang, X., Wang, W., Yang, C., Jin, L., Lu, T.J., Solidification of fluid saturated in open-cell metallic foams with graded morphologies, Int. J. Heat Mass Transfer, vol. 98, pp. 60-69, 2016b.

Zhao, C.-Y., Wu, Z., Heat transfer enhancement of high temperature thermal energy storage using metal foams and expanded graphite, Sol. Energy Mater. Sol. Cells, vol. 95, pp. 636-643, 2011.

Zhu, F., Experimental and numerical study of metal foam composite in innovative application of thermal energy storage, Lasmis. Universitt of Technology of Troyes, Troyes, France.

Chuan ZHANG

Doctorat : Matériaux, Mécanique, Optique et Nanotechnologie

Année 2017

Mousses d'aluminium composites : élaboration et propriétés thermiques pour le stockage d'énergie

L'objectif de cette thèse est d'étudier et d'optimiser le processus de fabrication des mousses métalliques et le comportement thermique du matériau de la mousse d'aluminium/matériau de changement de phase (MCP) par des méthodes expérimentales et numériques. Le processus d'élaboration de la mousse d'aluminium à pore ouvert est développé et optimisé pour contrôler précisément les paramètres de fabrication. Deux modèles de mousse d'aluminium à haute porosité (MAHP)/MCP composite et à faible porosité (MALP)/MCP composite sont établis pour la simulation numérique. En simulant le processus de fusion d'un système de stockage d'énergie, les composites MAHP/MCP et MALP/MCP sont comparés numériquement afin d'évaluer la performance de stockage d'énergie thermique. Les résultats montrent que la mousse d'aluminium améliore nettement le processus de transfert de chaleur dans MCP en raison de sa haute conductivité thermique. La porosité des mousses d'aluminium influence non seulement le processus de fusion du composite mais aussi la performance de stockage d'énergie thermique. Grâce à la collaboration avec EPF, une nouvelle méthode d'élaboration des mousses périodiques d'aluminium à pore ouvert est développée dans cette thèse sur la base d'impression 3D. Le comportement thermique des mousses d'aluminium périodiques à pore ouvert/MCP est analysé expérimentalement et numériquement.

Mots clés : mousses métalliques - chaleur, stockage - composites à matrice métallique - analyse thermique - simulation, méthodes de – impression 3D.

Aluminum Foams Composite: Elaboration and Thermal Properties for Energy Storage

The objective of this thesis is to study and optimize the manufacturing process of metal foams and the thermal behavior of the aluminum foam/phase change material (PCM) composite by experimental and numerical methods. The manufacturing process of open-cell aluminum foam is developed and optimized to precisely control the parameters of mufacturing. Two pore-scale models of high porosity aluminum foams (HPAF)/PCM composite and low porosity aluminum foams (LPAF)/PCM composite are established for numerical simulation. By simulating the melting process of a layer energy storage system, the HPAF/PCM and LPAFS/PCM composite are compared numerically in order to evaluate the energy storage performance. The results show that aluminum foam improves greatly the heat transfer process in PCM due to its high thermal conductivity. The porosity of aluminum foams could not only influence the melting process of composite but also the energy storage performance. Thanks to the collaboration with EPF, a new manufacturing method of periodic open-cell aluminum foams is developed based on 3D rapid tooling. The thermal behavior of the periodic open-cell aluminum foams/PCM composite is experimentally and numerically analyzed.

Keywords: metal foams - heat storage - metallic composites - thermal analysis - simulation methods - three-dimensional printing.

Thèse réalisée en partenariat entre :

Ecole Doctorale "Sciences et Technologies"